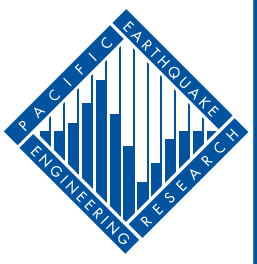

PACIFIC EARTHQUAKE ENGINEERING
RESEARCH CENTER

Seismic Evaluation of 196 kV Porcelain Transformer Bushings

Amir S. Gilani
Juan W. Chavez
Gregory L. Fenves
Andrew S. Whittaker
University of California, Berkeley

PEER 1998/02
MAY 1998

Seismic Evaluation of 196 kV Porcelain Transformer Bushings

by

Amir S. Gilani
Juan W. Chavez
Gregory L. Fenves
Andrew S. Whittaker
University of California, Berkeley

Report Number PEER-1998/02

Pacific Earthquake Engineering Research Center
College of Engineering
University of California, Berkeley

May 1998

ABSTRACT

Two identical 196 kV porcelain transformer bushings were evaluated for their response to severe earthquake shaking. Tri-directional earthquake simulator testing was undertaken to investigate the dynamic response of the bushing, to provide data for correlation with the analytical studies, to qualify one of the bushings for moderate earthquake shaking (per IEEE 693), and to evaluate the response of one bushing to extreme shaking effects. For earthquake testing, the bushing was mounted at 20° to the vertical in a stiff support frame. Spectrum-compatible ground motion records derived from earthquake motions recorded during the 1978 Tabas earthquake in Iran and the 1994 Northridge earthquake in California were used for testing. One bushing passed the IEEE 693 qualification tests for moderate shaking, and the other bushing survived extreme earthquake shaking with negligible damage and passed the IEEE 693 qualification tests for earthquake shaking at the High Level. The modal properties calculated by linear dynamic analysis and experimentation correlated reasonably well. Parametric studies identified the mechanical properties of the rubber gaskets separating the porcelain units as the key factor influencing the dynamic response of a transformer bushing.

ACKNOWLEDGMENTS

The work described in this report was funded by the Pacific Gas and Electric (PG&E) Company by a contract with the Pacific Earthquake Engineering Research (PEER) Center. This financial support is gratefully acknowledged. The transformer bushings were supplied by Asea Brown Boveri (ABB) of Alamo, Tennessee.

The significant technical contributions of Messrs. Ed Matsuda and Eric Fujisaki of PG&E, Mr. Lonnie Elder of ABB, and Mr. Don Clyde of the University of California at Berkeley made possible the work described in this report. The authors also thank Ms. Carol Cameron for editing this report.

TABLE OF CONTENTS

LIST OF TABLES

LIST OF FIGURES

CHAPTER 1
INTRODUCTION

1.1 Overview

The reliability of a power transmission and distribution system in a region exposed to earthquake shaking is dependent upon the seismic response of its individual components. One of the key components in a power transmission system are transformer bushings, which are insulated conductors that provide the electrical connection between a high-voltage line and an oil-filled transformer. Bushings are typically mounted on the top of a transformer (see Figure 1-1) using a bolted flange connection.

Porcelain bushings and other porcelain components (e.g., disconnect switches and live-tank circuit breakers) have proven vulnerable to moderate and severe earthquake shaking (EERI, 1990; EERI, 1995; Shinozuka, 1995). Following the 1994 Northridge earthquake, EERI (1995) wrote

> The Northridge earthquake confirmed the vulnerability of some types of substation equipment, especially those in higher-voltage classifications that contain large porcelain components. The vast majority of damage was to 500 kV and 230 kV equipment ... A large number of bushings failed from gasket oil leaks caused by the movement of porcelain relative to the metal base that connects the bushing to the top of the transformer body. Several transformer bushings failed when the porcelain bushing fractured.
>
> These failures confirmed the importance of the interutility/vendor effort started prior to the Northridge earthquake to ensure that new bushings are seismically rugged and to develop retrofit schemes for improving the performance of existing bushings.

The research described in this report addresses the vulnerability of high-voltage porcelain transformer bushings during moderate and severe earthquake shaking. This work was made possible by a partnership between the Pacific Earthquake Engineering Research (PEER) Center and Pacific Gas & Electric (PG&E) that was formed to investigate the seismic reliability of utility lifelines. One component of the PEER-PG&E Directed Studies Research Program focuses on the vulnerability of electrical transmission equipment: porcelain transformer bushings are one such piece of equipment.

This report documents the seismic response of 196 kV transformer bushings manufactured by Asea Brown Boveri (ABB) of Alamo, Tennessee. The six key objectives of the studies described in the following chapters were:

1. Develop a three-dimensional mathematical model of a 196 kV porcelain bushing for parametric and future studies using material properties obtained from laboratory testing.

2. Analyze, design, and build a mounting frame suitable for seismic testing of bushings ranging in rating between 196 kV and 550 kV.

3. Develop earthquake ground motion records suitable for the seismic evaluation, qualification, and fragility testing of 196 kV bushings.

4. Test two 196 kV bushings on the earthquake simulator at the Pacific Earthquake Engineering Research (PEER) Center using levels of earthquake shaking consistent with those adopted for seismic qualification and fragility testing of electrical equipment.

5. Reduce the data acquired from the earthquake simulator tests to serve four purposes: a) determine the dynamic properties of the bushings, b) evaluate the seismic response of the bushings during moderate and severe earthquake shaking, c) qualify one of the 196 kV bushings for moderate shaking, and d) determine the failure mode, if any, of the second bushing subjected to extreme earthquake shaking (fragility testing).

6. Draw conclusions about a) the performance of porcelain transformer bushings, b) the likely failure modes of a bushing during severe earthquake shaking, c) methods for modeling porcelain bushings, and d) improved procedures for judging the seismic response of transformer bushings.

1.2 Seismic Qualification and Fragility Testing

Structural and nonstructural components that do not lend themselves to analysis are often *qualified* for use in specific applications by full-scale testing. Qualification has long been used by the Nuclear Regulatory Commission (NRC) for equipment and hardware (e.g., valves and snubbers) in nuclear power plants, and by the Departments of Defense and Energy for military hardware. Qualification is a binary decision-making process: equipment or hardware either passes or fails.

The objective of fragility testing is to establish a relation between limiting states of response (e.g., electrical connectivity, gasket failure, and cracking of porcelain) and peak ground acceleration for a selected piece of equipment. This information is then used to develop fragility curves that plot the cumulative probability of reaching a limit state as a function of peak ground acceleration.

In California, electrical equipment is seismically qualified using a standard developed by the Institute of Electrical and Electronic Engineers (IEEE 693). The draft IEEE standard (IEEE, 1997) entitled *IEEE 693 Recommended Practices for Seismic Design of Substations* details procedures for qualification of electrical substation equipment for different seismic performance levels. The key features of the draft standard as they pertain to this report are described in Section 3.2. Additional information is presented in Appendix A.

1.3 ABB 196 kV Transformer Bushings

Two Model 196W0800AY, 196 kV transformer bushings, manufactured by Asea Brown Boveri (ABB) Power Transmission & Distribution (T&D) Company, Inc. were tested as part of the research program described in this report. Figure 1-2 is a photograph of a 196 kV bushing.

A longitudinal section through a 196 kV bushing is shown in Figure 1-3. The overall length of the transformer bushing is 166 in. (4.2 m). The segment of the bushing above the cast aluminum flange plate (which protrudes above the top of the transformer as seen in Figure 1-1) is 106 in.

(2.7 m) long and includes three porcelain insulator units (hereafter referred to as UPPER-1, UPPER-2, and UPPER-3), and a metallic dome at the top of the bushing (adjacent porcelain unit UPPER-3). The porcelain units, the cast flange, and the metallic dome are separated by gaskets made of nitrile rubber. The gasket between the flange plate and porcelain unit UPPER-1 is a flat annular strip of rubber. The remaining gaskets above the flange plate are flat annular strips of rubber with an outside perimeter lip. The segment of the bushing below the flange plate includes an extension of the cast aluminum flange plate, one porcelain insulator, and a cast aluminum lower support. Flat annular gaskets separate these components. The flange plate, which is used to connect the bushing to the transformer, is cast with two lifting lugs to facilitate movement and installation of the bushing.

In cross-section, the bushing has an aluminum core, which houses copper cables that provide the electrical connection; a multi-layered kraft paper condenser wrapped around the core; an annular gap between the porcelain and condenser that is filled with an oil to provide electrical insulation; and a porcelain insulator. The bushing is post-tensioned along its longitudinal axis through the aluminum core with a force of 27 kip (120 kN). Springs in the metallic dome ensure a uniform distribution of compression around the perimeter of the porcelain units and the gaskets. The weight of the bushing is approximately 1,050 lb (4.7 kN), and its center of mass is located 84 in. (2.1 m) above the lower tip of the bushing.

The two bushings tested as part of this research program where identified by the Serial Numbers 7T00525802 and 7T00525801. These bushings were designated Bushing-1 and Bushing-2, respectively.

1.4 Report Organization

This report is divided into seven chapters and three appendices. Chapter 2 provides information on the simulator used for earthquake testing, the mounting frame designed to support the bushings during testing, and a list of the transducers used to monitor the response of the bushings. Chapter 3 describes the earthquake histories developed for qualification and testing, and the schedule of tests on the earthquake simulator. Chapter 4 provides a summary of the key test results. A mathematical model of a 196 kV bushing is presented in Chapter 5, together with the results of selected parametric studies. Chapter 6 includes a summary of the key findings and conclusions drawn from the research project. References are listed following Chapter 6. The IEEE Recommended Practice for earthquake testing of transformer bushings is summarized in Appendix A. The results of the electrical testing of the bushing, conducted by others but included herein for completeness, are presented in Appendix B. Appendix C reproduces Annex S of IEEE 693 and presents a table cross-referencing the information documenting the qualification of a transformer bushing per IEEE 693 and the appropriate section numbers in this report. Appendix D lists instrument and calibration data for each of the transducers used to record the response of the bushings. Raw data and video images from all earthquake tests were supplied to Pacific Gas & Electric under separate cover.

Figure 1-1 Photograph of a bushing mounted on an oil-filled transformer

Figure 1-2 196 kV transformer bushing

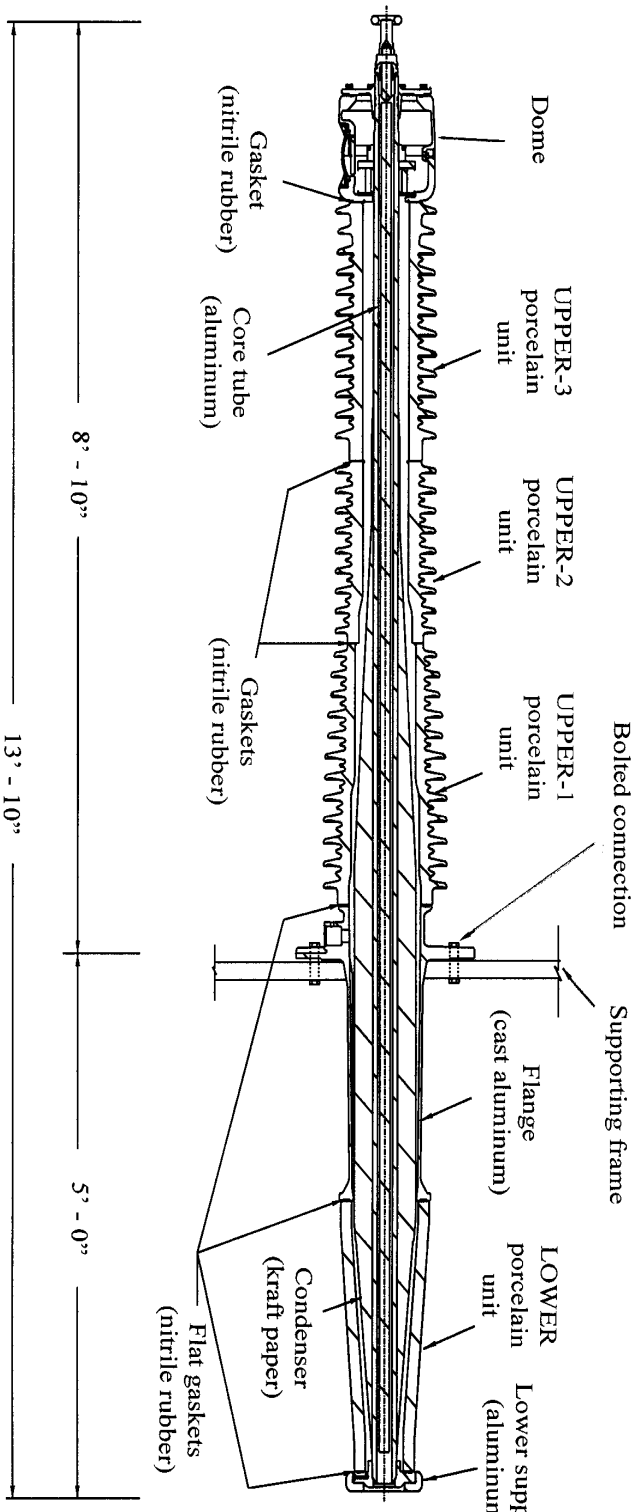

Figure 1-3 Geometry and longitudinal section of a 196 kV transformer bushing

CHAPTER 2
EARTHQUAKE SIMULATOR TESTING

2.1 Introduction

Triaxial earthquake simulator testing was used to evaluate the seismic behavior of two 196 kV transformer bushings. The earthquake testing protocol for transformer bushings set forth in IEEE 693 (IEEE, 1997) was adopted for this study. The following sections in this chapter describe the earthquake simulator used for testing the bushings, the *rigid* mounting frame used to support the bushings during testing, and the instrumentation scheme used to monitor the response of the bushings during earthquake testing.

2.2 Earthquake Simulator

The earthquake simulator at the Pacific Earthquake Engineering Research (PEER) Center at the University of California at Berkeley was used for the seismic evaluation and qualification studies described in this report. The simulator, also known as a shaking table, measures 20 ft by 20 ft (6.1 by 6.1 m) in plan; the maximum payload is 140 kips (623 kN). Models up to 40 ft (12.2 m) in height can be tested. The six-degree-of-freedom simulator can be programmed to reproduce any wave form (e.g., sinusoidal, white noise, earthquake history). The maximum stroke and velocity of the simulator are ± 5 inches (± 127 mm) and 25 inches/second (635 mm/sec), respectively.

2.3 Mounting Frame

IEEE 693 states that bushings rated at 161 kV and above must be qualified using three-component earthquake-simulator testing. Because it is impractical to test bushings mounted on a transformer, IEEE specifies that bushings must be mounted on a rigid stand for earthquake testing and qualification. IEEE also recommends that a transformer bushing be tested at 20 degrees measured from the vertical because a bushing, if so tested and qualified, is assumed to be qualified for use on all transformers with angles from vertical to 20 degrees.

Figures 2-1a and 2-1b are photographs of the mounting frame used for the earthquake simulator testing. Drawings of the frame are shown in Figure 2-2. The mounting frame was designed to support bushings ranging in size up to 550 kV, and is constructed of four 5”x5”x0.38” tubular steel columns, 5”x5”x0.75” angle braces, and a 2-inch (51 mm) thick steel mounting plate (sloping at 20 degrees to the horizontal). ASTM A36 steel was used for all components, and welding was used to join the columns, braces, and plate. Table 2-1 reports the modal properties of the mounting frame considering a) the frame alone (columns 2 and 3) per Figure 2-2, and b) the frame, adaptor plate, and 196kV bushing (columns 4 and 5), all as calculated by analysis.

Table 2-1 Modal properties of mounting frame by analysis

	Frame Only		*Frame, Adaptor Plate, and Bushing*	
Mode	*Frequency (Hz)*	*Predominant direction*[1]	*Frequency (Hz)*	*Predominant direction*[1]
1	72	X	58	X
2	78	Y	70	Y
3	88	Z	74	Z
4	113	θ_z	107	θ_z

1. See Figure 2-3 for coordinate system

The mounting frame was post-tensioned to the earthquake simulator platform using 15 1-inch (25 mm) diameter high-strength threaded rods. A 1.5-inch (38 mm) thick adaptor plate was used to attach the bushing to the mounting plate (see Figure 2-1b). Twelve 1.25-inch (32 mm) diameter high-strength bolts were used for the adaptor plate-to-mounting plate connection The flange of the bushing was joined to the adaptor plate with 12 0.75-inch (19 mm) diameter Grade 2 stainless steel bolts (equivalent to A307 steel) torqued to 100 ft-lb (136 m-N) per the ABB installation specification.

2.4 Instrumentation

For seismic testing, IEEE 693 states that porcelain bushings must be instrumented to record a) maximum vertical and horizontal accelerations at the top of the bushing, at the bushing flange, and at the top of the earthquake simulator platform, b) maximum displacement of the top of the bushing relative to the flange, and c) maximum porcelain stresses at the base of the bushing near the flange.

The instrumentation scheme developed for the tests described in this report exceeded the IEEE requirements. Fifty channels of data were recorded for each test. Table 2-2 lists the channel number, instrument type, response quantity, coordinate system, and location for each transducer. Figure 2-3 presents information on the instrumentation of the earthquake simulator platform (Figure 2-3a), the bushing and the mounting frame (Figure 2-3b), and the porcelain unit immediately above the flange (UPPER-1) of the bushing (Figure 2-3c). The global (X, Y, Z) and local (*x, y, z*) coordinate systems adopted for the testing program are shown in the figure. Figure 2-4 is a photograph of the bushing instrumentation above the flange plate. The calibration factor for each transducer is listed in Appendix D.

Sixteen channels (channels 3 through 18) recorded the acceleration and displacement of the earthquake simulator platform in the global coordinate system. The accelerations of the mounting frame in the local coordinate system (channels 28, 29, and 30) and the absolute displacements of the mounting frame in the global coordinate system (channels 37 and 38) were recorded. The accelerations of the bushing in the local coordinate system and the absolute displacements of the bushing in the global coordinate system were measured at the top, midheight, and bottom of the bushing. Four strain gages (channels 39 through 42) monitored the axial strains in the UPPER-1

porcelain unit. Four displacement transducers (channels 47 through 50) measured displacements across the gasket (located immediately above the flange) parallel to the axis of the bushing. Another four displacement transducers (channels 43 through 46) measured slip of the UPPER-1 porcelain unit relative to the adaptor plate.

Table 2-2 Instrumentation for bushing tests

Channel Number	*Transducer*[1]	*Response Quantity*	*Coordinate System and Orientation*	*Transducer Location*
1	-	date	-	-
2	-	time	-	-
3	A	table acceleration	global X	simulator platform
4	A	table acceleration	global X	simulator platform
5	A	table acceleration	global Y	simulator platform
6	A	table acceleration	global Y	simulator platform
7	A	table acceleration	global Z	simulator platform
8	A	table acceleration	global Z	simulator platform
9	A	table acceleration	global Z	simulator platform
10	A	table acceleration	global Z	simulator platform
11	LVDT	table displacement	global X	simulator platform
12	LVDT	table displacement	global Y	simulator platform
13	LVDT	table displacement	global X	simulator platform
14	LVDT	table displacement	global Y	simulator platform
15	LVDT	table displacement	global Z	simulator platform
16	LVDT	table displacement	global Z	simulator platform
17	LVDT	table displacement	global Z	simulator platform
18	LVDT	table displacement	global Z	simulator platform
19	A	bushing acceleration	local x	bottom of bushing
20	A	bushing acceleration	local y	bottom of bushing
21	A	bushing acceleration	local z	bottom of bushing
22	A	bushing acceleration	local x	midheight of bushing
23	A	bushing acceleration	local y	midheight of bushing
24	A	bushing acceleration	local z	midheight of bushing
25	A	bushing acceleration	local x	top of bushing
26	A	bushing acceleration	local y	top of bushing
27	A	bushing acceleration	local z	top of bushing
28	A	frame acceleration	local x	top of mounting frame

Table 2-2 Instrumentation for bushing tests

Channel Number	*Transducer*[1]	*Response Quantity*	*Coordinate System and Orientation*	*Transducer Location*
29	A	frame acceleration	local y	top of mounting frame
30	A	frame acceleration	local z	top of mounting frame
31	LP	bushing displacement	global X	bottom of bushing
32	LP	bushing displacement	global Y	bottom of bushing
33	LP	bushing displacement	global X	midheight of bushing
34	LP	bushing displacement	global Y	midheight of bushing
35	LP	bushing displacement	global X	top of bushing
36	LP	bushing displacement	global Y	top of bushing
37	LP	frame displacement	global X	top of mounting frame
38	LP	frame displacement	global Y	top of mounting frame
39	SG	porcelain strain	-	UPPER-1 porcelain unit
40	SG	porcelain strain	-	UPPER-1 porcelain unit
41	SG	porcelain strain	-	UPPER-1 porcelain unit
42	SG	porcelain strain	-	UPPER-1 porcelain unit
43	DCDT	gasket slip	relative to frame	UPPER-1 porcelain unit
44	DCDT	gasket slip	relative to frame	UPPER-1 porcelain unit
45	DCDT	gasket slip	relative to frame	UPPER-1 porcelain unit
46	DCDT	gasket slip	relative to frame	UPPER-1 porcelain unit
47	DCDT	gasket opening	relative to frame	UPPER-1 porcelain unit
48	DCDT	gasket opening	relative to frame	UPPER-1 porcelain unit
49	DCDT	gasket opening	relative to frame	UPPER-1 porcelain unit
50	DCDT	gasket opening	relative to frame	UPPER-1 porcelain unit

1. A = accelerometer; LVDT = displacement transducer; LP = linear potentiometer; SG = strain gage; DCDT = displacement transducer

a. View of the mounting frame showing angle braces

b. View of adaptor plate

Figure 2-1 Photographs of the mounting frame

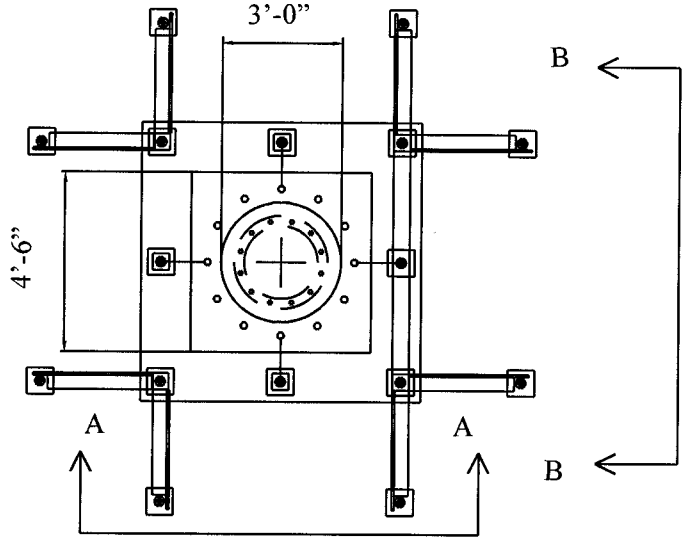

Plan view of the mounting frame

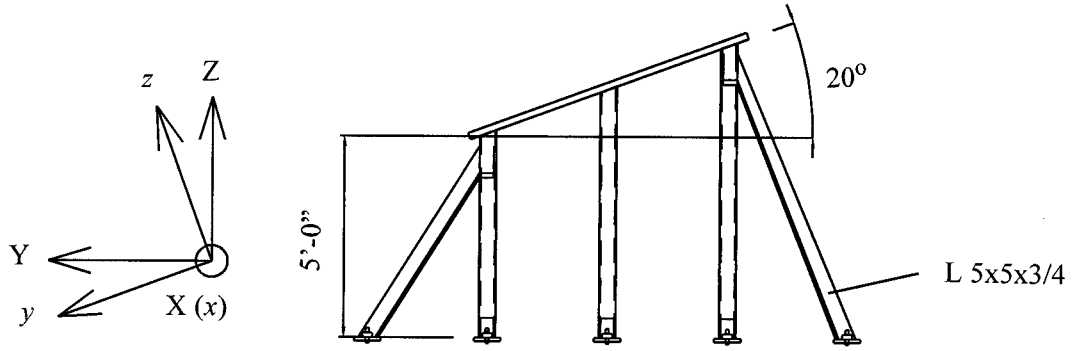

Elevation A-A

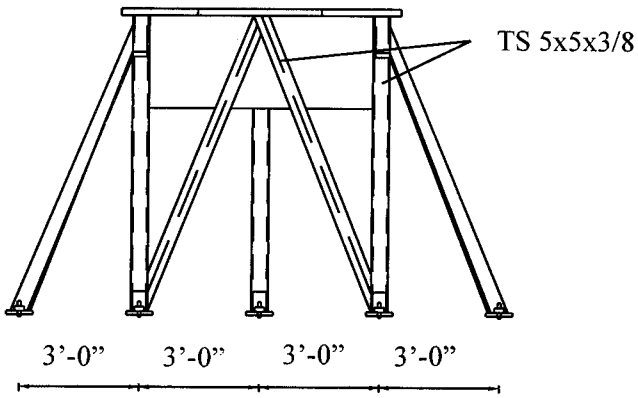

Elevation B-B

Figure 2-2 Mounting frame construction drawings

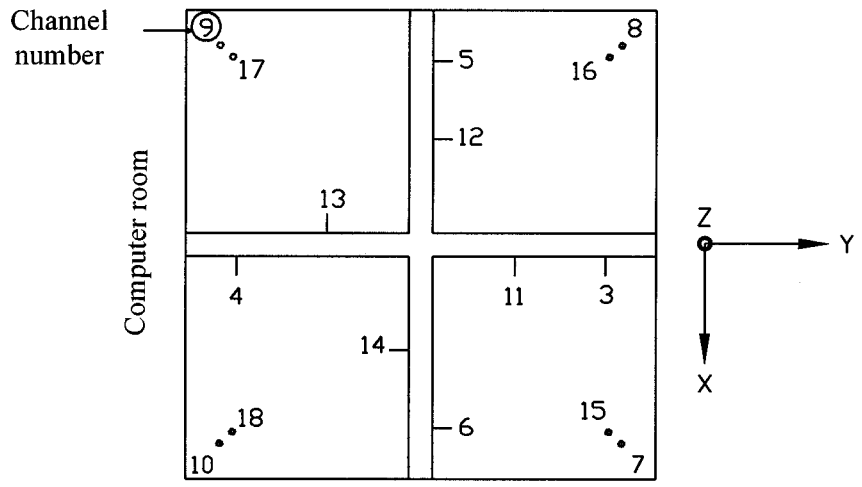

(a) Earthquake simulator (view from beneath)

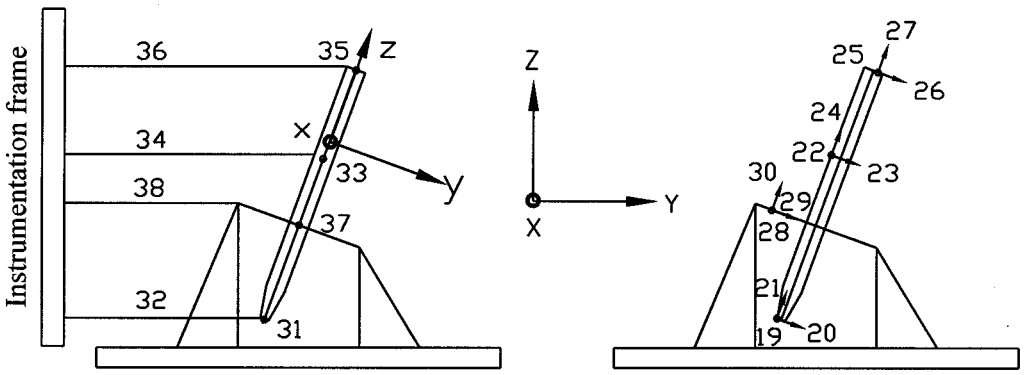

(b) Bushing and mounting frame

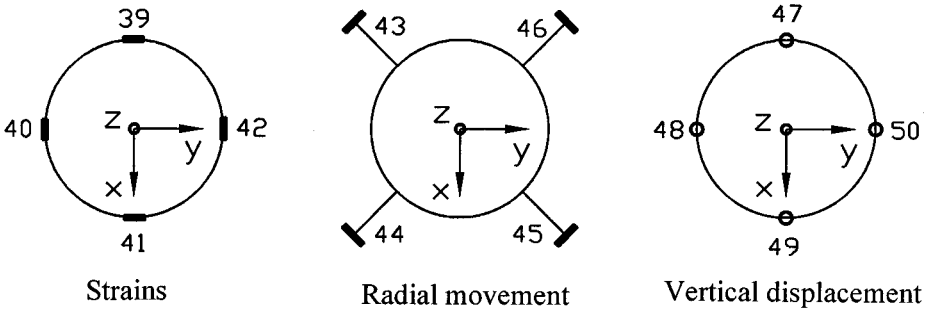

(c) UPPER-1 porcelain unit

Figure 2-3 Bushing instrumentation

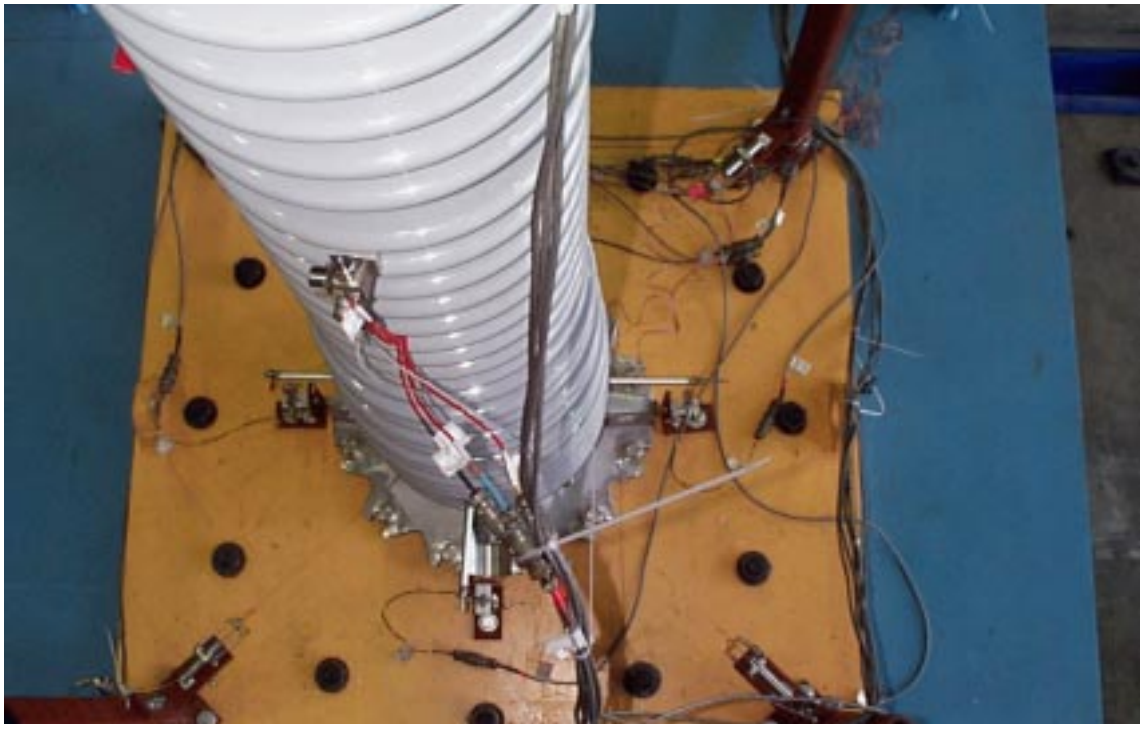

Figure 2-4 Photograph of bushing and selected instrumentation

CHAPTER 3
EARTHQUAKE HISTORIES FOR TESTING

3.1 Introduction

Recorded earthquake ground motion histories were used to evaluate the seismic response of two 196 kV transformer bushings (hereafter termed Bushing-1 and Bushing-2). The following sections describe the requirements of IEEE 693 (IEEE, 1997) for qualification of transformer bushings (Section 3.2), the procedures used to develop earthquake histories for testing (Section 3.2), the schedule of tests on the earthquake simulator (Section 3.3), and analysis of the response of the earthquake simulator platform (Section 3.4).

3.2 Earthquake Histories for Bushing Qualification

Three types of earthquake-simulator testing are identified in IEEE 693 for the seismic qualification of transformer bushings: 1) earthquake ground motions, 2) resonant frequency search, and 3) sine-beat testing. Earthquake ground motion tests (termed *time-history shake table tests* in IEEE 693) and resonant frequency tests are mandatory; information on these two types of tests follow.

3.2.1 Resonant search tests

Sine-sweep or broad-band white noise tests are used to establish the dynamic characteristics (natural frequencies and damping ratios) of a bushing. These so-called *resonant search* tests are undertaken using uni-directional excitation along each global axis of the earthquake simulator platform. If broadband white noise tests are performed, the amplitude of the white noise must not be less than 0.25g.

If sine-sweep tests are used, IEEE 693 specifies that the resonant search be conducted at a rate not exceeding one octave per minute in the range for which the equipment has resonant frequencies but at least at 1 Hz; frequency searching above 33 Hz is not required. Modal damping is calculated using the half-power bandwidth method. Because both sine-sweep and white-noise tests were used in this testing program to identify the modal properties of the transformer bushings, the recommendations of IEEE 693 were not adhered to exactly.

The history for the sine-sweep test was developed using a rate of two octaves per minute, that is, the input frequency doubles every 30 seconds. A continuous frequency function of the form

$$f(t) = 2^{t/30} \tag{3-1}$$

where t is time in seconds, was used to develop the sine-sweep function

$$x(t) = x_0 \sin\left(2\pi\left[\frac{30}{\log 2}\right]2^{t/30}\right) \tag{3-2}$$

where x is the displacement, and x_0 is the maximum displacement.

The history for the banded white-noise tests was prepared using a random signal generator.

3.2.2 Earthquake tests

For earthquake simulator testing, IEEE 693 states that the Test Response Spectrum (TRS) for each horizontal earthquake motion must match or exceed the target spectrum and that the TRS for vertical earthquake motion be no less than 80 percent of target spectrum. IEEE 693 recommends that 2-percent damping be used for spectral matching and requires at least 20 seconds of strong motion shaking be present in each earthquake record. Earthquake motions can be established using either synthetic or recorded histories. Recorded motions formed the basis of the earthquake histories used to test the 196 kV bushings.

IEEE 693 represents a Performance Level (PL) for substation equipment by a response spectrum. The two PLs relevant to California are *High* and *Moderate*. The Moderate PL was selected for the studies reported herein. Equipment that is shown to perform acceptably in ground shaking consistent with the Moderate Seismic Performance Level (see Figure 3-1) is said to be seismically qualified to the Moderate Level.

It is often impractical or not cost effective to test to the Moderate PL. As such, IEEE 693 permits equipment to be tested using accelerations that are one-half of the PL. The reduced level of shaking is called the Required Response Spectrum (RRS). The ratio of PL to RRS, termed the performance factor in IEEE 693, is equal to 2. The Moderate RRSs are shown in Figure 3-2. The shapes of the RRS and the PL are identical, but the ordinates of the RRS are one-half of the PL. Equipment tested or analyzed using the RRS is expected to have acceptable performance at the PL. This assumption is checked by measuring the stresses obtained from testing at the RRS, and a) comparing the stresses to 50 percent (equal to the inverse of the performance factor) of the ultimate strength of the porcelain (assumed to be brittle) or cast aluminum components, and b) using a lower factor of safety against yield combined with an allowance for ductility of steel and other ductile materials.

To account for the amplification of earthquake motion due to the influence of the transformer body and local flexibility of the transformer near the bushing mount, IEEE 693 states that the input motion *as measured at the bushing flange* shall match a spectrum with ordinates twice that of the Required Response Spectrum. The resulting spectra, termed the Test Response Spectra (TRS), for Moderate Level qualification are shown in Figure 3-3. These spectra are identical to those shown in Figure 3-1. The key requirements of IEEE 693 for earthquake-history testing of bushings are summarized in Table 3-1.

The earthquake histories used for the qualification and fragility testing were developed using two recorded (three-component) sets of near-fault ground motion records: Tabas (1978 Iran earthquake) and Newhall (1994 Northridge earthquake). These records are representative of earthquakes known to have high potential for damaging building structures and equipment. Figures 3-4 to 3-9 show the three component normalized acceleration histories, power spectra, and pseudo-acceleration response spectra for the Tabas and Newhall records.

Table 3-1 Summary of IEEE earthquake-history testing requirements

Peak Ground Acceleration	*Comments*
0.5g	Moderate Seismic Performance Level for substation equipment
0.25g	Required Response Spectrum for Moderate Seismic Performance Level for substation equipment
0.5g	Test Response Spectrum for Moderate Seismic Performance Level for bushing supported on a transformer
1.0g	Response spectrum for checking porcelain stresses and oil leakage; see Section 4.4.4 for more details

These normalized acceleration records were modified using a non-stationary response-spectrum matching technique developed by Abrahamson (Abrahamson, 1996). The method generates spectrum-compatible histories from reference histories by adding short wavelets to the reference history. Figures 3-10 to 3-15 show the three component normalized acceleration histories, Fourier spectra, and response spectra for spectrum-compatible Tabas and Newhall records.

The low frequency components of the spectrum-compatible, normalized Tabas and Newhall histories produce displacements that exceed the displacement limits of the earthquake simulator. To reduce the displacements to 5 inches (127 mm) or less, the spectrum-compatible records were high-pass filtered using a cut-off frequency of 1 Hz. The resonant frequency of the 196 kV bushing was known to range between 10 Hz and 15 Hz. The removal of low frequency input will therefore have little to no impact on the dynamic response of the bushing. The resulting earthquake histories and the corresponding response spectra are shown in Figures 3-16 through 3-19.

3.3 Schedule of Experimental Testing

The experimental program for the two 196 kV transformer bushings is summarized in Table 3-2. Resonant search (banded white-noise and sine-sweep) tests were performed to determine the dynamic characteristics (modal frequencies and damping ratios) of the bushings. In Table 3-2, these tests are designated as WN and SS, respectively. The suffixes X, Y, and Z refer to the direction of testing; see Figure 2-3 for the global coordinate system. The resonant searches were low-amplitude, uni-directional tests carried out at a nominal peak acceleration of 0.1g.

For the seismic qualification and fragility tests, three-component earthquake histories were used (see Section 3.2.2). In Table 3-2, these histories are denoted as Tabas*** or Newhall***, where *** is the nominal amplitude of the target peak acceleration (e.g., 050 = 50 percent gravity and Tabas050 are the earthquake histories of Figure 3-16 normalized to a peak acceleration of 0.5g).

Bushing-1 was designated for seismic qualification testing. Bushing-2 was designated for fragility testing. Tabas100 was selected for the Moderate Level seismic qualification of Bushing-1. The Tabas and Newhall earthquake histories of Section 3.2.2 were used for the fragility testing of Bushing-2. Due to response interaction along the three axes of the earthquake simulator, the mea-

sured peak accelerations of the simulator platform along the X-, Y-, and Z-axes did not match the target values. Values of the measured accelerations for the key earthquake simulations are shown in Table 3-3. Test Number 8 (using Tabas100) was used for the Moderate Level seismic qualification of Bushing-1.

The schedule of the fragility tests is presented in Table 3-2. The Tabas and Newhall earthquake histories were used for simulations with target peak accelerations of less than 1.0g. The Tabas earthquake histories were used for target peak accelerations greater than 1.0g (Test Numbers 18 through 22). For fragility test numbers 19 through 22, the peak horizontal accelerations exceeded the target value and the peak vertical accelerations were smaller than the target value.

3.4 Earthquake Simulator Response Characteristics

3.4.1 Translational response

The key tests of Bushing-1 and Bushing-2 were Test Numbers 8 and 21, respectively. The three-component, 2-percent damped, response spectra computed using the measured acceleration histories of the simulator platform, are shown in Figures 3-20 (Test Number 8, Tabas100, Moderate Level Qualification of Bushing-1) and 3-21 (Test Number 21, Tabas180, Fragility Testing of Bushing-2).

Test Number 8: Tabas100

In the frequency range of interest for the 196 kV bushings (10 to 20 Hz), the 2-percent damped spectra for longitudinal (X direction) and lateral (Y direction) response equal or exceed the target spectrum that is anchored to a peak acceleration of 1.0g. The spectrum for vertical response is substantially smaller than the target spectrum that is anchored to a peak acceleration of 0.8g. The spectra were generated using the measured acceleration histories of the earthquake-simulator platform. The durations of strong-motion shaking, as calculated using the procedure set forth in IEEE 693 (IEEE 1997) were 19, 13, and 16 seconds in the X-, Y-, and Z-directions, respectively. These values are less than the 20-second requirement in IEEE (see Appendix A).

Test Number 21: Tabas180

The 2-percent damped spectra for longitudinal (X direction) and lateral (Y direction) response equal or exceed the target spectrum that is anchored to a peak acceleration of 2.0g. The spectrum for vertical response is substantially less than the target spectrum that is anchored to a peak acceleration of 1.6g. The spectra were generated using the measured acceleration histories of the earthquake-simulator platform. The durations of strong-motion shaking, as calculated using the procedure set forth in IEEE 693, were 26, 15, and 18 seconds in the X-, Y-, and Z-directions, respectively. Two of the three values are less than the 20-second requirement in IEEE.

Table 3-2 Schedule of earthquake testing

Test No.	*Test date*	*Bushing*	*Test*[1]
1	8/11/97	1	WN-X
2	8/11/97	1	WN-Y
3	8/11/97	1	WN-Z
4	8/11/97	1	SS-X
5	8/11/97	1	SS-Y
6	8/11/97	1	SS-Z
7	8/11/97	1	Tabas100[2]
8	8/11/97	1	Tabas100
9	8/14/97	2	WN-X
10	8/14/97	2	WN-Y
11	8/14/97	2	WN-Z
12	8/14/97	2	Tabas050
13	8/14/97	2	Newhall050[3]
14	8/14/97	2	Newhall080
15	8/14/97	2	Tabas080
16	8/14/97	2	Tabas100
17	8/14/97	2	Newhall100
18	8/15/97	2	Tabas120
19	8/15/97	2	Tabas140
20	8/15/97	2	Tabas160
21	8/15/97	2	Tabas180
22	8/15/97	2	Tabas200
23	8/15/97	2	WN-X
24	8/15/97	2	WN-Y
25	8/15/97	2	WN-Z

1. WN = white noise, SS = sine sweep; -X, -Y, and -Z denote direction of testing.
2. Tabas = Tabas earthquake histories; 050 denotes target peak acceleration in percent of g.
3. Newhall = Newhall earthquake histories.

Table 3-3 Peak accelerations of the earthquake simulator platform

		Peak Acceleration (g)		
Test Number	*Identification*	*X-direction*[1]	*Y-direction*	*Z-direction*
7	Tabas100	0.6	2.1	0.7
8	Tabas100	1.3	2.0	0.7
12	Tabas050	0.7	0.9	0.5
13	Newhall050	0.5	0.6	0.4
14	Newhall080	0.9	0.9	0.5
15	Tabas080	1.0	1.5	0.7
16	Tabas100	1.3	1.5	0.9
17	Newhall100	1.3	1.1	0.5
18	Tabas120	1.7	1.8	1.1
19	Tabas140	2.0	2.0	1.1
20	Tabas160	2.3	2.2	1.1
21	Tabas180	2.5	2.5	1.1
22	Tabas200	2.3	2.6	0.8

1. See Figure 2-3 for information on the coordinate system

3.4.2 Rotational response

The three rotational displacement signals were set equal to zero for all earthquake simulations. However, due to interaction of the servo-actuators and pitching and rolling of the simulator platform, some rigid body rotation of the platform was measured. The rigid body rotations of the platform were estimated using the measured displacements of the platform (channels 15 through 18). Herein, the rotations are defined as twist (rotation about the vertical [ZZ] axis), pitch (rotation about the longitudinal [XX] axis), and roll (rotation about the lateral [YY] axis). Figure 3-22 shows the rotational response of the simulator platform during the Tabas180 test. A rigid body rotation of 0.0005 radian (see Figure 3-22) will produce a displacement at the tip of the bushing equal to 0.1 inch (2.5 mm).

Data from the Tabas180 run was used to estimate the rotational accelerations of the earthquake simulator platform. Rotational accelerations at the center of the platform were estimated using the measured acceleration histories (channels 7 through 10). The history and frequency response of these accelerations are shown in Figures 3-23 and 3-24, respectively. The peak rotational acceleration about the horizontal axes of the simulator platform is approximately 0.005 radian/ sec^2, producing a peak translational acceleration at the tip of the bushing equal to approximately 1.0g. As seen in Figure 3-24, the rotational accelerations have significant components between 10 and 20 Hz. These components could amplify the motion of the mounting frame and increase the translational acceleration response of the bushing.

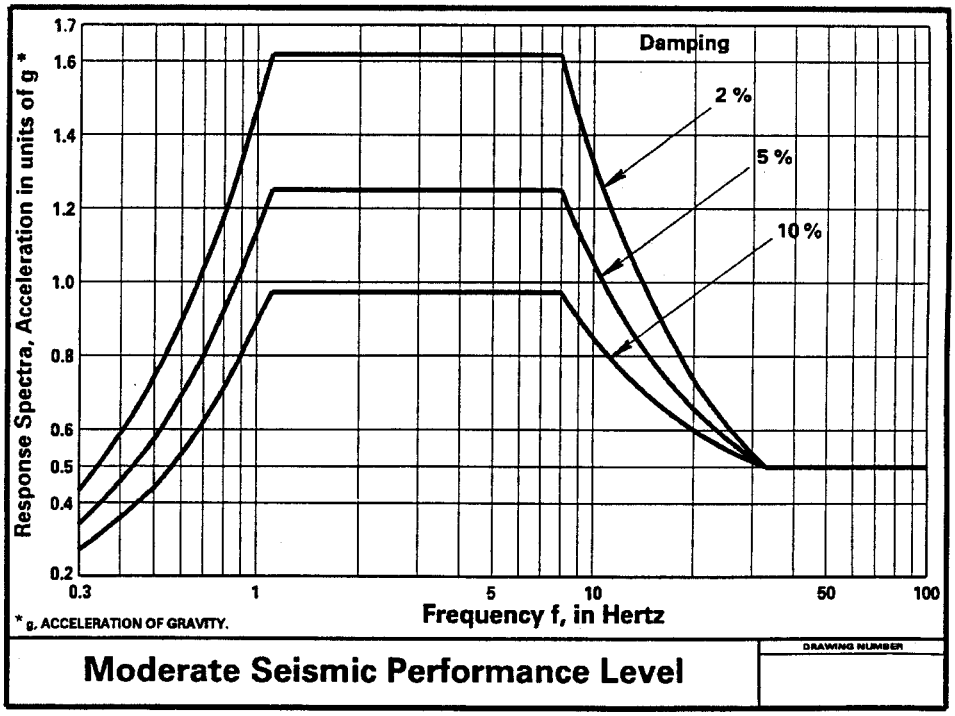

Figure 3-1 Spectra for the Moderate Seismic Performance Level (IEEE, 1997)

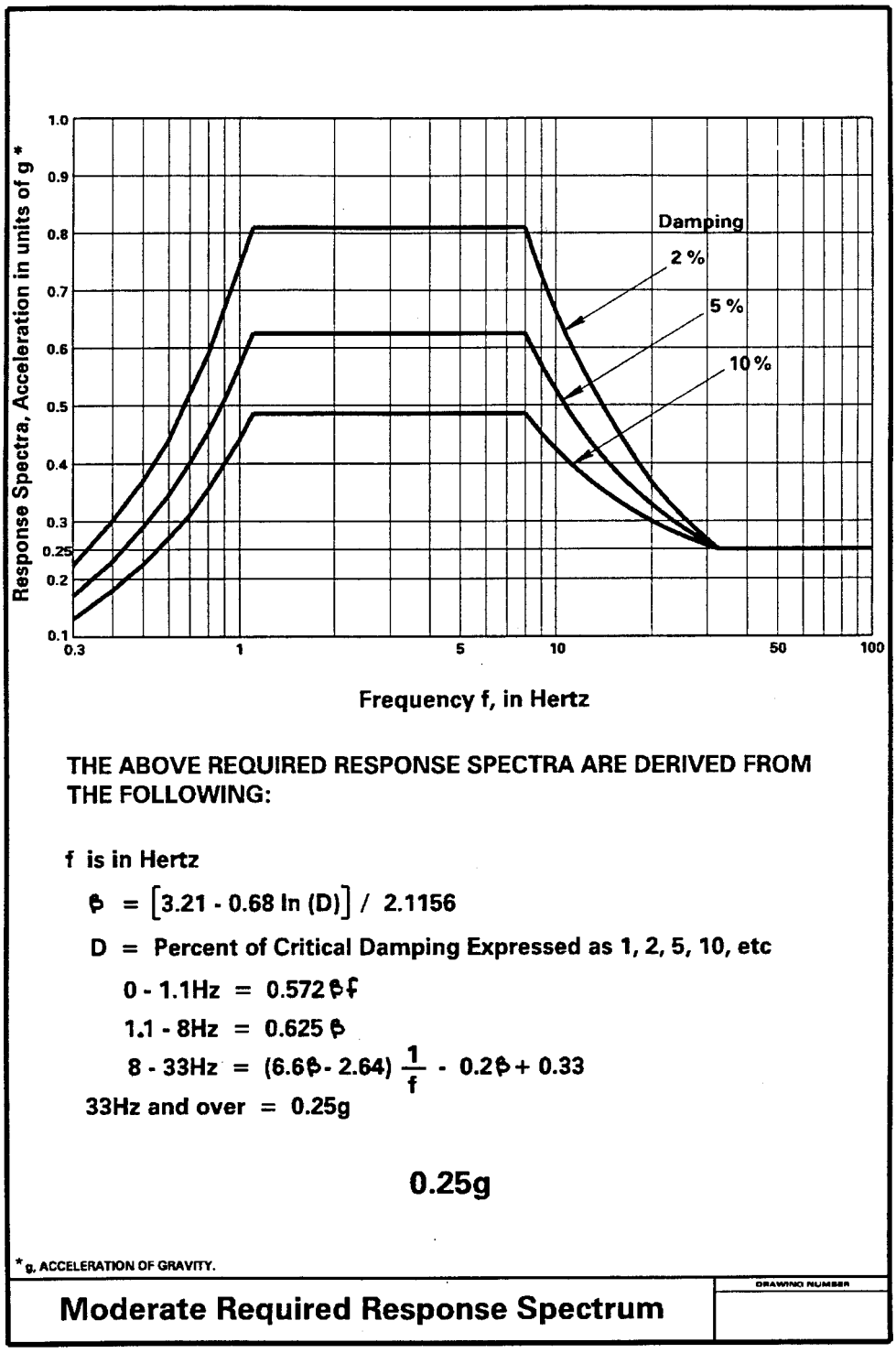

Figure 3-2 Required Response Spectra for Moderate PL (IEEE, 1997)

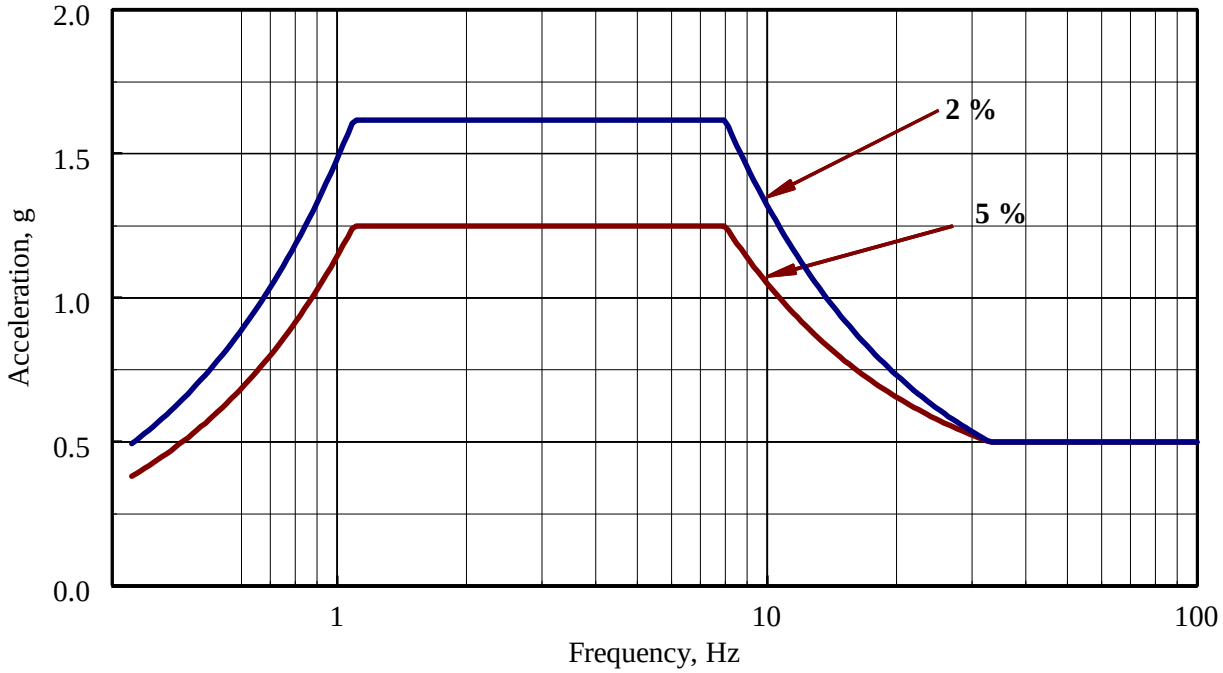

Figure 3-3 Test Response Spectra at bushing flange for Moderate PL

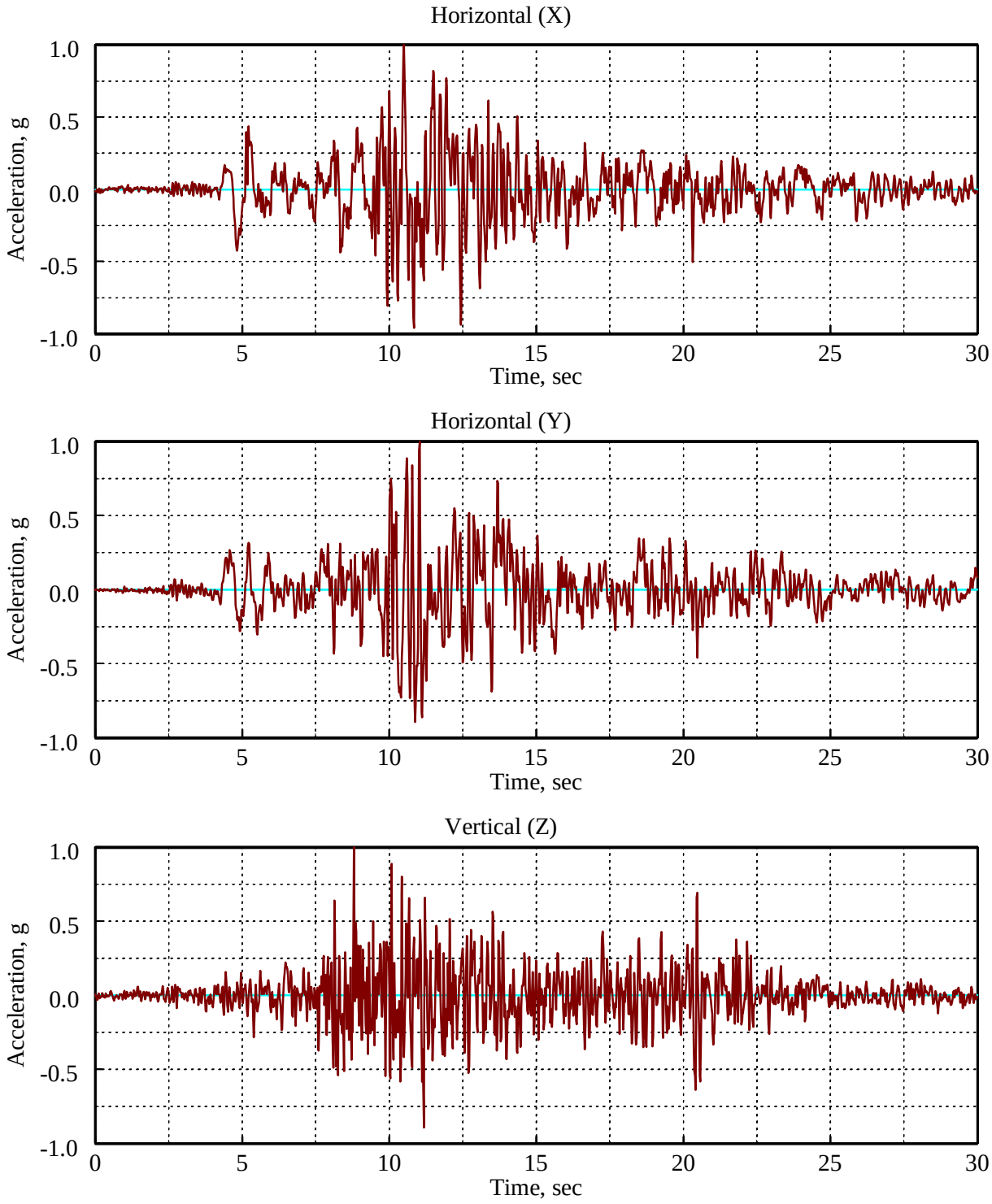

Figure 3-4 Normalized acceleration histories, Tabas record

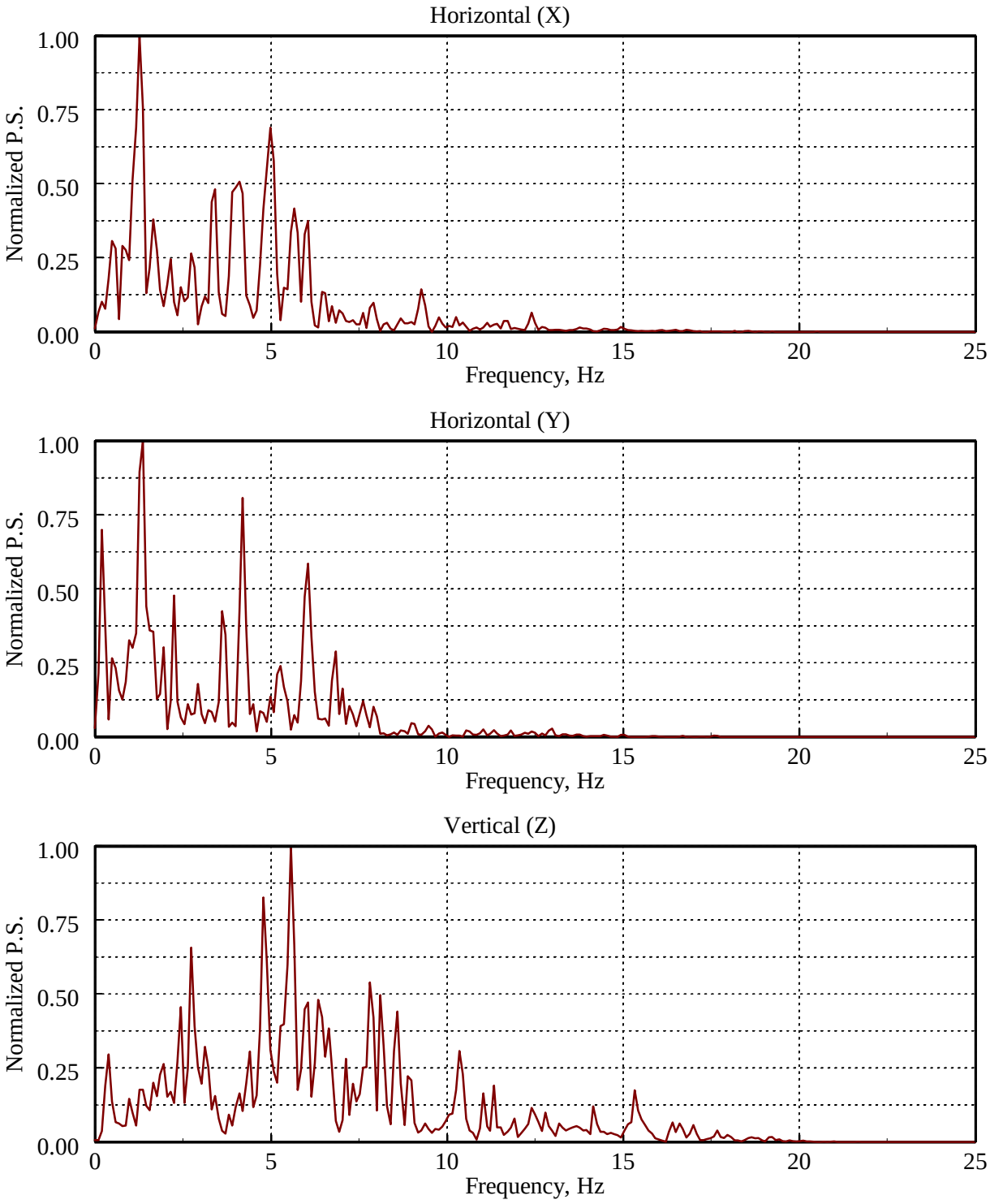

Figure 3-5 Power spectra for normalized acceleration histories, Tabas record

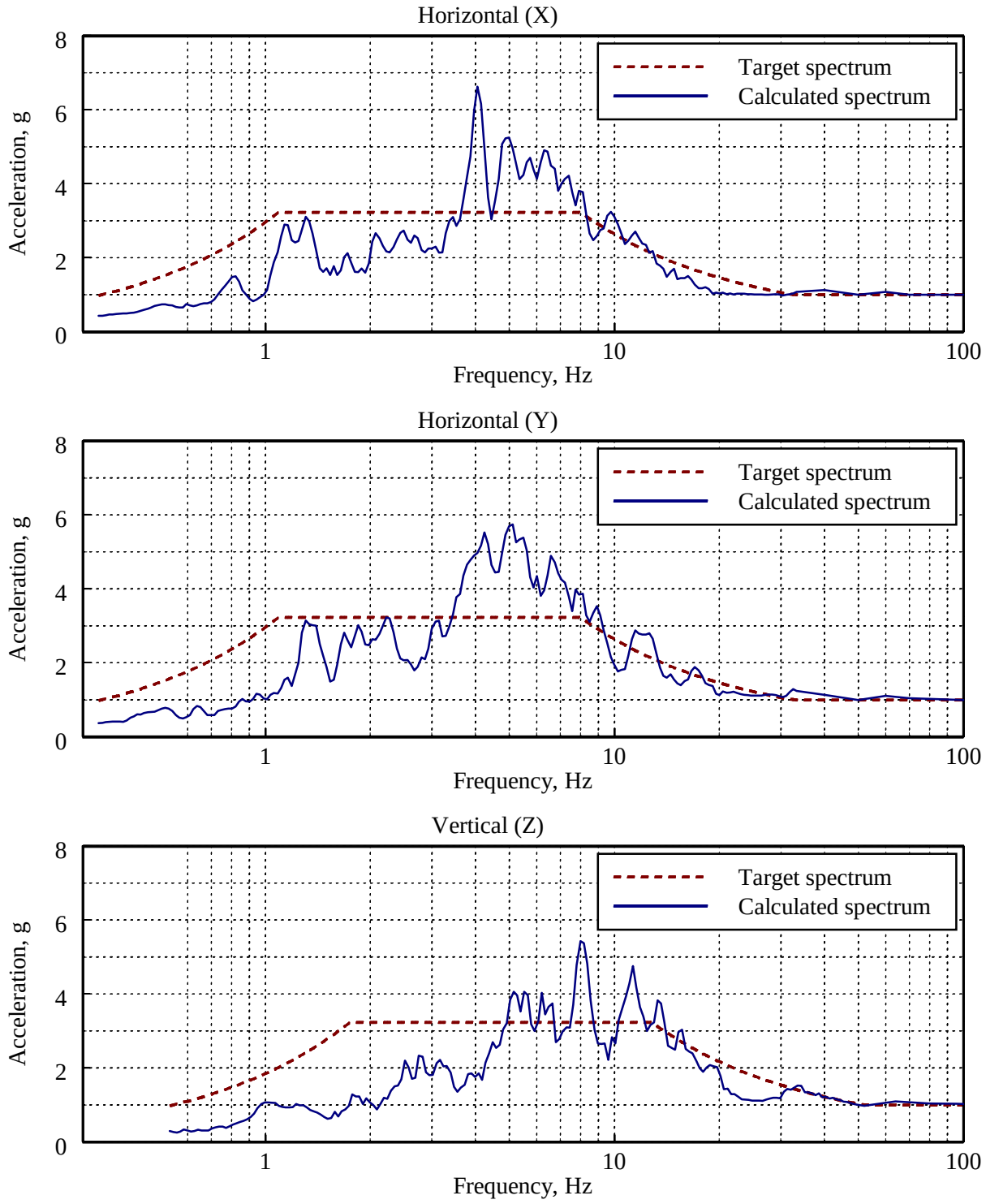

Figure 3-6 Response spectra for normalized acceleration histories, Tabas record

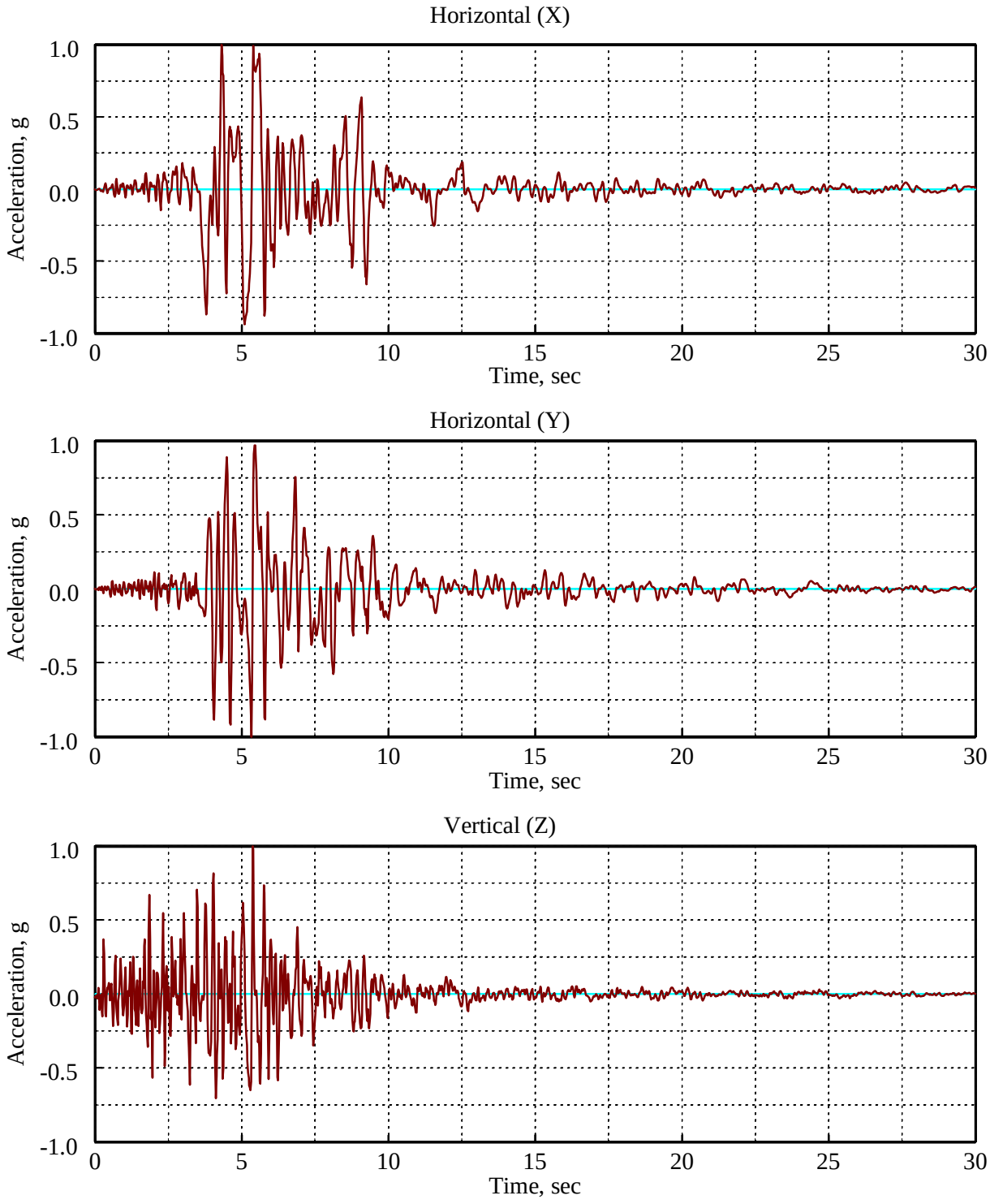

Figure 3-7 Normalized acceleration histories, Newhall record

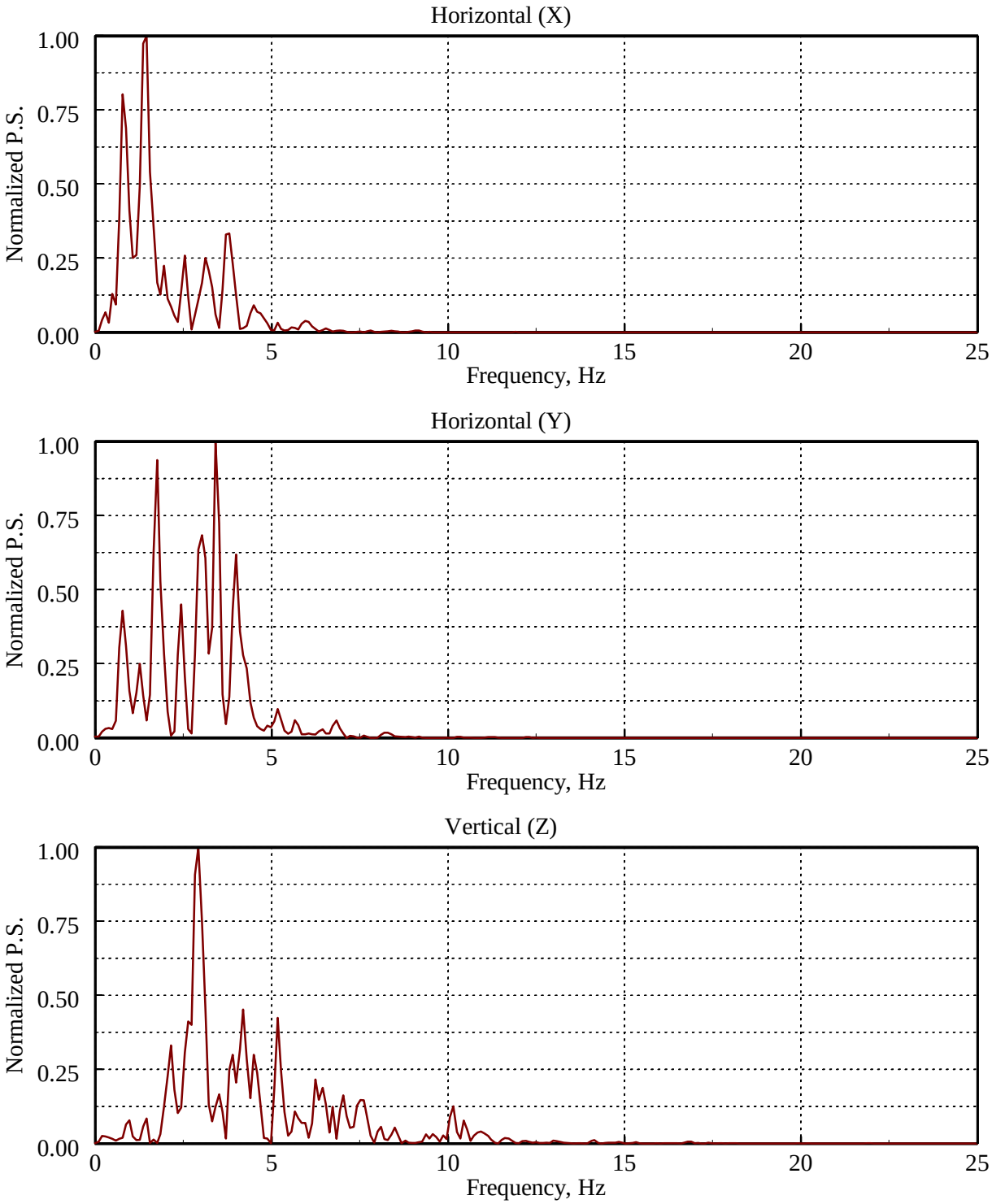

Figure 3-8 Power spectra for normalized acceleration histories, Newhall record

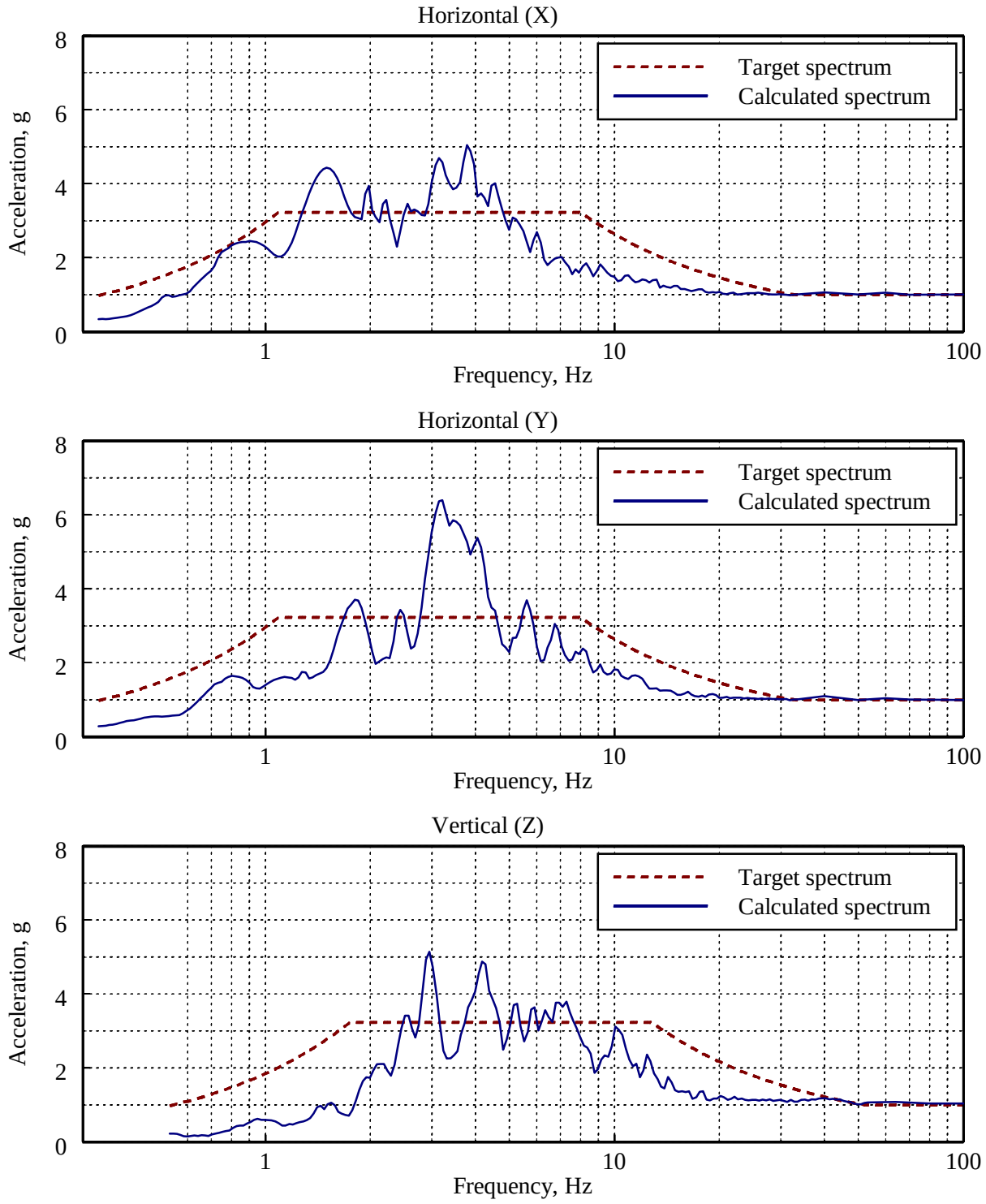

Figure 3-9 Response spectra for normalized acceleration histories, Newhall record

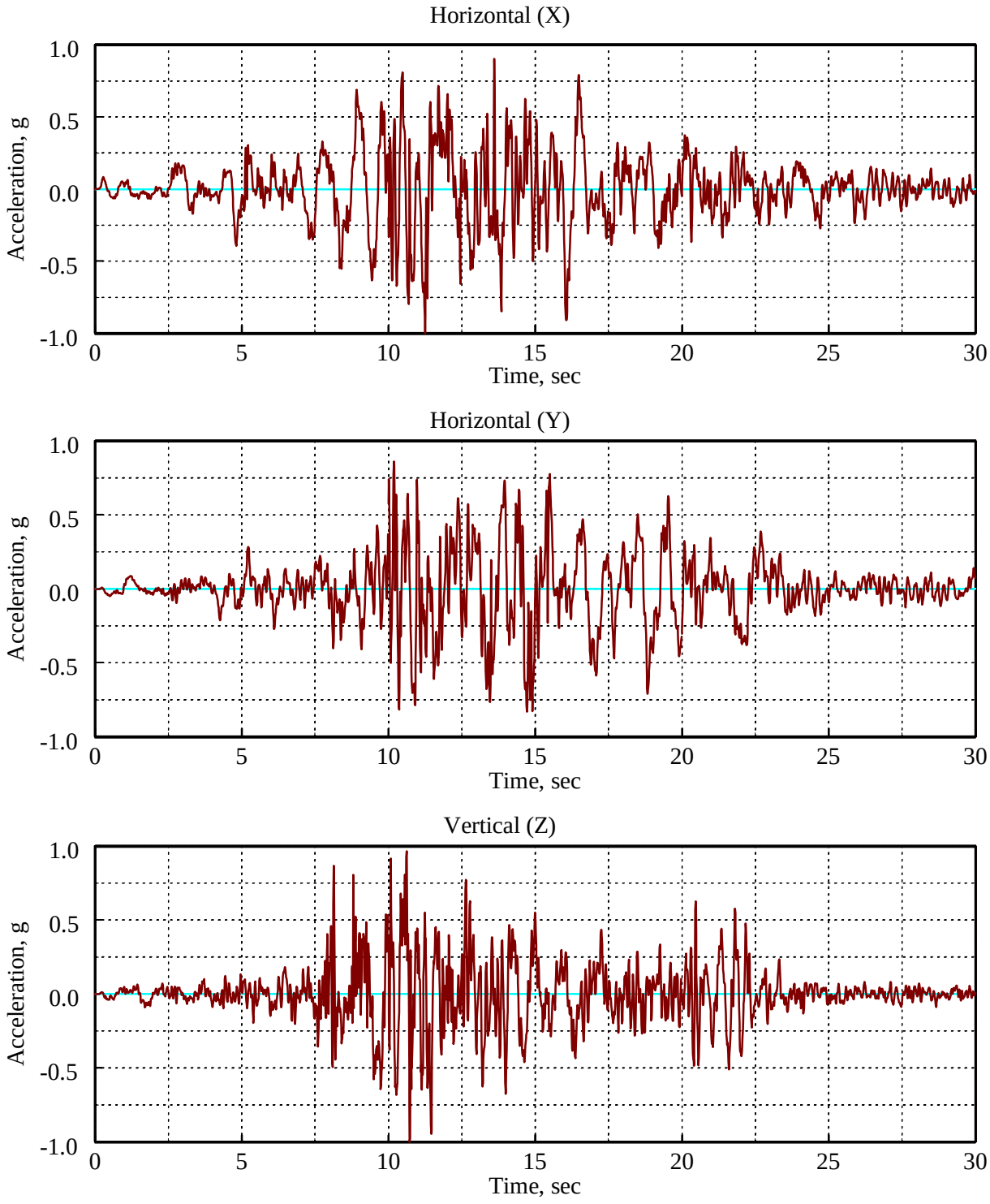

Figure 3-10 Spectrum-compatible, normalized acceleration histories, Tabas record

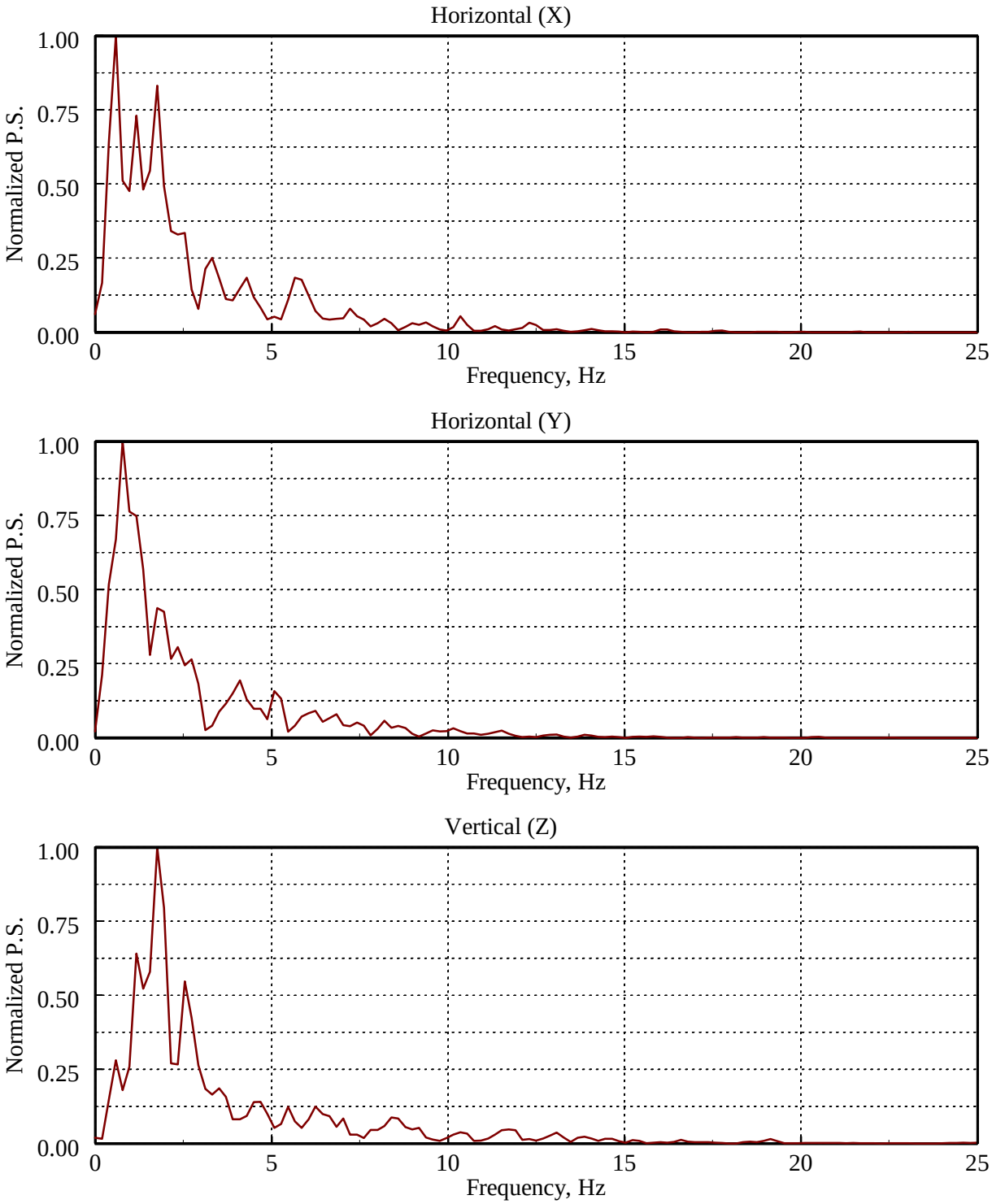

Figure 3-11 Power spectra for spectrum-compatible, normalized acceleration histories, Tabas record

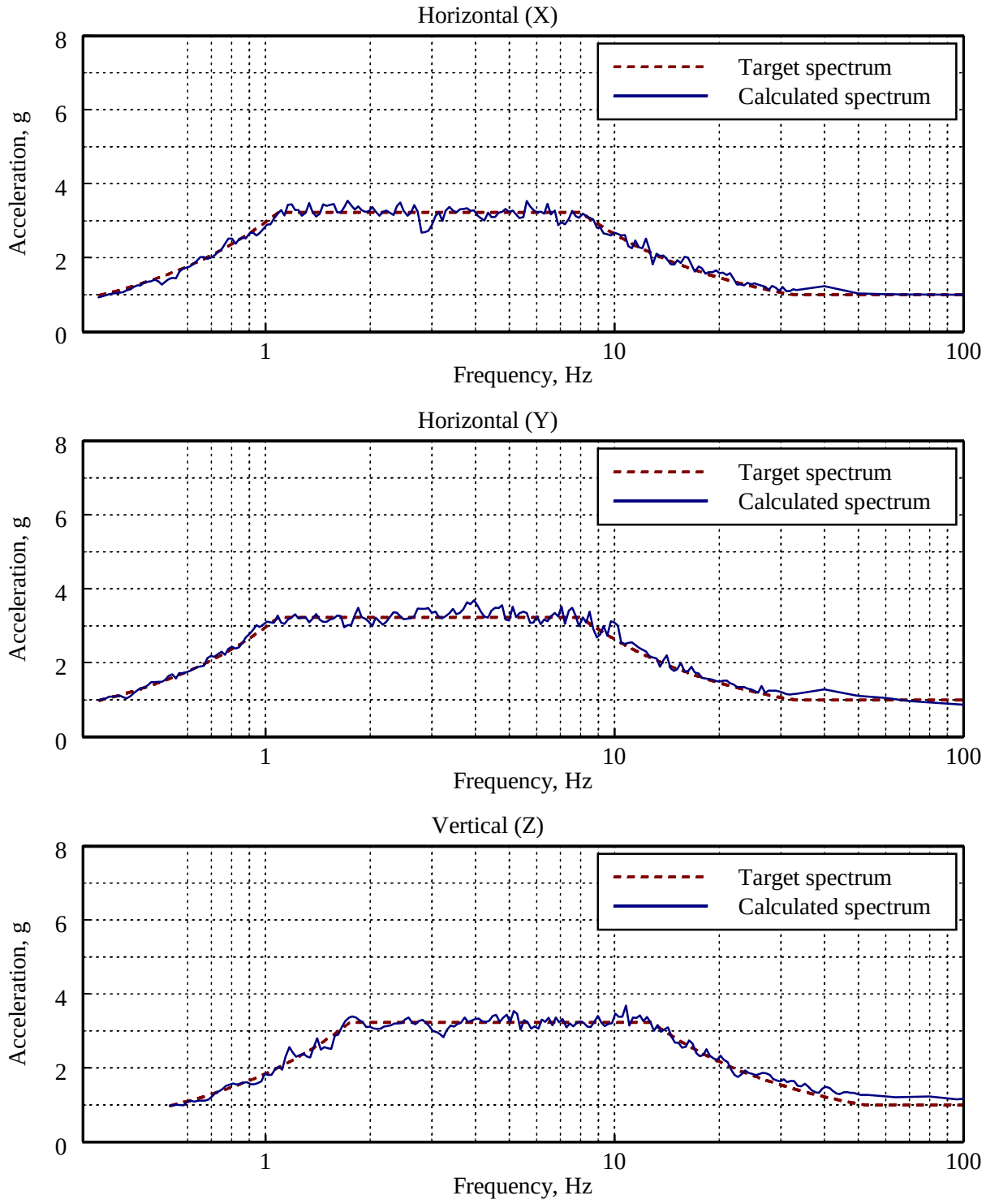

Figure 3-12 Response spectra for spectrum-compatible, normalized acceleration histories, Tabas record

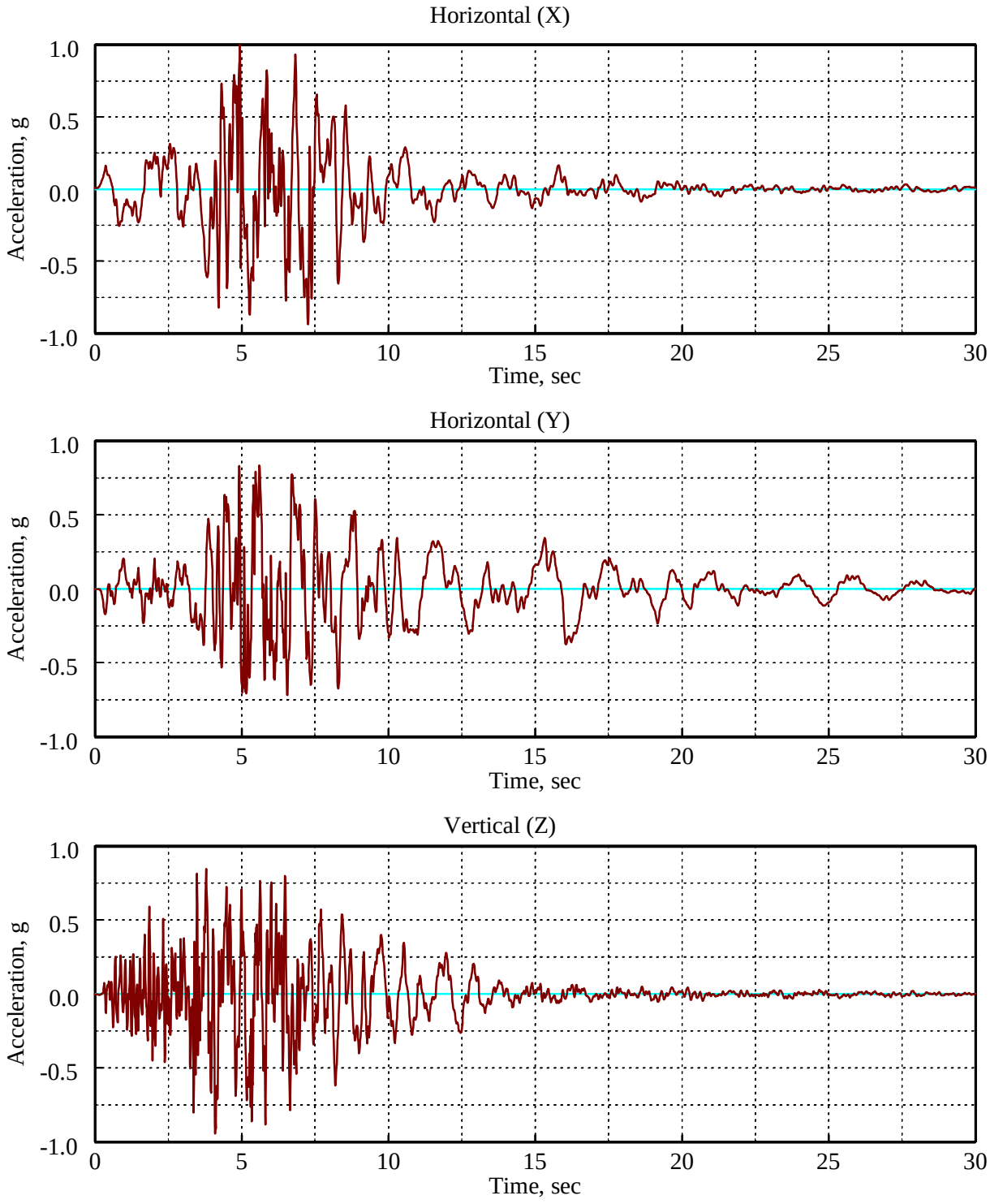

Figure 3-13 Spectrum-compatible, normalized acceleration histories, Newhall record

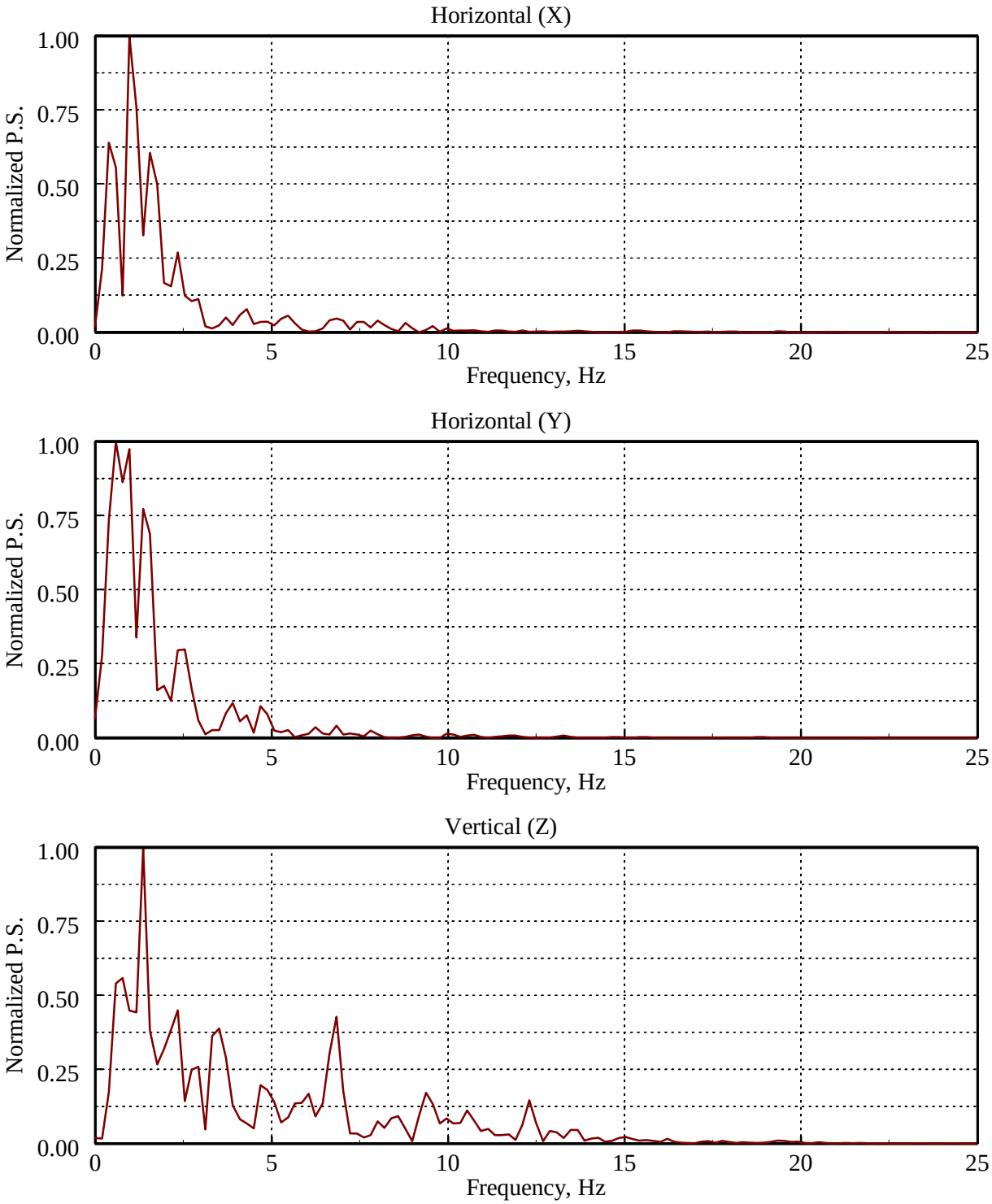

Figure 3-14 Power spectra for spectrum-compatible, normalized acceleration histories, Newhall record

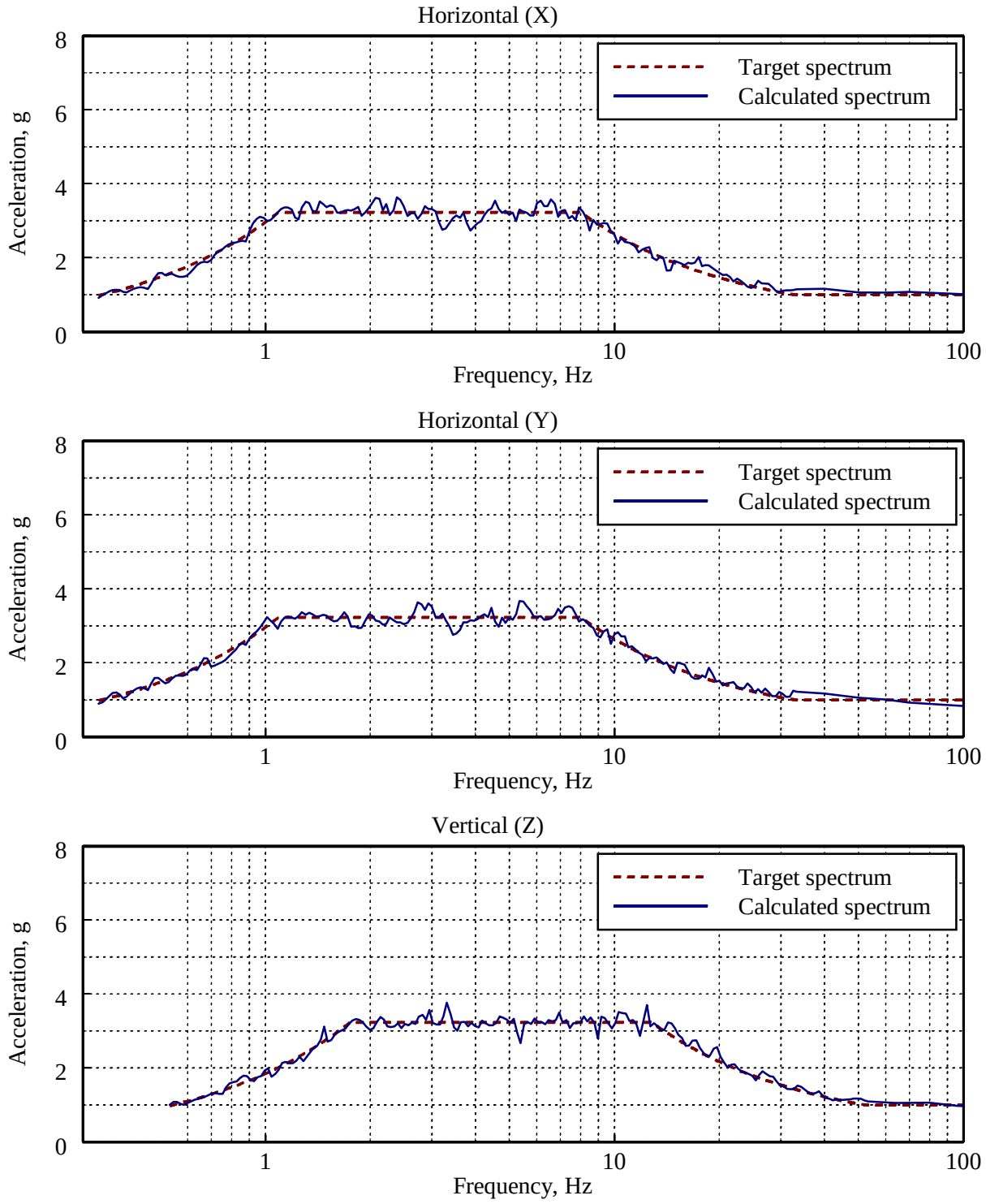

Figure 3-15 Response spectra for spectrum-compatible, normalized acceleration histories, Newhall record

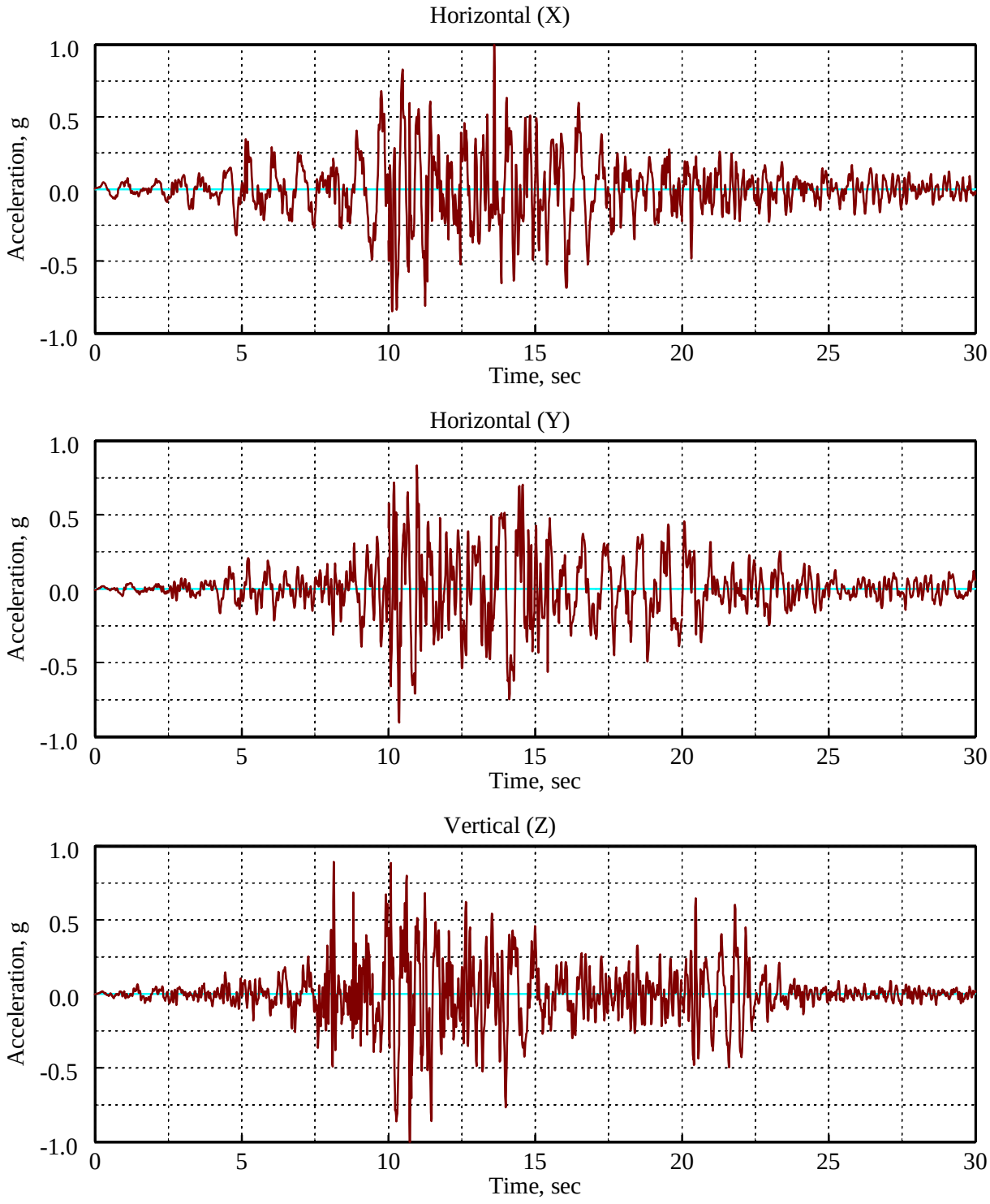

Figure 3-16 High-pass filtered, spectrum-compatible, normalized acceleration histories, Tabas record

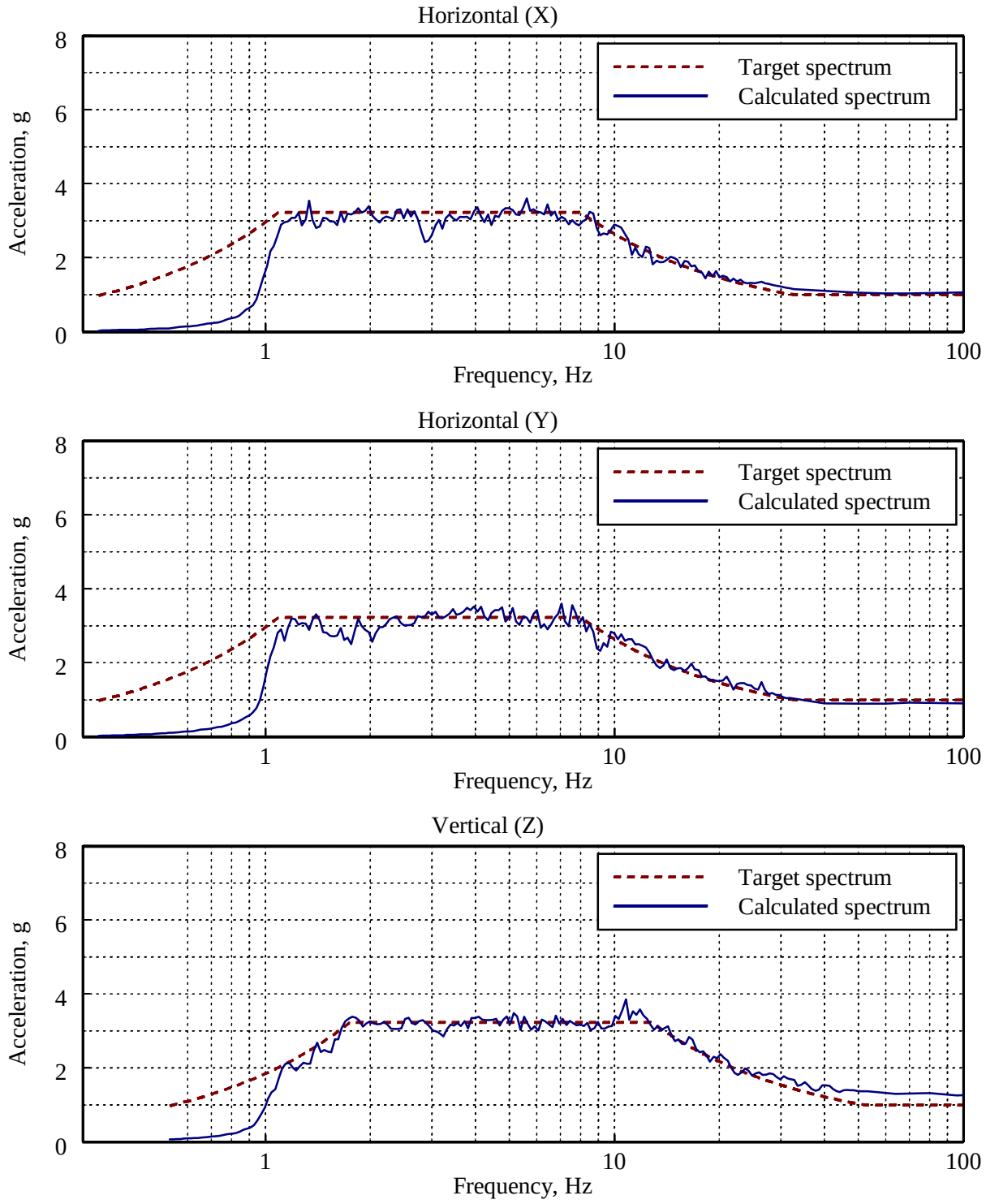

Figure 3-17 Response spectra for high-pass filtered, spectrum-compatible, normalized acceleration histories, Tabas record

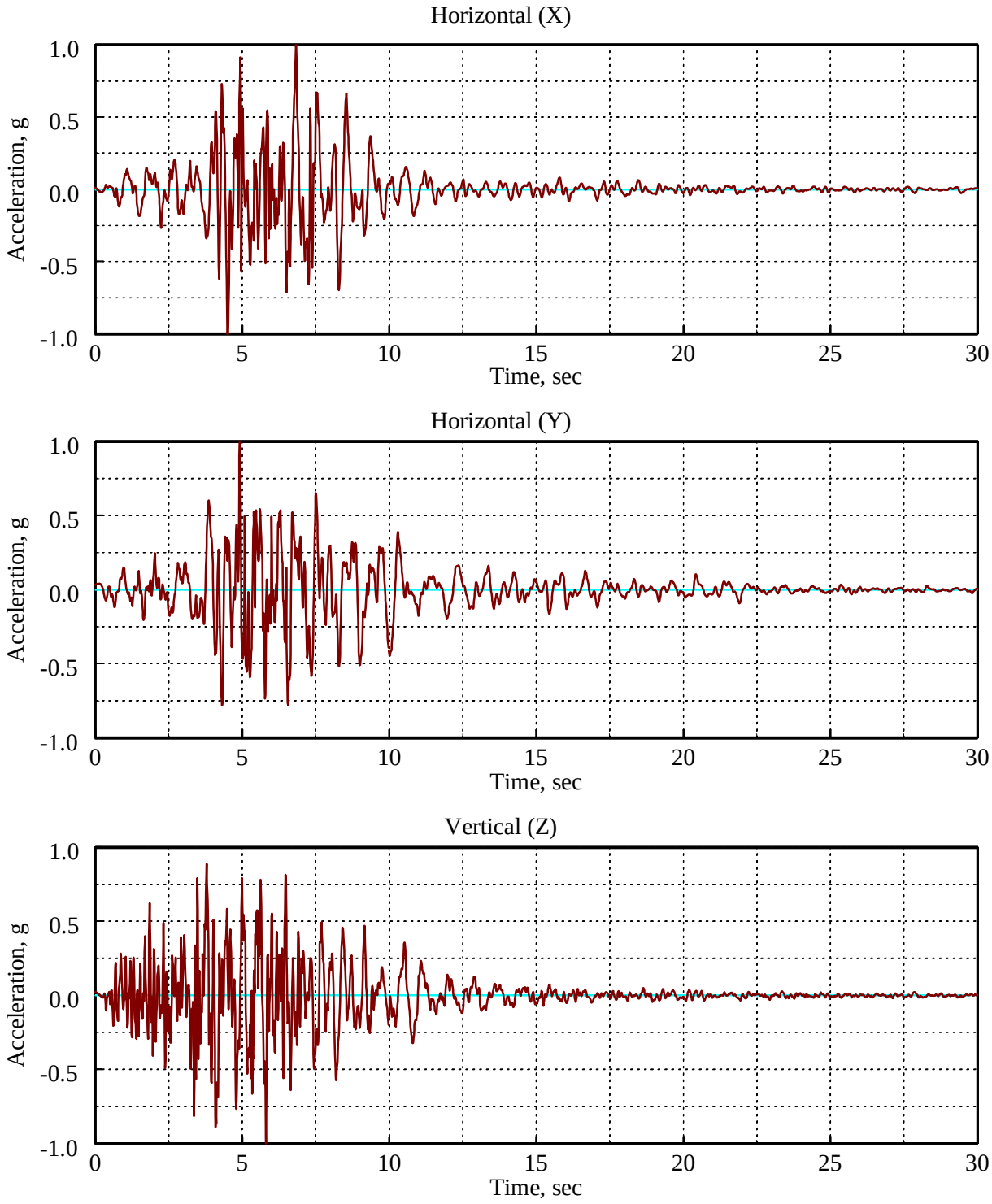

Figure 3-18 High-pass filtered, spectrum-compatible, normalized acceleration histories, Newhall record

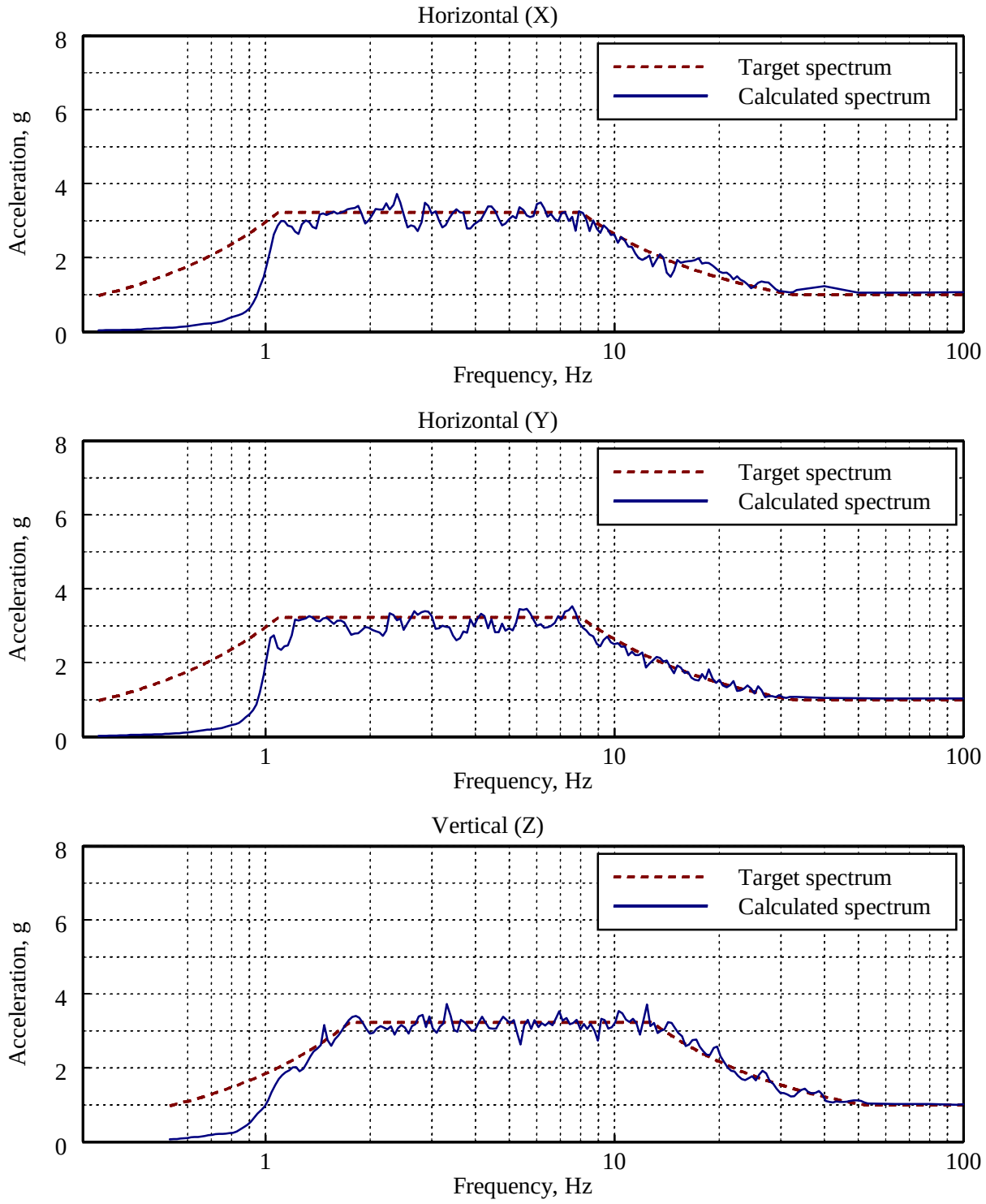

Figure 3-19 Response spectra for high-pass filtered, spectrum-compatible, normalized acceleration histories, Newhall record

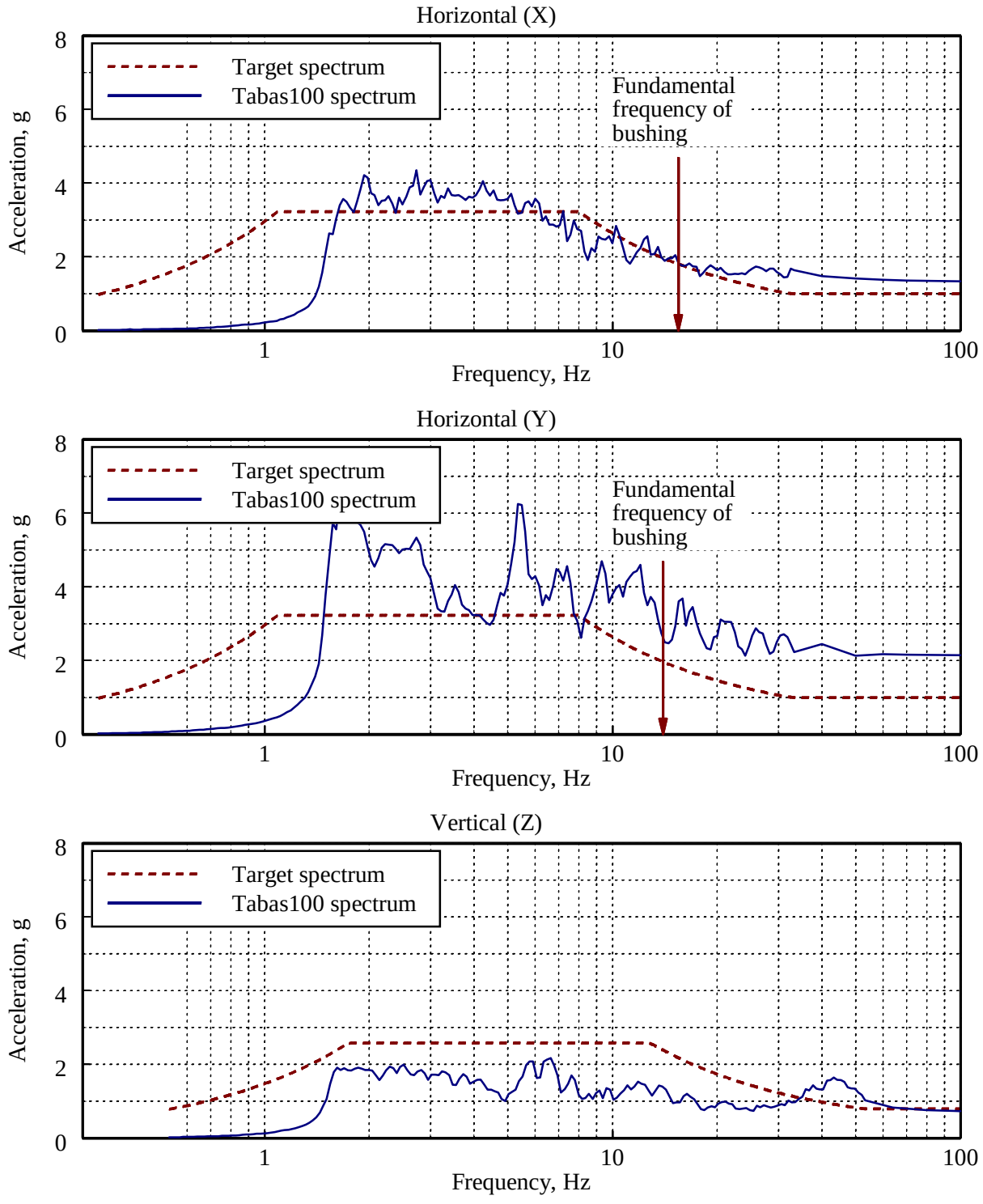

Figure 3-20 Response spectra, Test Number 8, Tabas100, Moderate Level qualification of Bushing-1

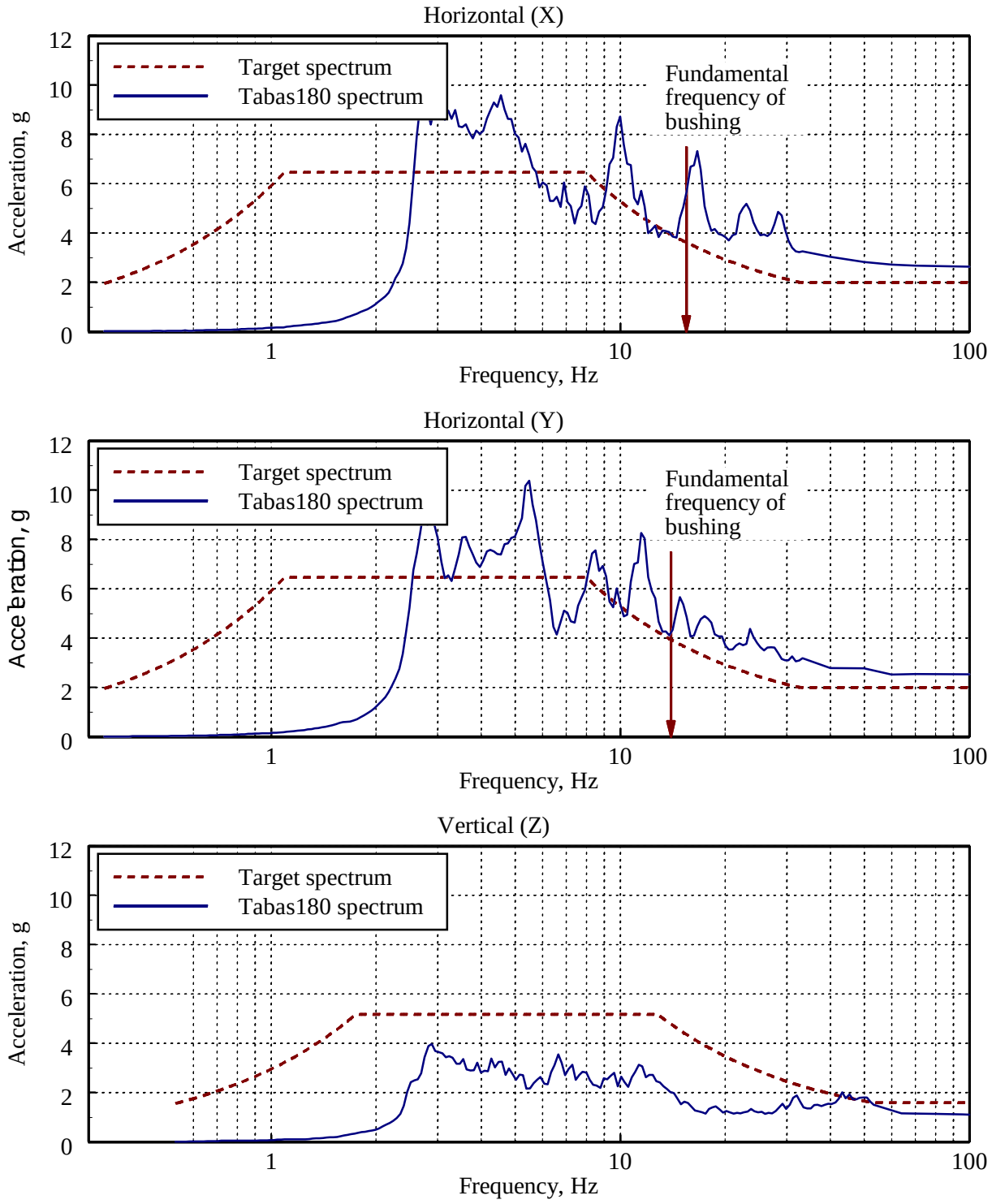

Figure 3-21 Response spectra, Test Number 21, Tabas180, fragility testing of Bushing-2

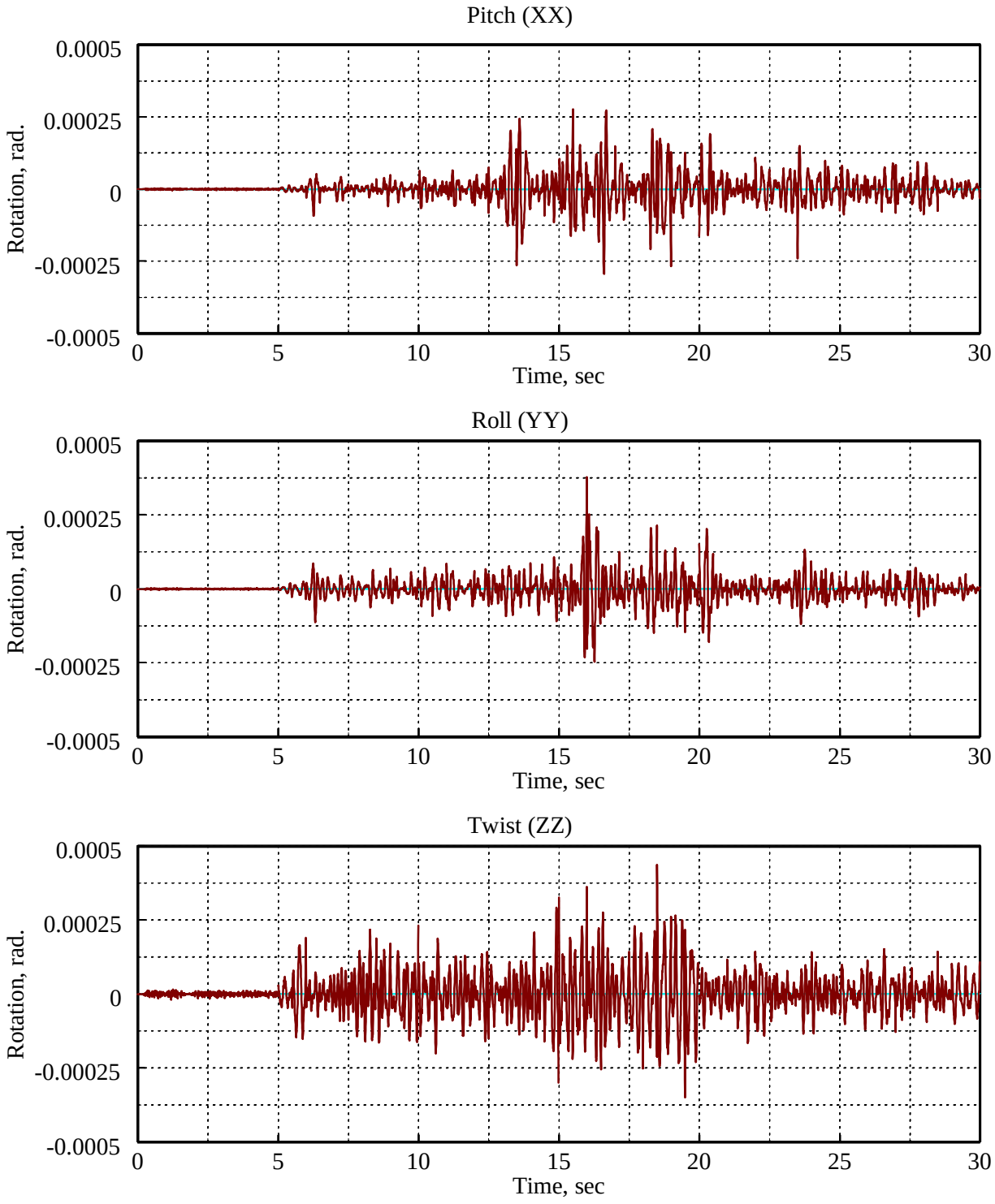

Figure 3-22 Rigid body rotational response of the earthquake-simulator platform, Tabas180

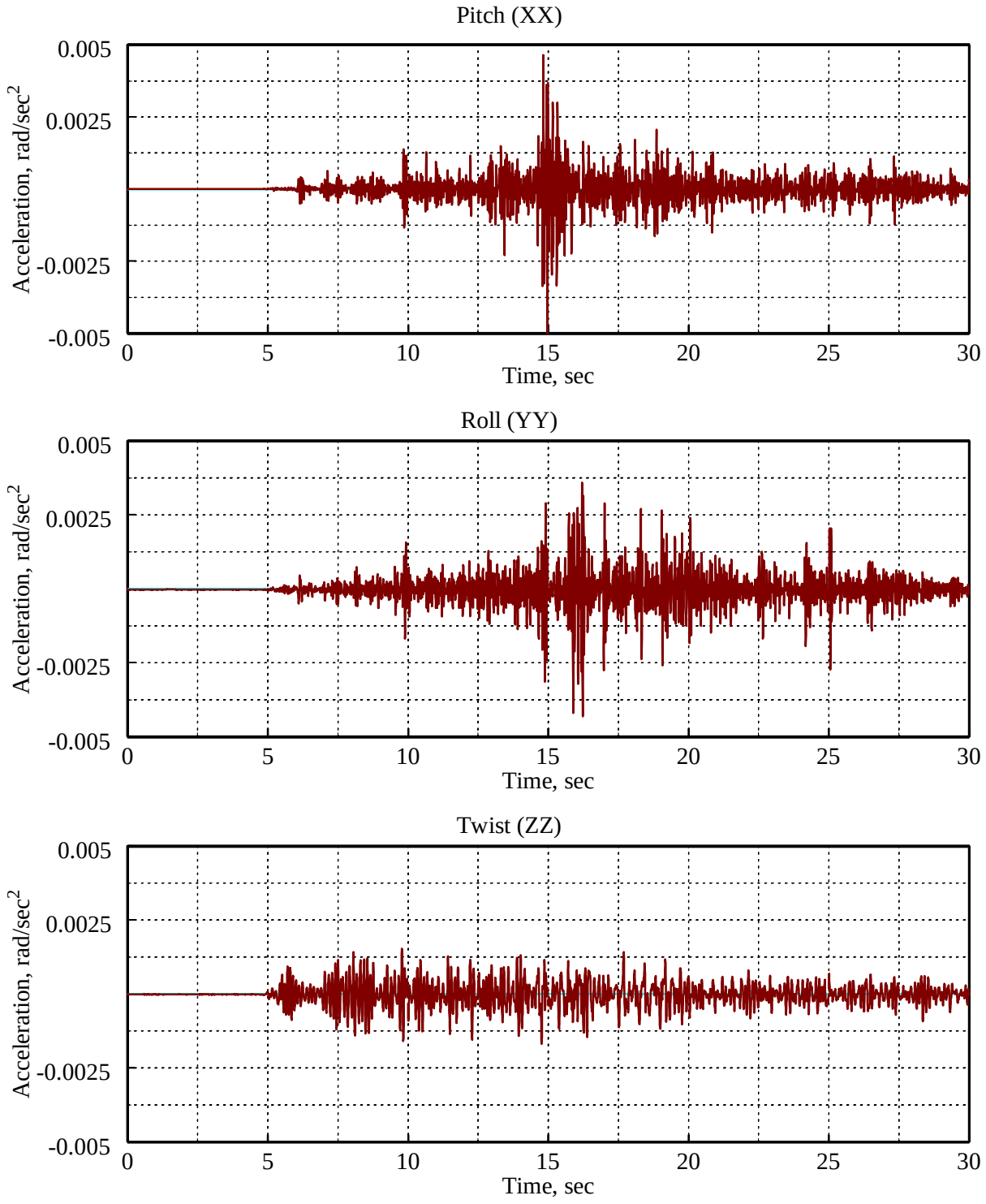

Figure 3-23 Response histories of earthquake-simulator platform rotational accelerations, Tabas180

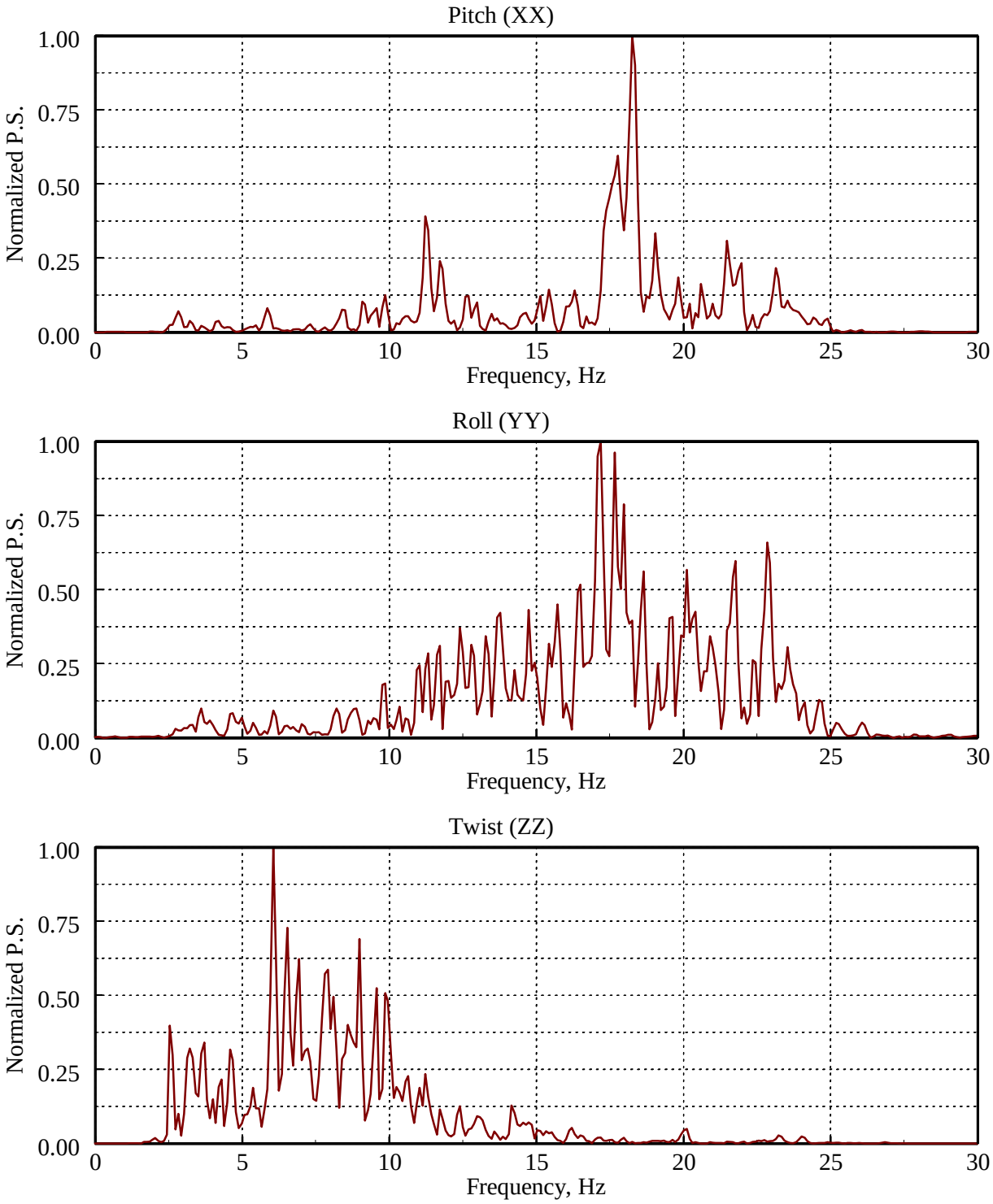

Figure 3-24 Power spectra of response histories of earthquake-simulator platform rotational accelerations, Tabas180

CHAPTER 4
SUMMARY OF EXPERIMENTAL DATA

4.1 Overview

The objectives of the testing program were to evaluate the seismic behavior of 196 kV transformer bushings, to qualify Bushing-1 to the Moderate Level, and to test Bushing-2 to failure. For testing, each bushing was installed in the rigid mounting frame described in Section 2.3. A photograph of Bushing-1 installed in the mounting frame is presented in Figure 4-1.

The following sections summarize results from the compression testing of porcelain cylinders and nitrile rubber gaskets (Section 4.2), the dynamic testing of the bushings (Section 4.3), and the earthquake testing of Bushing-1 and Bushing-2 (Section 4.4).

4.2 Testing of Porcelain Cylinders and Nitrile Rubber Gaskets

4.2.1 Porcelain cylinders

IEEE 693 states that the maximum stress in porcelain components of a transformer bushing shall not exceed 50 percent of the ultimate value during earthquake shaking associated with the Test Response Spectrum (TRS). To determine the stress-strain characteristics of the porcelain insulators, two porcelain cylinders were individually tested in uniaxial compression. The porcelain cylinders, supplied by Asea Brown Boveri (ABB), were 9.65 inches (245 mm) long, had an outside diameter of 3.15 inches (80 mm), and an inside diameter of 2.22 inches (56 mm). The stress-strain relation for one of the cylinders is shown in Figure 4-2a. The ultimate compression strain for the porcelain is approximately 4000E-6 in/in. Young's modulus for the porcelain is approximately 14,200 ksi (98 GPa).

4.2.2 Nitrile rubber gaskets

One flat nitrile rubber gasket with an outside diameter of 11.79 inches (299 mm), an inside diameter of 9.97 inches (253 mm), and a thickness of 0.238 inches (6 mm) was tested in uniaxial compression to determine its stress-strain characteristics. The rubber gasket was supplied by ABB and was identical to one of the three types of gasket used in the construction of Bushing-1 and Bushing-2. The stress-strain relation for the gasket is shown in Figure 4-2b. (A similar relation is reported by the manufacturer for a 6-inch (152 mm) long, 1-inch wide gasket.) The nominal precompression on the gasket under operating conditions is approximately 0.870 ksi (= 27 kips/31.10 sq. in). The tangent compression modulus for the gasket at this contact pressure is approximately 9.4 ksi (65 MPa).

4.3 Dynamic Properties of the 196 kV Bushings

Sine-sweep and white-noise tests were used to assess the modal frequencies and modal damping ratios for each bushing. Both of these tests involve running the earthquake simulator. The simulator is a dynamic mechanical system: the oil columns in the servoactuators have finite stiffness and damping. Detailed analysis of the results of the resonant search tests should consider the flexibility and damping of the simulator. Although the modal frequencies of the bushing alone will likely not be altered by the flexibility of the simulator, the modal damping ratios of the bushing will be overestimated by resonant search testing.

The results of the resonant search tests were checked by impact (hammer) and pull-back tests. The impact tests involved hitting the upper tip of the bushing and monitoring its free-vibration history using accelerometers. For these tests, the earthquake simulator was locked in position. The pull-back tests were conducted by ABB staff in their manufacturing facility. This test involved imposing a horizontal load of 500 lbs at the upper tip of the bushing, releasing the load, and monitoring the free-vibration history of the bushing.

Matlab (Mathworks, 1997) was used to process the experimental data. The data was zero-corrected, rotated to eliminate drift, and low-pass filtered with a cut-off frequency of 50 Hz. Figure 4-3 shows the transfer functions between the upper tip of the bushing and the mounting frame in the three local directions (*x, y, z*) of the bushing using data from Test Numbers 1, 2, and 3. The resonant frequencies in the local *x*- and *y*-directions are each approximately 15 Hz. Damping ratios of between 2 and 3 percent of critical were obtained using the half-power bandwidth method.

Table 4-1 summarizes the measured dynamic properties of the bushings. Modal data could not be determined for the local *z*-direction. The bushing is slightly stiffer in the local *x* direction due to the lifting lugs on the bushing flange (see Figure 4-4). The properties of the bushings did not change appreciably over the course of the testing program.

Table 4-1 Modal properties of the bushings

			Frequency Hz		*Damping Ratio % of critical*	
Test Number	*Test Type*	*Bushing*	*x direction*	*y direction*	*x direction*	*y direction*
1, 2, 3	White Noise	1	15.6	14.1	2.8	3.0
4, 5, 6	Sine Sweep	1	15.8	14.1	2.6	2.5
23, 24, 25	White Noise	2	15.4	14.0	3.6	3.9
After 25	Hammer	2	15.6	14.0	NA	NA
NA	Pull-back		NA	14.4	NA	2.5

1. NA = Not Applicable or Not Available

4.4 Earthquake Testing of Bushing-1 and Bushing-2

4.4.1 Introduction

The schedule of testing and key observations are presented in Table 4-2. After each earthquake test (Tabas*** or Newhall *** in Table 4-2), the response data were analyzed, the bushing was inspected for damage and oil seepage, and the bolts joining the bushing flange plate to the adaptor plate, and the adaptor plate to the mounting plate, were checked for tightness. All bolts that were found to be loose were retightened using a calibrated torque wrench.

No structural damage or oil seepage was observed prior to Test Number 22 (Tabas200) of Bushing-2. After this test, a tiny amount of oil was found on the aluminum flange-plate casting immediately below the gasket. Fragility testing was terminated following Test Number 22 so that the manufacturer could perform electrical testing and tear down the bushing to look for evidence of internal damage.

The following sub-sections present information on the peak responses of the mounting frame and the bushings; data related to the qualification and fragility testing of Bushing-1 and Bushing-2, respectively; and local response characteristics of the bushing as measured at the junction of the UPPER-1 porcelain unit and the flange plate.

4.4.2 Peak responses

The transducer response histories were processed using the computer program Matlab (Mathworks, 1997). The experimental histories were low-passed filtered with a cut-off frequency of 50 Hz, and zero-corrected as necessary.

The peak acceleration responses of the mounting frame and the bushings are presented in Tables 4-3 and 4-4, respectively. Only the peak responses at the upper tip of each bushing are reported; the maximum accelerations at the lower tip of the bushings were always less than those at the upper tip of the bushings.

A total of twelve transducers measured porcelain strain (channels 39 through 42), local radial motion of the UPPER-1 porcelain unit with respect to the flange plate (channels 43 through 46), and local vertical motion of the UPPER-1 porcelain unit with respect to the flange plate (channels 47 through 50). Maximum values, computed as the peak value of the four transducers, for porcelain strain, local radial motion, and local vertical motion, are presented in Table 4-4. The local radial motions include both slip of the flange plate over the adaptor plate and slip of the UPPER-1 porcelain unit over the flange plate.

4.4.3 Response of the mounting frame

The mounting frame was designed to be *rigid* and thus not amplify the motions of the earthquake simulator. Figure 4-5 shows the mounting frame-to-earthquake simulator transfer functions (in the X-, Y-, and Z-directions) calculated from the sine-sweep tests of Bushing-1 (Test Numbers 4 through 6). The mounting-frame accelerations were transformed into the global coordinate system

Table 4-2 Summary of earthquake testing program

Test No.	*Bushing*	*Identification*[1]	*Comments*
1	1	WN-X	
2	1	WN-Y	
3	1	WN-Z	
4	1	SS-X	
5	1	SS-Y	
6	1	SS-Z	
7	1	Tabas100[2]	
8	1	Tabas100	Moderate Level qualification test for Bushing-1
9	2	WN-X	
10	2	WN-Y	
11	2	WN-Z	
12	2	Tabas050	
13	2	Newhall050[3]	
14	2	Newhall080	Flange plate-to-adaptor plate bolts loose after test; bolts tightened to 100 ft-lbs
15	2	Tabas080	
16	2	Tabas100	Moderate Level qualification for Bushing-2
17	2	Newhall100	
18	2	Tabas120	
19	2	Tabas140	
20	2	Tabas160	
21	2	Tabas180	High Level qualification for Bushing-2; fragility test for Bushing-2
22	2	Tabas200	Minor oil seepage at the gasket immediately above the flange plate
23	2	WN-X	
24	2	WN-Y	
25	2	WN-Z	

1. WN = white noise, SS = sine sweep; -X, -Y, and -Z denote direction of testing
2. Tabas = Tabas earthquake histories; e.g., 050 denotes target peak acceleration of 50% of g
3. Newhall = Newhall earthquake histories

Table 4-3 Peak accelerations of the mounting frame

			Peak Acceleration (g)		
Test Number	*Bushing*	*Identification*	*x direction*[1]	*y direction*	*z direction*
7	1	Tabas100	0.6	2.0	1.1
8	1	Tabas100[2]	1.4	2.0	1.1
12	2	Tabas050	0.8	1.0	0.4
13	2	Newhall050	0.6	0.7	0.5
14	2	Newhall080	1.0	0.9	0.7
15	2	Tabas080	1.1	1.7	0.6
16	2	Tabas100[2]	1.4	1.8	0.8
17	2	Newhall100	1.4	1.1	1.0
18	2	Tabas120	2.0	2.1	1.1
19	2	Tabas140	2.4	2.3	1.0
20	2	Tabas160	2.6	2.4	1.1
21	2	Tabas180[3]	2.9	2.8	1.1
22	2	Tabas200	2.7	2.9	1.2

1. See Figure 2-3 for definition of the local coordinate system for the mounting frame
2. Moderate Level qualification test
3. High Level qualification test for Bushing-2; fragility test for Bushing-2

for these calculations. If the mounting frame were truly rigid, the transfer function would be flat with a value equal to 1.0 across the entire frequency range. The transfer functions show little amplification of motion in the frequency range of 0 to 10 Hz, but significant amplification of horizontal motion for frequencies between 10 and 20 Hz. The amplification of motion above 10 Hz is due to rotational accelerations of the simulator platform which produce translational accelerations in the mounting frame. The rotational accelerations of the simulator platform are related to the oil-column frequencies of the vertical actuators that support the platform: the pitch and roll frequencies of the simulator are in the range of 13 to 18 Hz.

4.4.4 Seismic qualification of Bushing-1 and Bushing-2

To satisfy the IEEE 693 requirements for Moderate Level qualification, the measured peak horizontal acceleration at the bushing flange is required to be 0.50g (see Appendix A). For this level of shaking, IEEE 693 states that the stresses in the porcelain components must be less than 50 percent of the ultimate stress, and the factor of safety against oil leakage must be greater than or equal to 2.0.

Table 4-4 Peak acceleration responses of the upper tip of the bushings

			Peak Acceleration Response (g)		
Test Number	*Bushing*	*Identification*	*x-direction*[1]	*y-direction*	*z-direction*
7	1	Tabas100	1.7	3.6	1.1
8	1	Tabas100[2]	3.6	3.4	1.1
12	2	Tabas050	3.3	2.7	0.4
13	2	Newhall050	2.1	2.2	0.6
14	2	Newhall080	2.8	2.7	0.7
15	2	Tabas080	2.9	3.8	0.6
16	2	Tabas100[2]	3.7	3.7	0.8
17	2	Newhall100	3.1	2.7	0.7
18	2	Tabas120	4.7	4.5	1.1
19	2	Tabas140	5.2	5.0	1.0
20	2	Tabas160	5.0	5.3	1.1
21	2	Tabas180[3]	5.3	6.0	1.1
22	2	Tabas200	5.3	6.4	1.2

1. See Figure 2-3 for definition of the local coordinate system for the bushings
2. Moderate Level qualification test
3. High Level qualification test for Bushing-2; fragility test for Bushing-2

An alternate approach that is identified in Annex D5.1(d) of IEEE 693 was used to qualify Bushing-1. Namely, earthquake histories with spectral ordinates twice those of the Test Response Spectrum were used for testing: the target peak horizontal acceleration at the bushing flange was 1.0g. Porcelain stresses at this level of earthquake shaking were required to be less than or equal to the ultimate value, and there was to be no evidence of oil leakage. Test Number 8 (Tabas100) was therefore used for the Moderate Level Qualification of Bushing-1. Figure 4-6 shows the measured spectra in the local (*x*, *y*, *z*) and global (X, Y, Z) coordinate systems and the target spectrum (anchored to a peak horizontal acceleration of 1.0g) for 2-percent damping. The spectral ordinates associated with longitudinal and lateral response histories of the mounting frame in the local co-ordinate system exceed those of the target spectrum in the frequency range of interest (10 to 20 Hz). The spectral ordinates associated with the vertical motion (local *z*-direction) of the mounting frame are approximately equal to those of the target spectrum for frequencies between 10 and 20 Hz. Given that a) the maximum porcelain strains were less than the ultimate strain ($34.9\mu\varepsilon$ versus $4000\mu\varepsilon$), and b) there was no evidence of oil leakage, *Bushing-1 was qualified by test to the Moderate Level.*

Table 4-5 Peak responses of UPPER-1 porcelain unit

			Maximum response		
Test Number	*Bushing*	*Identification*	*Porcelain strain (με)*	*Radial motion (inches/1000)*	*Vertical motion (inches/1000)*
7	1	Tabas100	25.6	12	10
8	1	Tabas100[2]	34.9	13	10
12	2	Tabas050	30.6	17	9
13	2	Newhall050	19.1	11	6
14	2	Newhall080	26.6	13	8
15	2	Tabas080	41.6	22	11
16	2	Tabas100	48.0	20	11
17	2	Newhall100	27.7	15	12
18	2	Tabas120	64.0	22	13
19	2	Tabas140	74.0	27	16
20	2	Tabas160	64.8	28	18
21	2	Tabas180	86.0	42	26
22	2	Tabas200	80.0	95	42

Qualification of transformer bushings at the High Level requires the use of earthquake histories with spectral ordinates twice those of the target spectrum described in the previous paragraph. Using a target peak acceleration for these histories of 2.0g, a bushing would be qualified at the High Level if the porcelain stresses were less than the ultimate value and there was no evidence of oil leakage.

Fragility testing of Bushing-2 used severe earthquake shaking histories as input to the earthquake simulator. Consider the measured spectra in the local (*x, y, z*) and global (X, Y, Z) coordinate systems and the target spectrum (anchored to a peak horizontal acceleration of 2.0g) for Test Number 21 (Tabas180) as shown in Figure 4-7. The spectral ordinates associated with longitudinal and lateral response histories of the mounting frame in the local coordinate system substantially exceed those of the target spectrum in the frequency range of interest (10 to 20 Hz). The spectral ordinates associated with the vertical motion of the mounting frame (local *z*-direction) are slightly less than those of the target spectrum. Given that a) the maximum porcelain strains were less than the ultimate strain (86.0με versus 4000με), and b) there was no evidence of oil leakage, *Bushing-2 was qualified by test to the High Level.*

The bushings were attached to the adaptor plate with torqued Grade 2 stainless steel bolts placed in over-sized, open-ended, slotted holes in the flange plate. This type of connection is used to join a bushing to a transformer. During earthquake testing, the bushing flange plate slipped with respect to the adaptor plate on a number of occasions; these bolts were checked and re-torqued to 100 ft-lbs. as necessary after each test.

4.4.5 Fragility testing of Bushing-2

Fragility curves for electrical equipment are often developed using information from testing programs such as the program described in this report. If a limiting state of response for a transformer bushing is oil leakage, Bushing-2 reached this limit state at a peak horizontal acceleration (in the local coordinate system) of 2.7g.

4.4.6 Bushing response characteristics

Global response

Test Number 21, Tabas180, was used to qualify Bushing-2 to the High Level. It is instructive to review the response of the 196 kV bushing during this severe shaking. Figure 4-8 shows the translational motions (global X- and Y-directions) of the upper tip of Bushing-2 relative to the mounting frame. The maximum relative displacement between the bushing and the mounting frame was 0.50 inches (13 mm). Figure 4-9 shows the total acceleration response of the upper tip of the bushing; the maximum total acceleration exceeded 6.0 g.

Response of UPPER-1 porcelain unit

Figure 4-10 shows the vertical displacement of the porcelain unit UPPER-1 relative to the flange plate, as measured at four locations around the circumference of the bushing during the last earthquake shaking test of Bushing-2 (Tabas200). A schematic plan view of the bushing showing the location of the four channels is included in the figure; see also Figure 2-3. The Tabas200 test (Test Number 22) damaged the bushing: minor oil leakage from the gasket immediately above the flange plate was discovered following the test.

Experimental studies at ABB have indicated that oil will leak from the bushing if the relative vertical displacement across the gasket exceeds approximately 0.03 inch (0.8 mm). This limiting value is shown as a solid line in Figure 4-10. A relative displacement of 0.03 inch (0.8 mm) was reached only once during the Tabas200 test. Given that the duration of the *gasket opening* was extremely short, it is not surprising that the loss of oil was minuscule.

Figure 4-11a shows the relation between the average vertical displacement in the local *z* direction and rocking about the local *y* axis. The average vertical displacement in the *z* direction was calculated as one-half of the sum of the channel 47 and channel 49 displacements; the rocking about the local *y*-axis was calculated as the difference between the channel 47 and 49 displacements divided by the distance between these transducers (= 24 inches). Figure 4-11b shows the relation between the average vertical displacement in the local *z* direction and rocking about the local *x*-axis. The average vertical displacement in the *z* direction was calculated as one-half of the sum of the channel 48 and channel 50 displacements; the rocking about the local *y* axis was calculated as the difference between the channel 48 and 50 displacements divided by the distance between these transducers (= 24 inches). Substantial rocking of UPPER-1 porcelain unit was accompanied by significant translation of the unit in the local *z*-direction.

Figure 4-12 shows the relative horizontal displacement (in the local coordinate system) of the UPPER-1 porcelain unit relative to the adaptor plate, measured at four locations around the circumference of the bushing, during the last earthquake shaking test of Bushing-2 (Tabas200). A schematic plan view of the bushing showing the location of the four transducers is included in the figure; see also Figure 2-3. The maximum relative horizontal displacement of the unit of approximately 0.1 inch (2.5 mm) coincided with the maximum relative vertical displacement of the unit with respect to the flange plate. The residual relative horizontal displacement was 0.02 inch (0.5 mm) in the negative local x-direction.

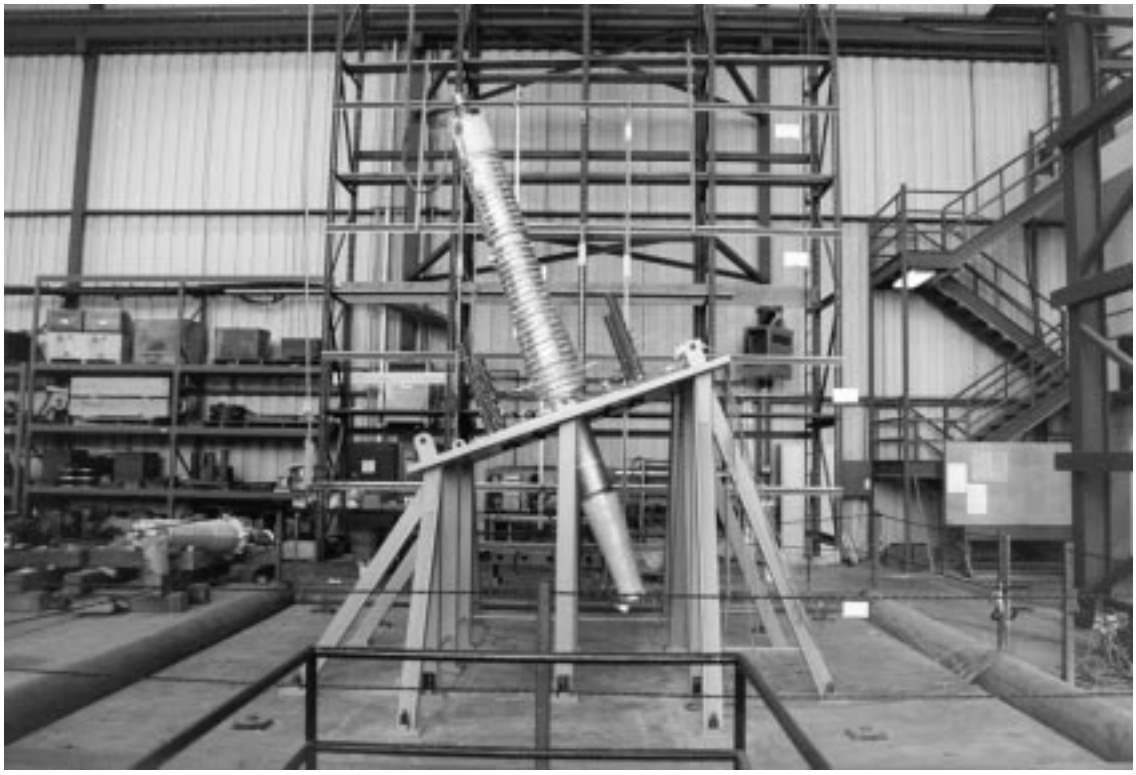

Figure 4-1 Photograph of Bushing-1 installed in the mounting frame prior to testing

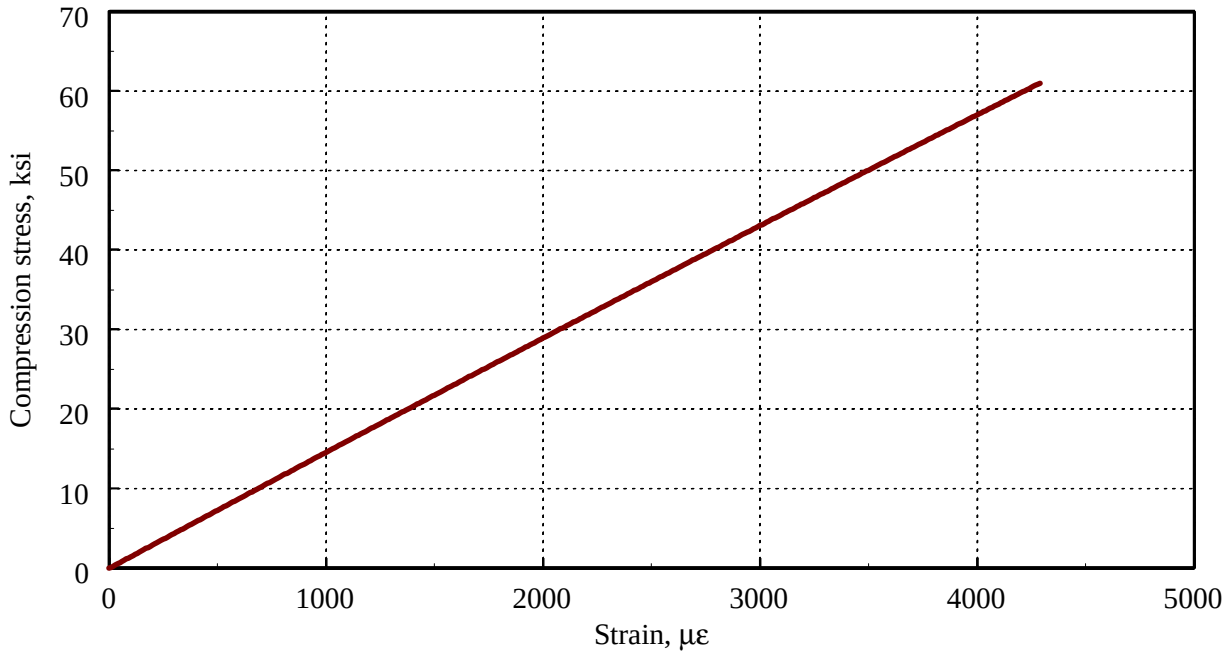

a. Porcelain cylinder

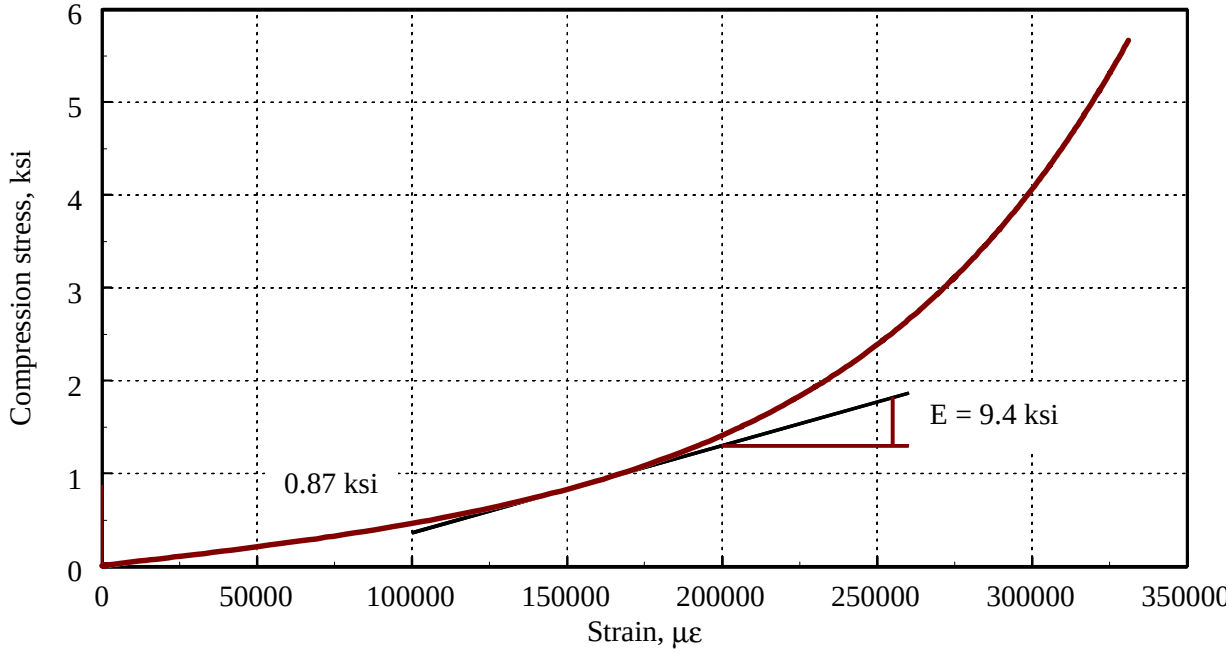

b. Nitrile rubber gasket

Figure 4-2 Stress-strain relations from compression testing of components of a bushing

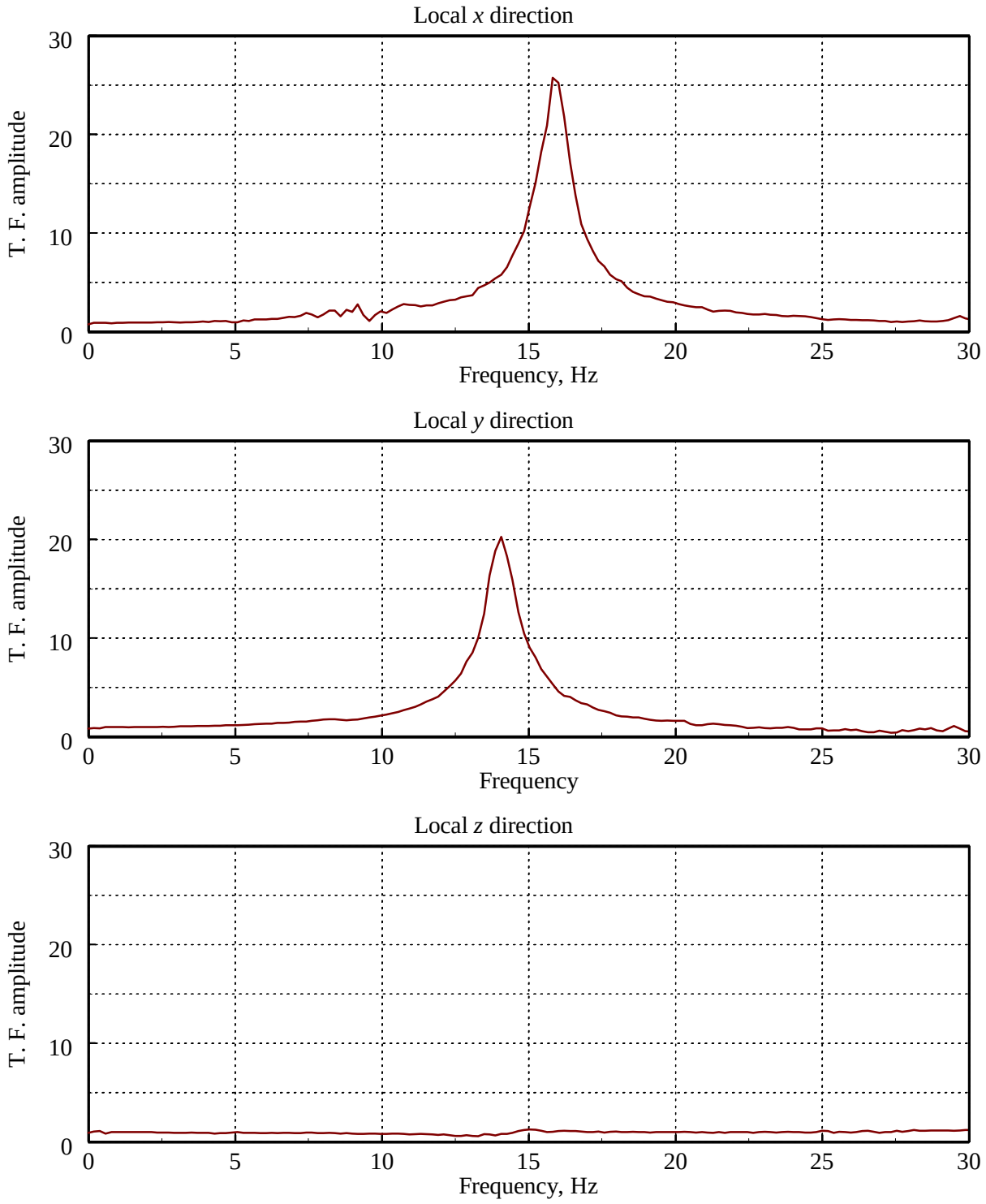

Figure 4-3 Bushing-to-mounting frame transfer functions for Bushing-1

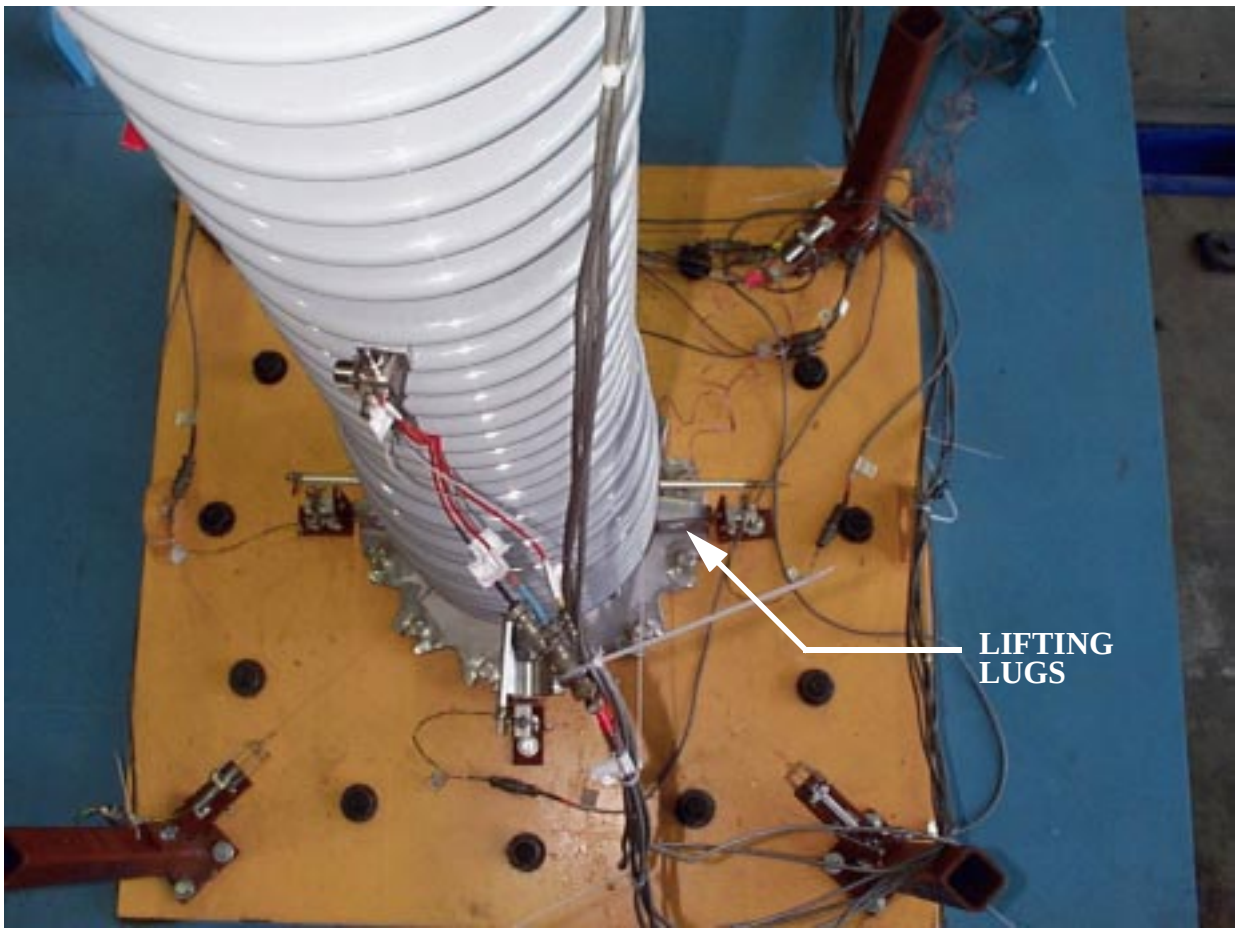

Figure 4-4 Bushing flange-to-adaptor plate connection showing lifting lugs

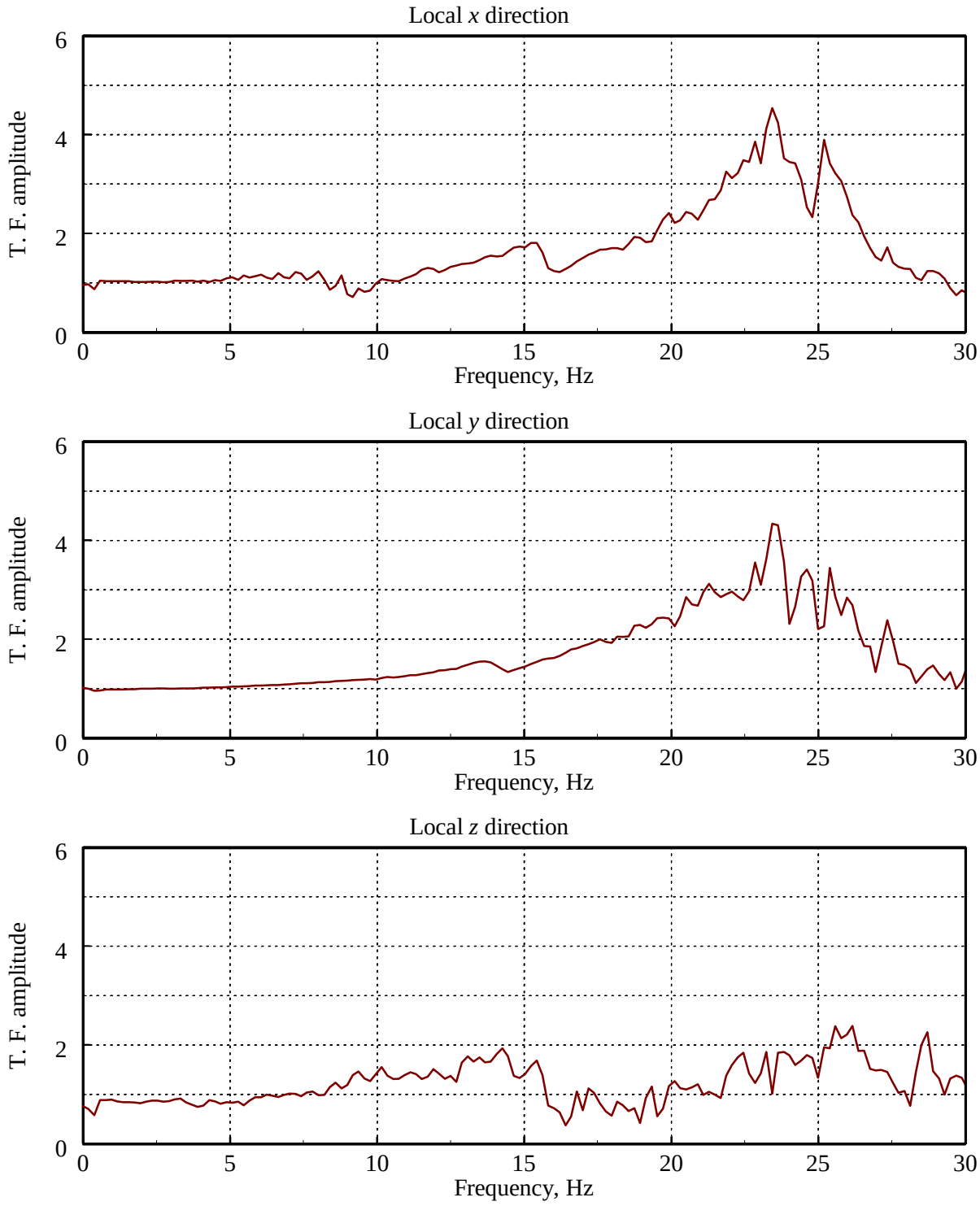

Figure 4-5 Mounting frame-to-earthquake simulator transfer functions for Bushing-1

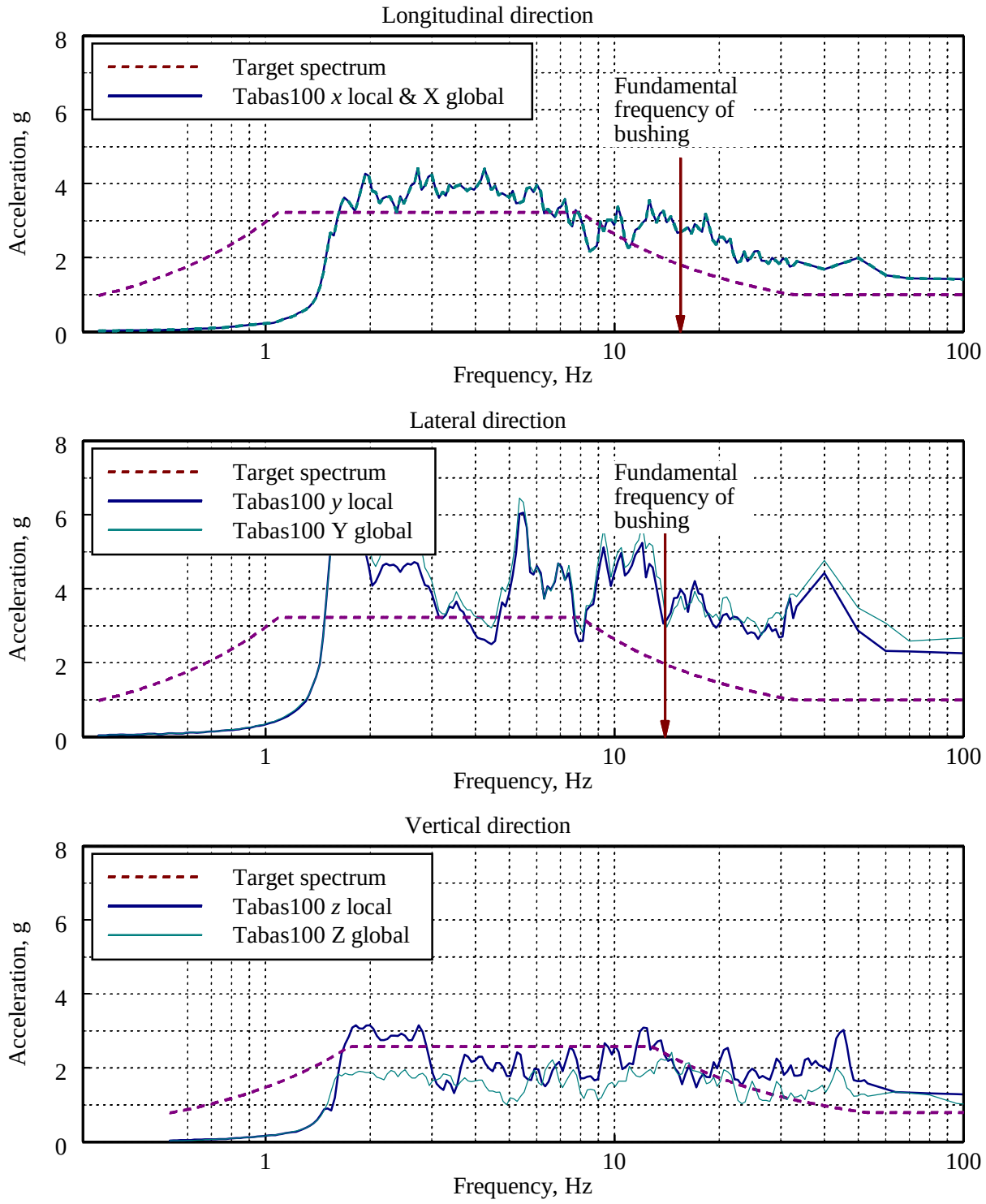

Figure 4-6 Response spectra (2-percent damping) for Bushing-1 Moderate Level qualification test (Test Number 8: Tabas100)

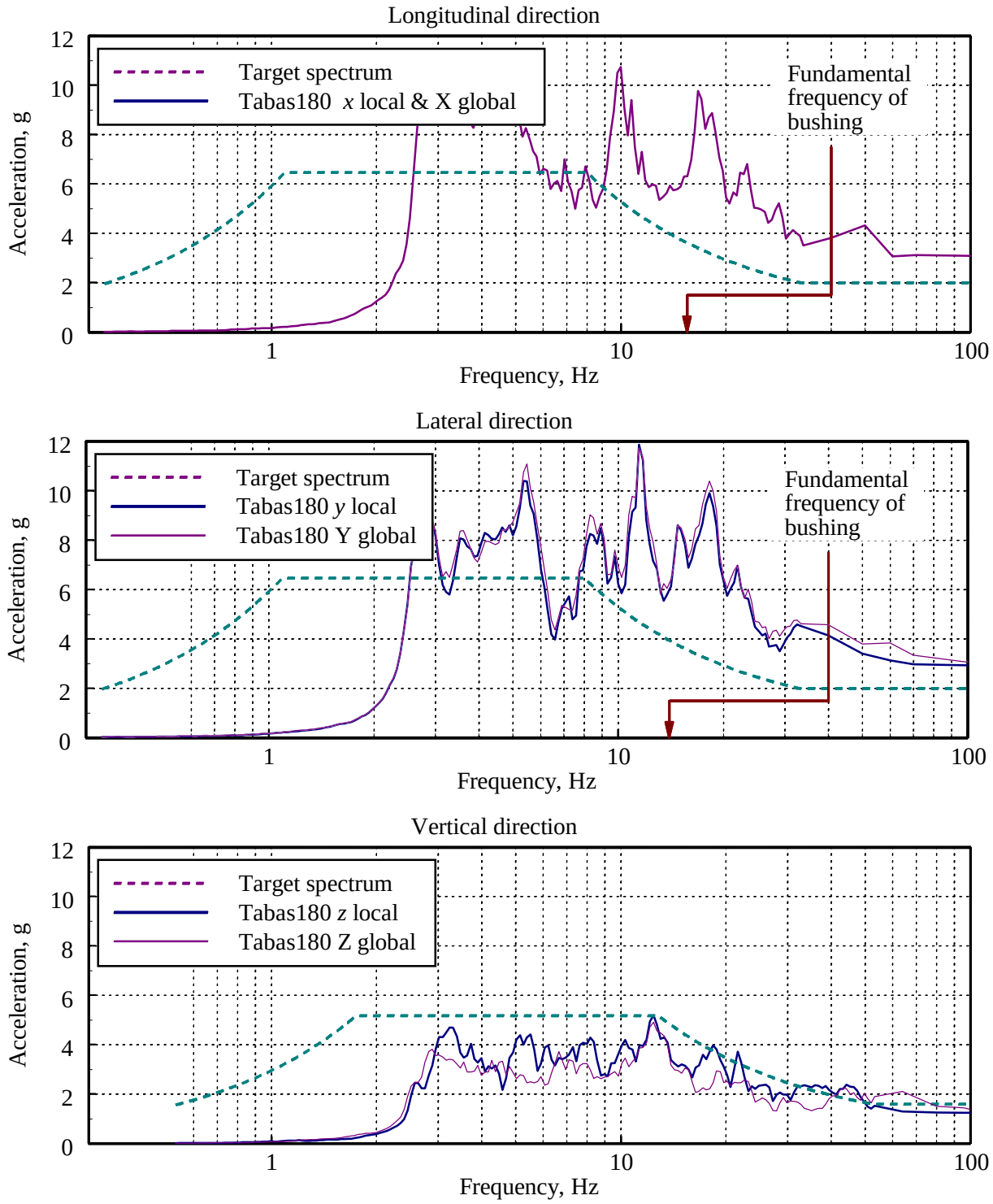

Figure 4-7 Response spectra (2-percent damping) for Bushing-2 fragility test (Test Number 21: Tabas180)

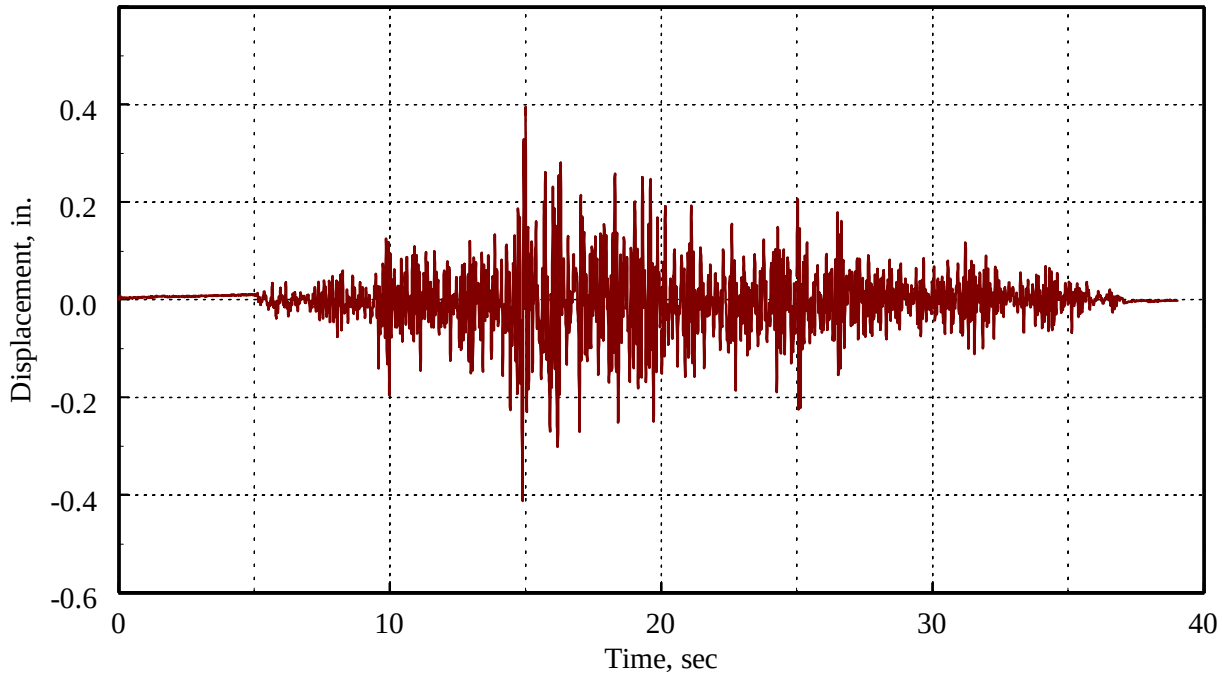

a. History in global X-direction

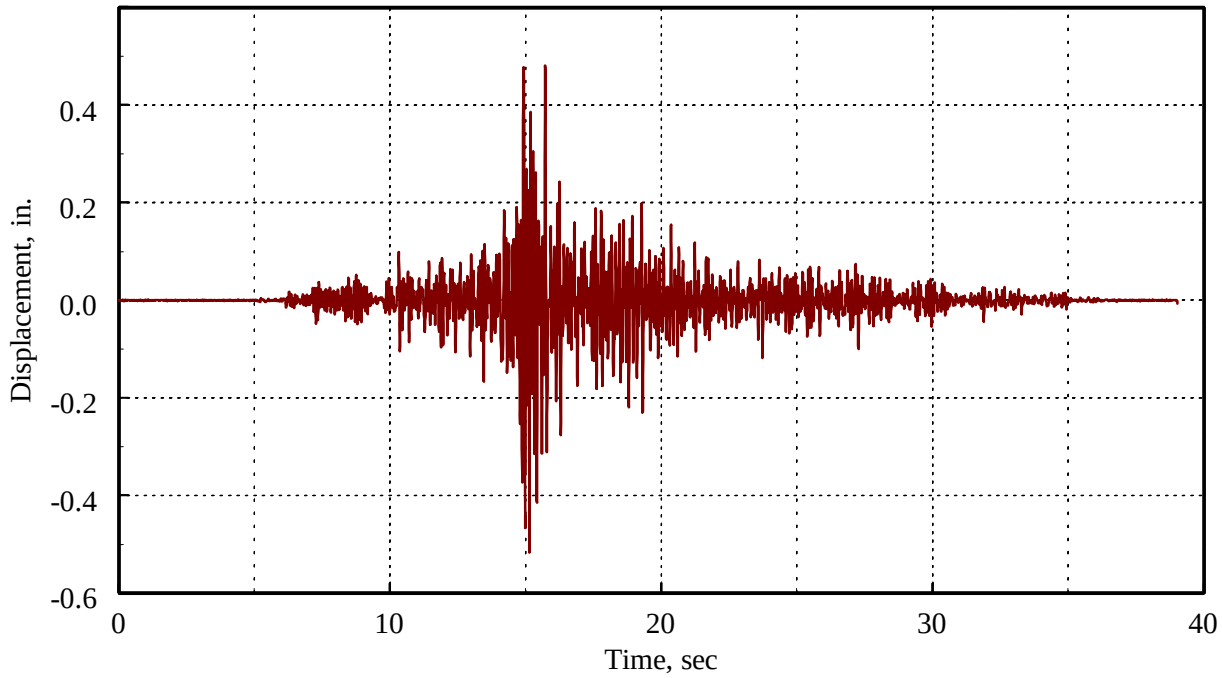

b. History in global Y-direction

Figure 4-8 Horizontal relative displacement histories of upper tip of bushing with respect to mounting frame, Test Number 21: Tabas 180

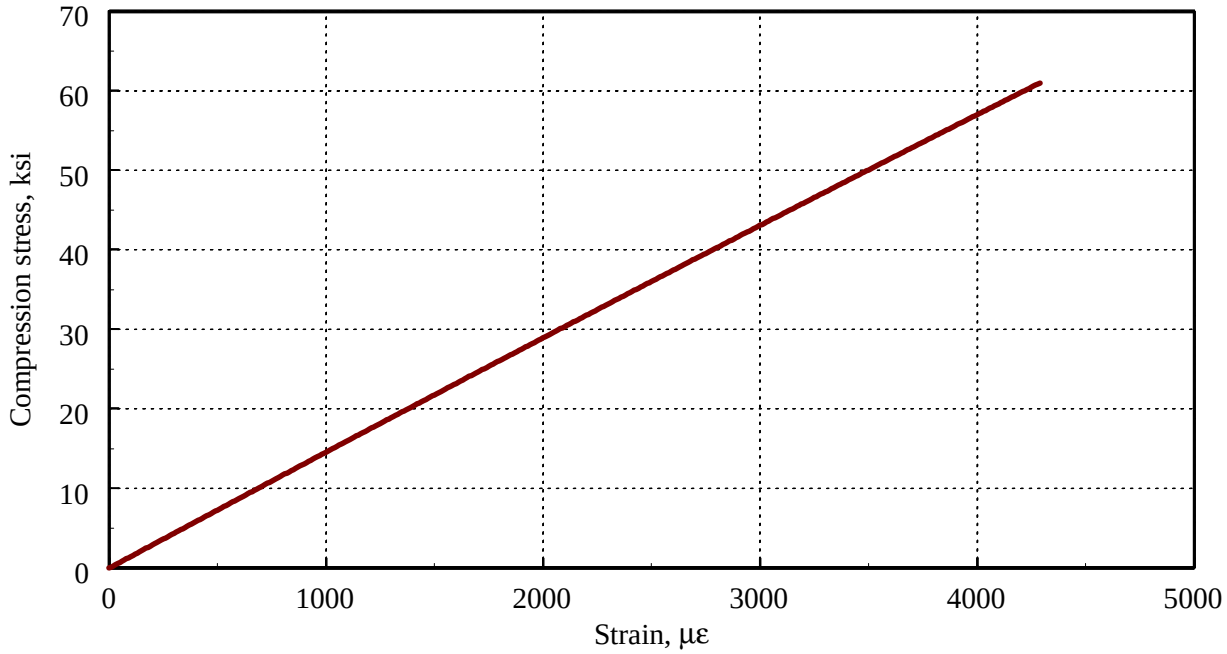

a. History in local *x*-direction

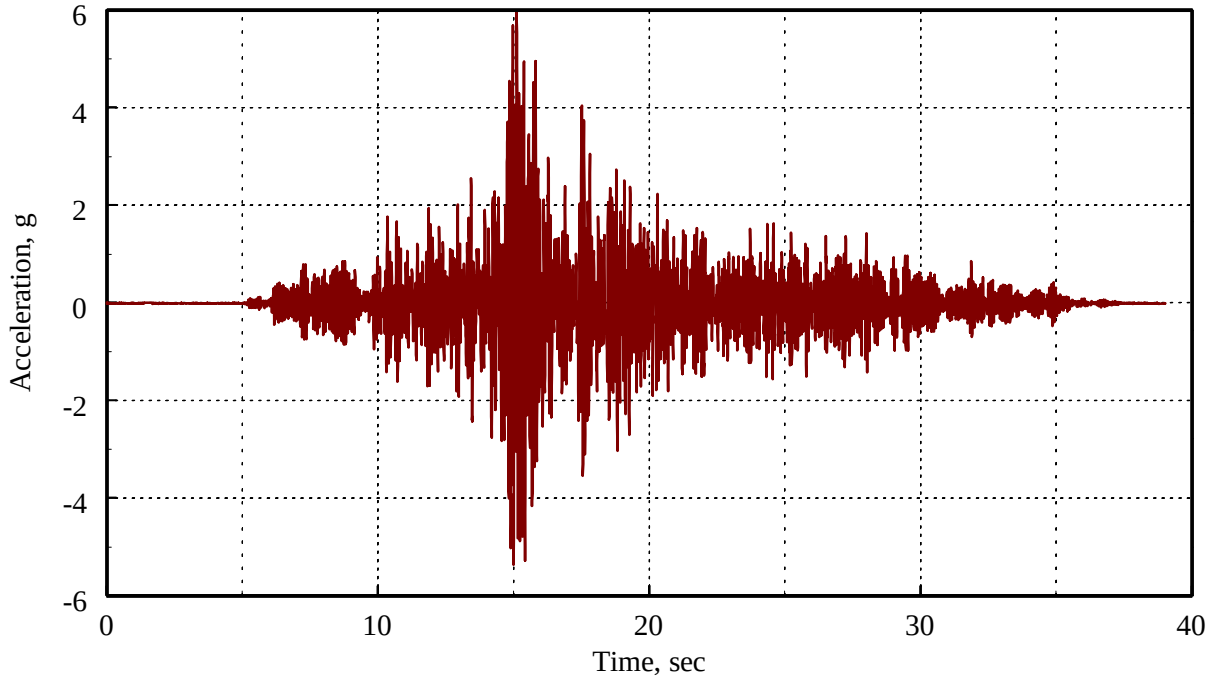

b. History in local *y*-direction

Figure 4-9 Horizontal acceleration histories of upper tip of bushing, Test Number 21: Tabas 180

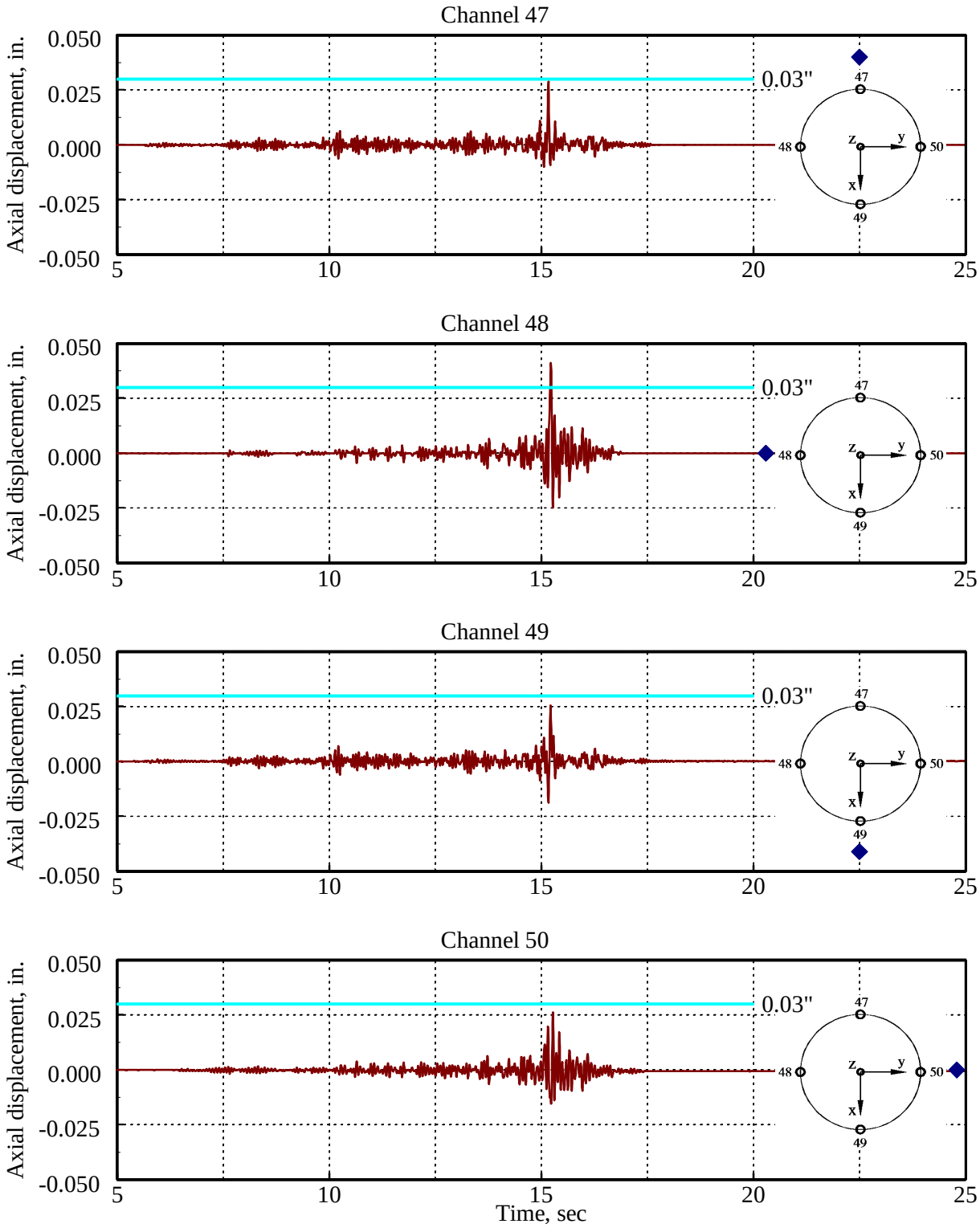

Figure 4-10 Relative vertical displacement histories across gasket adjacent UPPER-1 porcelain unit, Test Number 22: Tabas200 (local coordinate system)

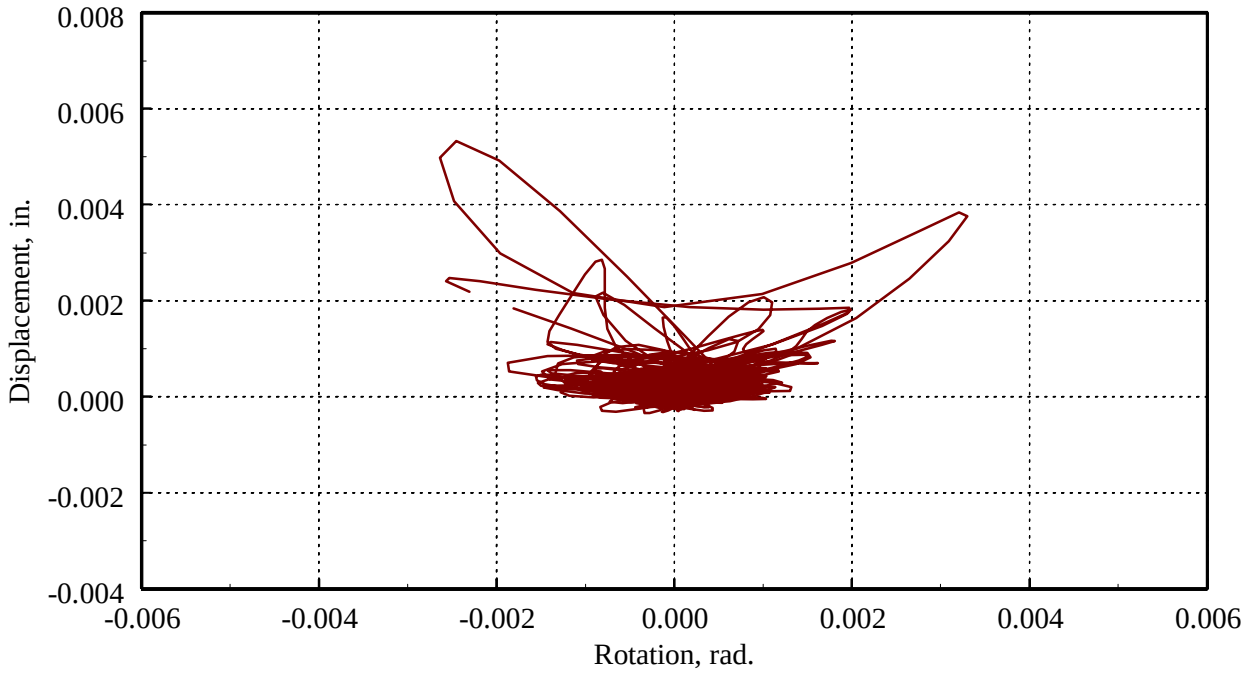

Figure 4-11 Relative vertical displacement versus rotation across gasket adjacent UPPER-1 porcelain unit, Test Number 21: Tabas180 (local coordinate system)

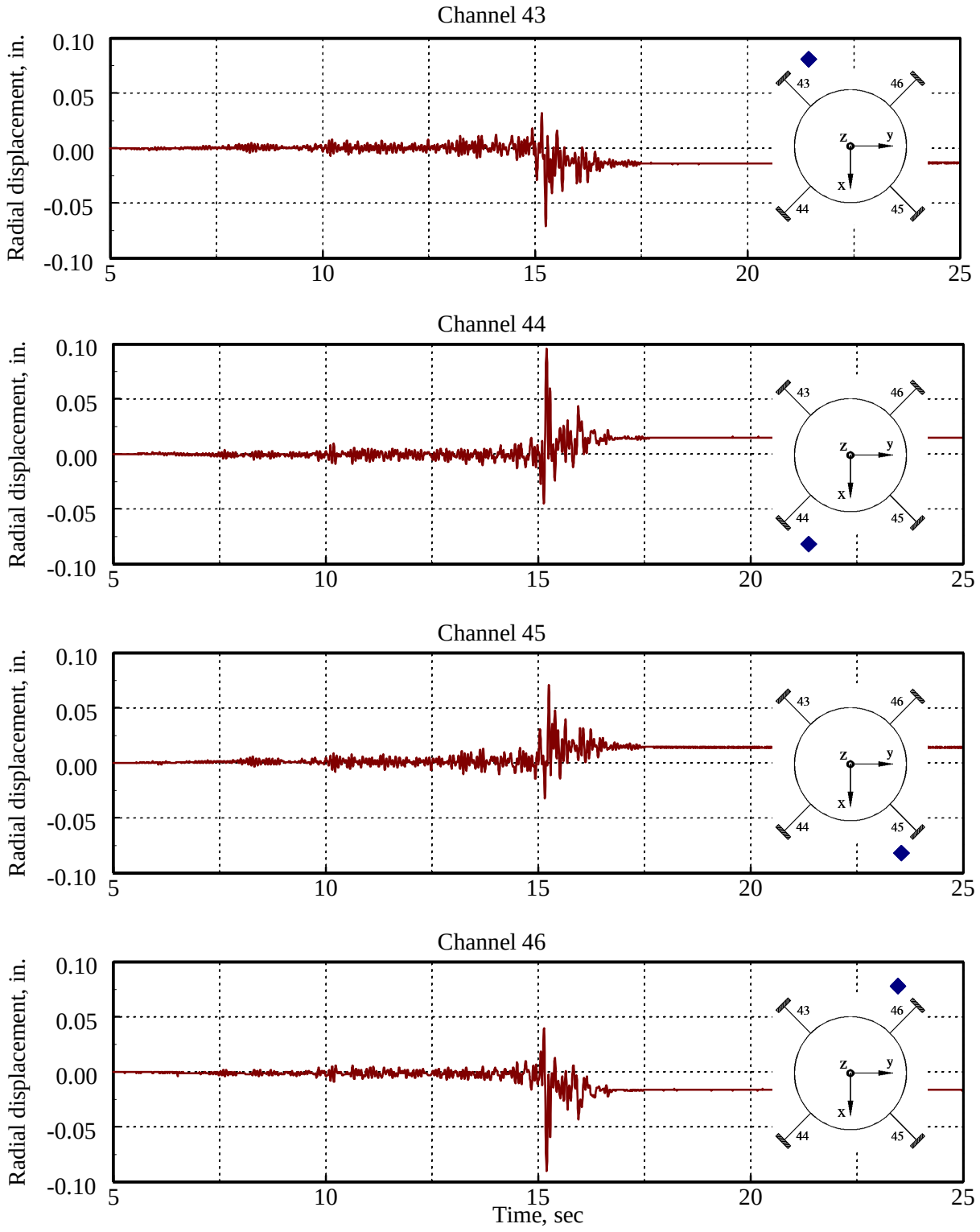

Figure 4-12 Relative radial displacement histories across gasket adjacent UPPER-1 porcelain unit, Test Number 22: Tabas200

CHAPTER 5
MODELING AND ANALYSIS

5.1 Overview

The earthquake-simulator testing program provided valuable information on the dynamic and earthquake-response characteristics of a 196 kV porcelain transformer bushing. The dynamic and earthquake response characteristics were further investigated by finite element analysis in order to a) ascertain whether porcelain bushings were readily amenable to such analysis, b) correlate the predicted and measured responses of a bushing to prescribed seismic input, and c) study the influence of gasket stiffness on the modal frequencies of a bushing. The following sections describe the finite element characterization of a 196 kV bushing (Section 5.2), the modal frequencies of the mathematical models of the bushing (Section 5.3), the predicted response of the models to earthquake shaking (Section 5.4), and the studies on gasket stiffness (Section 5.5).

5.2 Analytical Modeling

As described in Chapter 2, the 196 kV transformer bushing has an overall length of 166 in. (4.2 m). The portion of the bushing above the flange-plate connection includes three porcelain units, the upper segment of the flange-plate assembly, and a metallic dome. The porcelain units are separated by nitrile rubber gaskets. The portion of the bushing below the flange-plate connection includes the lower segment of the flange-plate assembly and one porcelain insulator, separated by a flat nitrile rubber gasket. The bushing has an internal aluminum core housing the copper cables, a condenser wrapped around the core, and oil filling the volume between the condenser and the porcelain. The aluminum core is pre-tensioned to a force of 27 kips (120 kN), which places the four porcelain units and the four gaskets under compression and stabilizes the bushing.

There are several alternatives for modeling porcelain bushings. The most rigorous approach is to develop a three-dimensional solid model of all components. However, data from the earthquake-simulator tests indicated that the seismically induced displacements in a bushing were primarily associated with deformations of the gaskets located between the porcelain units. This observation led the authors to develop a simpler mathematical model for the bushing.

Information on the analytical model of the bushing is shown in Figure 5-1. The model consists of two lines of beam-column elements in parallel running the length of the bushing. The first line of elements represents the mass and stiffness of the porcelain units, the flange, and the gaskets. The second line of elements represent the core, the condenser, the oil, and the copper leads. The longitudinal axis of the bushing was assumed to be vertical for analysis. The material properties for the bushing components listed in Table 5-1 were obtained from data supplied by the bushing manufacturer and the literature. The material properties for the porcelain units were obtained from the compression tests described in Chapter 4. The gasket properties listed in Table 5-2 were obtained from compression testing (see Chapter 4) of Gasket 1 and manufacturer data for Gaskets 2 and 3. At each cross section of the bushing, it was assumed that all components were placed concentrically with respect to the longitudinal axis of the bushing. Elementary mechanics of materials was used to compute section properties for the bushing components.

The earthquake response of a bushing is highly dependent on the assumed stiffness of its gaskets. As shown in Figure 4-2b, the stress-strain relation for the gaskets is nonlinear. However, because pre-compression on the gaskets was not lost during earthquake simulation, and the objective of the study was to develop a simple mathematical model of a bushing, the gaskets were modeled using equivalent linear axial and shear springs. Sixteen equally spaced axial springs were used to represent the axial stiffness of each gasket as shown in Figure 5-1. Two springs oriented in the local *x*- and *y*-directions of the bushing were used to capture shearing deformations in the gaskets. The spring properties used for the analysis were determined using the following two equations:

$$k_{ax} = \frac{A_g E_c}{16 T_r} \tag{5-1}$$

where k_{ax} is the stiffness of one axial spring, A_g is the cross-sectional area of the gasket (see Table 5-2), E_c is the tangent compression modulus of the gasket (see Table 5-2), and T_r is the thickness of the rubber layer. The shear stiffness of the gasket in the local *x*- and *y*-directions (k_{sh-x} and k_{sh-y}, respectively) were calculated as:

$$k_{sh-x} = k_{sh-y} = \frac{A_g G}{T_r} \tag{5-2}$$

where *G* is the shear modulus of nitrile rubber (assumed equal to 0.50 ksi). All other terms are defined above.

Mass was assigned to each component of the mathematical model. The mass of the metallic dome was lumped at the upper tip of the bushing. The bushing was fixed at the flange-plate connection for the purposes of analysis and comparison with the test data. The finite element analyses were performed with SADSAP (Wilson, 1992).

Two mathematical models were prepared for analysis. The only difference between the models was the connectivity between the outer and inner parallel elements. Some connectivity is provided by the oil between the porcelain units and the condenser that wraps around the aluminum core. Model A provides no connection between the outer and inner parallel elements. Model B constrains the lateral displacements of the outer and inner parallel elements.

5.3 Modal Properties of the Bushing

The fundamental frequency in the local *x*-*y* plane of Model A is 12.4 Hz and 16.3 Hz for Model B. The measured fundamental frequency of the 196 kV bushing was between 14 and 15 Hz. The computed mode shapes and frequencies are shown in Figure 5-2. The first mode shape for both models is a cantilever shape with much of the displacement associated with deformation in the gasket immediately above the flange plate. The second and third mode shapes for Model B correspond to the third and fifth mode shapes for Model A, and primarily capture the deformation of the porcelain units. The second and fourth modes of Model A correspond to the deformation of the aluminum core of the bushing. Since the model is axi-symmetric, identical resonant frequencies and mode shapes were obtained in the local *x*-*z* and *y*-*z* planes.

5.4 Influence of Gasket Properties on Modal Frequencies

The calculated fundamental frequency of the 196 kV bushing is highly dependent upon the assumed properties of the gaskets. These properties vary as a function of contact pressure (see Figure 4-2b), gasket width, and Durometer hardness of the nitrile rubber (Roberts, 1988).

The change in modal frequency as a function of gasket stiffness was investigated through a parametric study. Only the tangent modulus of the gasket immediately above the flange-plate assembly was varied in the study. Figure 5-3 shows the relation between the fundamental frequency of the bushing and the tangent modulus of the nitrile rubber gasket. A four-fold change in tangent modulus produced a 60-percent change in the first mode frequency for Model A and a 40-percent change in the first mode frequency for Model B. Figure 5-4 shows the contributions of the porcelain units, the gasket immediately above the flange-plate assembly, and the remaining gaskets to the first mode displacement of the upper tip of the bushing. It is evident from this figure that the gaskets must be correctly modeled if reasonable estimates are to be made of the dynamic properties and response of a porcelain transformer bushing.

5.5 Earthquake Response of the Bushing

5.5.1 Introduction

The translational and rotational motion of a bushing support (i.e., a transformer in the field or a mounting frame in the laboratory) will each affect the earthquake response of a bushing. Although rotational motion of the flange-plate assembly is routinely ignored for analysis and design, rotational motion may substantially amplify the acceleration and displacement histories of a bushing. Such motion might produce (additional) damage to the bushing and fail electrical connections to other hardware. Unfortunately, most commercially available finite element analysis programs only permit the user to input translational earthquake histories.

5.5.2 Earthquake input motions

The earthquake analysis of the model used the local *x*-, *y*-, and *z*- acceleration histories of the mounting frame measured during Test Number 21: Tabas180. The input acceleration histories are shown in Figure 5-5. The peak accelerations of the three components are 2.86g, 2.77g, and 1.14g, in the local *x*-, *y*, and *z*- axes of the bushing, respectively.

5.5.3 Bushing response histories

Figure 5-6 shows the computed and measured absolute accelerations at the top of the bushing for the first 20 sec of the Tabas180 test. The modal damping ratio assumed for the analysis was 3.75 percent of critical; this value is the average of the damping ratios measured by experiment during Tests 23, 24, and 25—see Table 4-1. Both the computed and measured histories were high-pass filtered at 25 Hz. The computed peak accelerations exceed the measured peak accelerations by up to 40 percent in the *x* direction (Model B) and 25 percent in the *y* direction (Model A). The com-

puted and measured relative displacements of the upper tip of the bushing with respect to the mounting frame, presented in Figure 5-7 for the first 20 sec of the Tabas180 test, are no better correlated than the absolute accelerations of Figure 5-6. Neither model (A or B) reproduced well the shape of the measured response histories.

One hypothesis for the poor correlation between the measured and predicted responses can be developed by review of the Tabas180 acceleration-response spectra. Consider Figure 5-8, which presents the 2.5-percent damped and 4.0-percent damped spectra for the local *x*- and *y*-acceleration histories of the mounting frame measured during the Tabas180 test. (The two damping ratios bracket the measured damping in the bushings—see Table 4-1.) Also shown in this figure are a) the measured fundamental frequencies of the bushing in the *x*- (=15.6 Hz) and *y*-directions (=14.0 Hz), and b) the fundamental frequencies for Model A (=12.4 Hz) and Model B (=16.3 Hz). It is evident from this figure that the acceleration-response ordinates at the measured frequencies of the bushing are substantially different from those associated with the fundamental frequencies of Models A and B. As such, unless a mathematical model exactly captures the modal properties of a bushing, it may be difficult to accurately predict the response of transformer bushings to earthquake shaking.

Figure 5-9 presents the computed and measured relative axial displacements across the gasket immediately above the flange-plate assembly. The measured relative axial displacements were calculated by dividing the sum of the displacements of Channels 48 and 50 by four. (The sum of the displacements is divided by two to calculate an average value and by two again to estimate the displacement at the face of the porcelain). Neither model (A or B) captures well either the shape or peak amplitude of the measured displacement history. This result is not surprising given the simplicity of the model of the gaskets adopted for the analysis.

Better correlation between the computed and measured acceleration and displacement histories would be achieved if a) the modal frequencies of the models better matched the measured frequencies of the bushing, b) improved models of the nitrile rubber gaskets were implemented in the mathematical models, and c) the mathematical model was extended to include the mounting frame, the earthquake simulator platform, and the vertical servo-actuators beneath the platform.

Table 5-1 Material properties for the bushing components

Component	*Material*	*Unit weight* $(lb^3/in.)$	*E* *(ksi)*
porcelain	porcelain	0.087	14,200
flange	356-T6P cast aluminum	0.097	10,100
transformer oil	oil	0.033	-
condenser	kraft paper	0.043	1,500
core tube	6063-T6 aluminum	0.097	10,000

Table 5-2 Gasket properties

Gasket	*Gasket area ($in.^2$)*	*Gasket thickness (in.)*	*Tangent compression modulus*[1]
1	31.0	0.24	10 ksi [2,3]
2	24.5	0.06	15 ksi [4]
3	29.3	0.06	12 ksi [4]

1. For gasket location refer to Figure 5-1
2. Tangent modulus for Gasket 1 determined from compression testing; see Chapter 4
3. Tangent modulus of 9.4 ksi from experiment rounded up to 10 ksi for analysis
4. Tangent modulus for Gaskets 2 and 3 determined from manufacturer's data

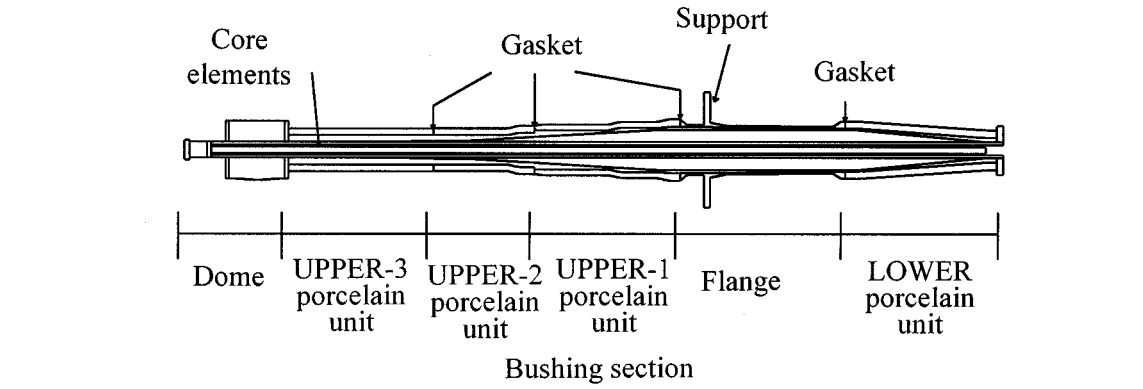

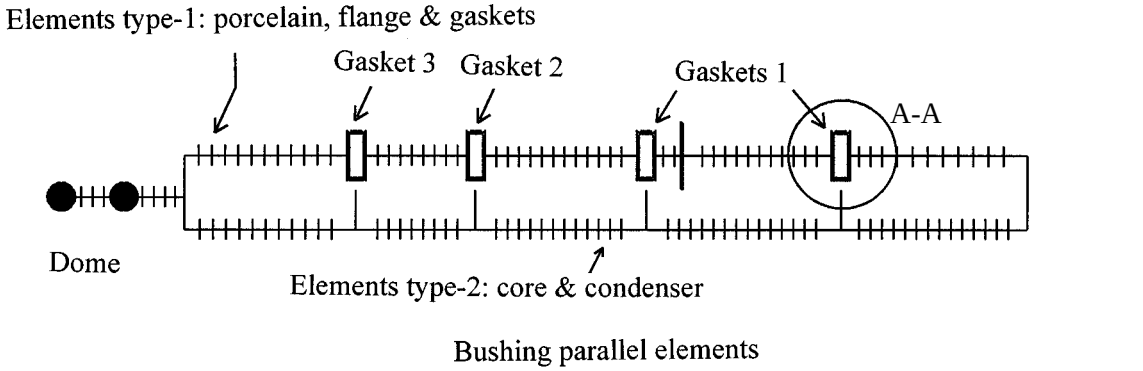

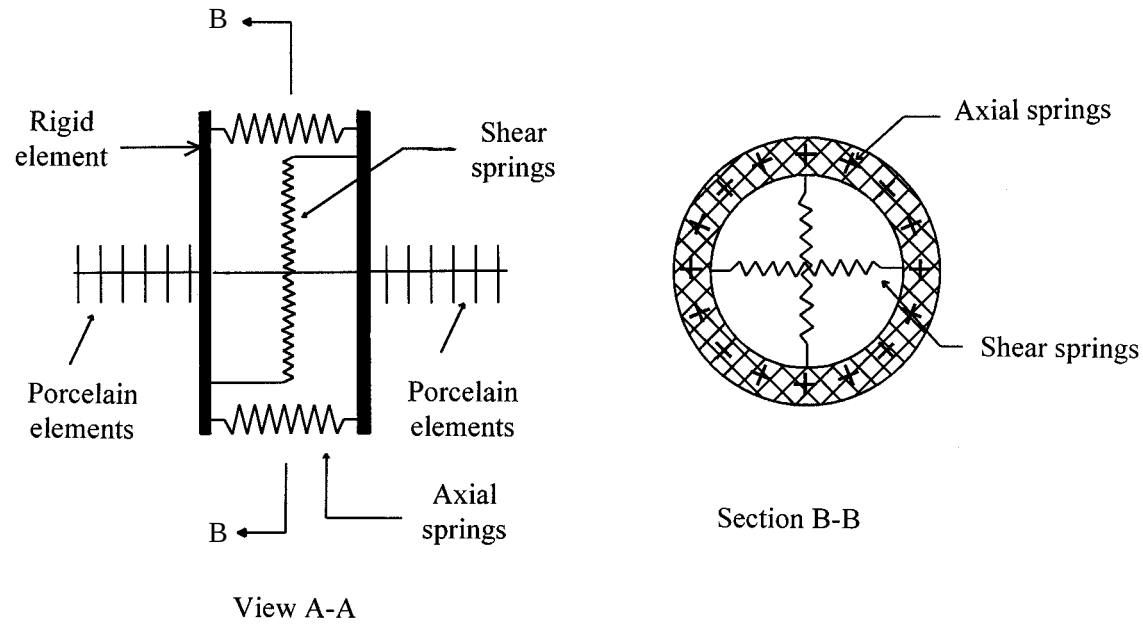

Figure 5-1 Mathematical modeling of a 196 kV bushing

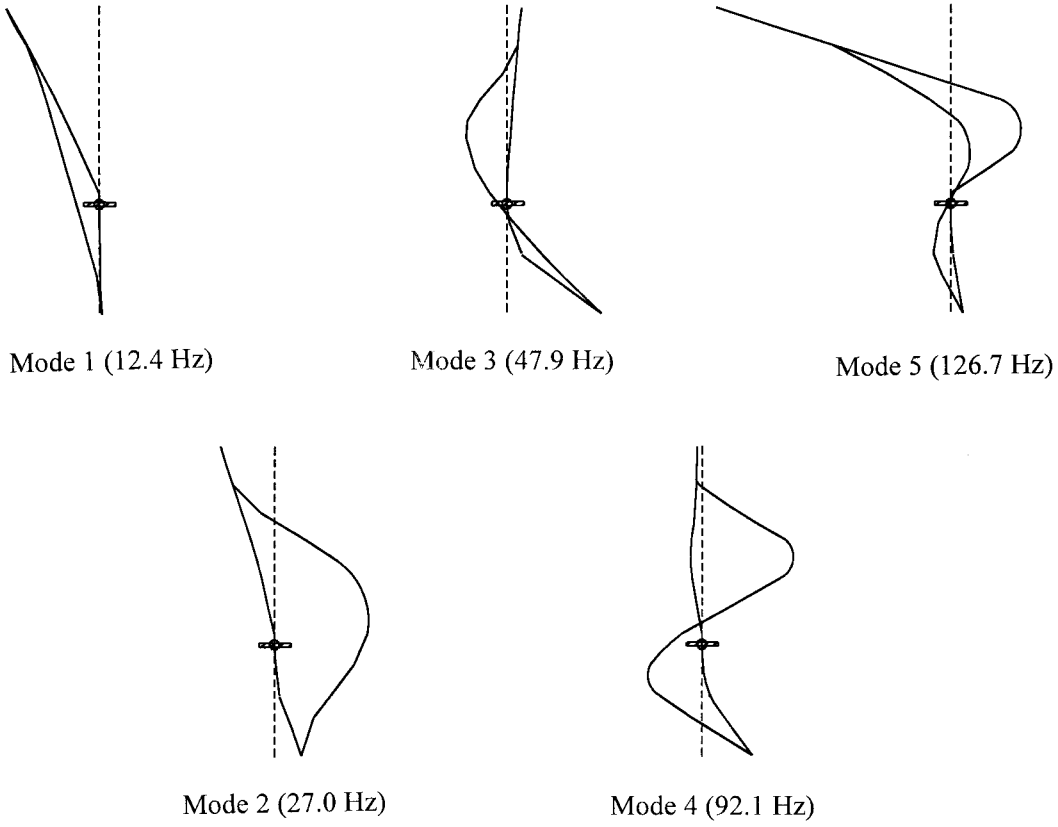

Figure 5-2 Mode shapes and frequencies (in parentheses) for bushing Model A and bushing Model B

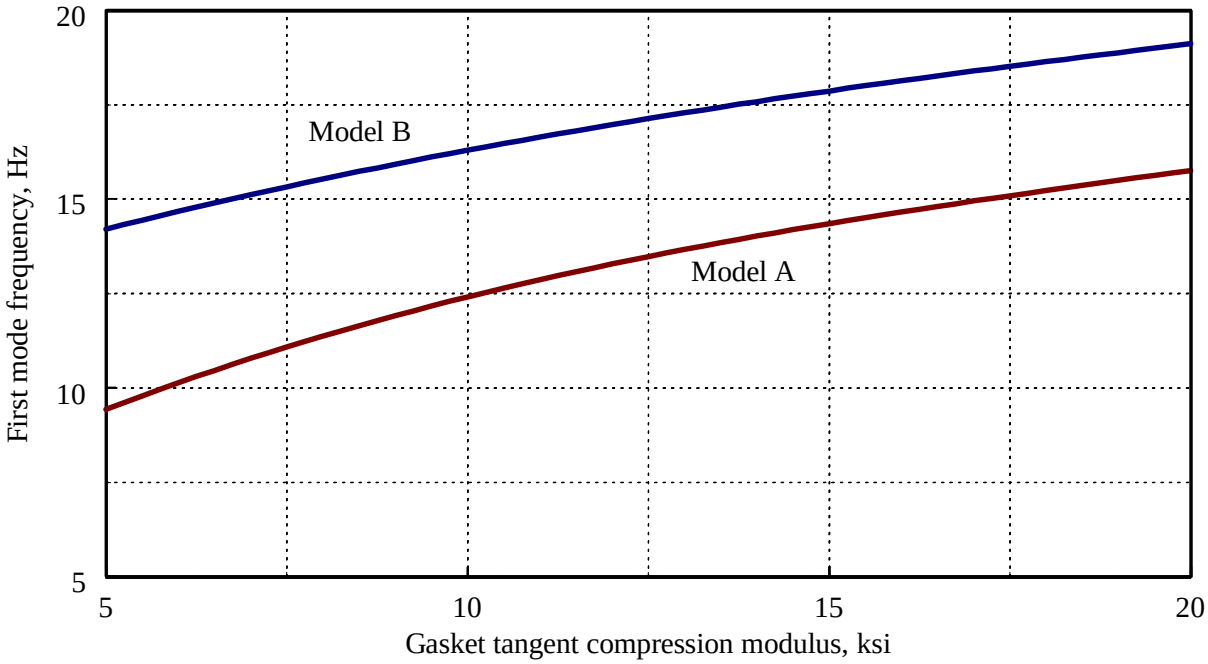

Figure 5-3 Influence of gasket (located immediately above the flange-plate) stiffness on the modal properties of a 196 kV bushing

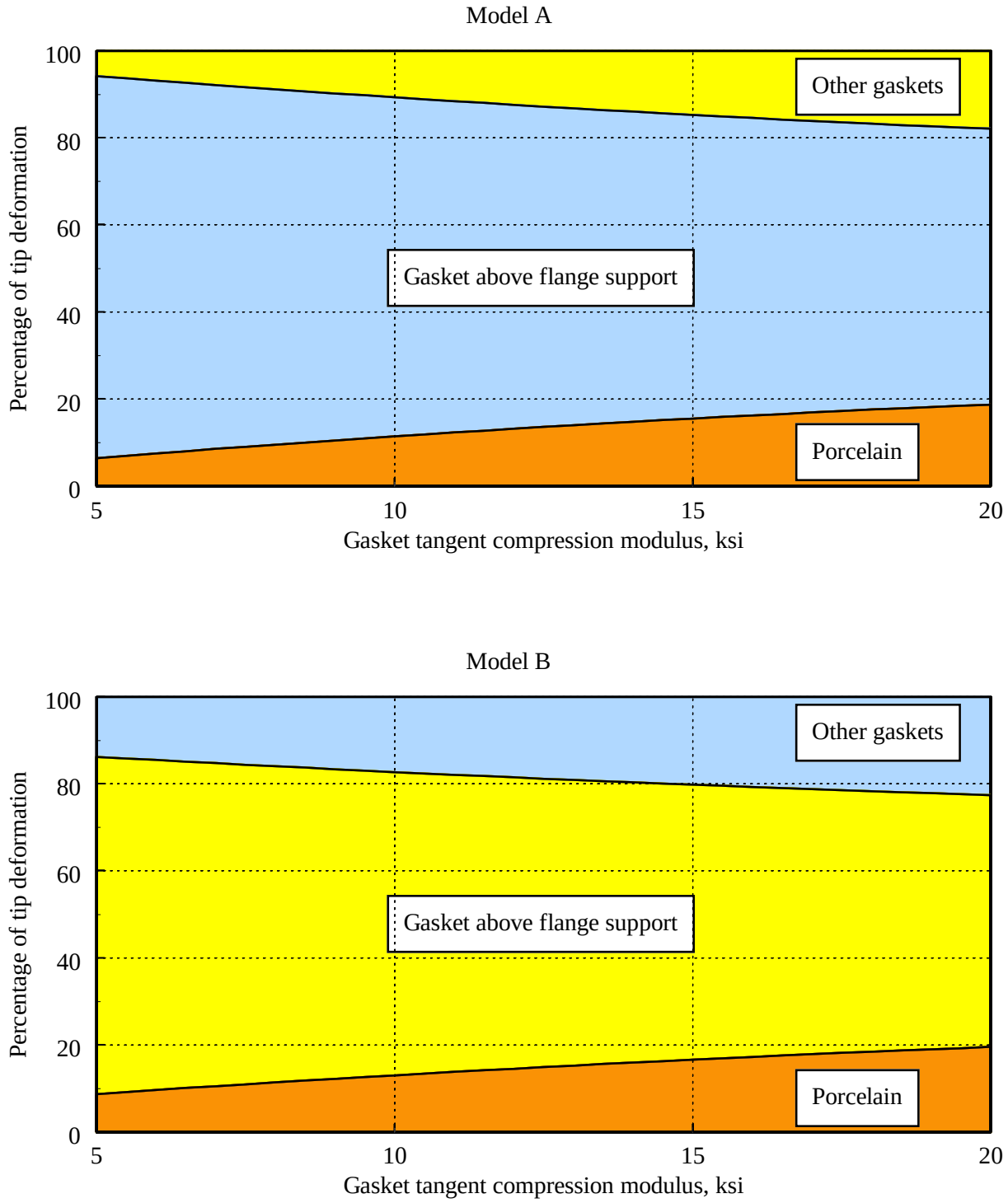

Figure 5-4 Contributions of porcelain and gasket flexibility to first mode tip displacement of a 196 kV bushing

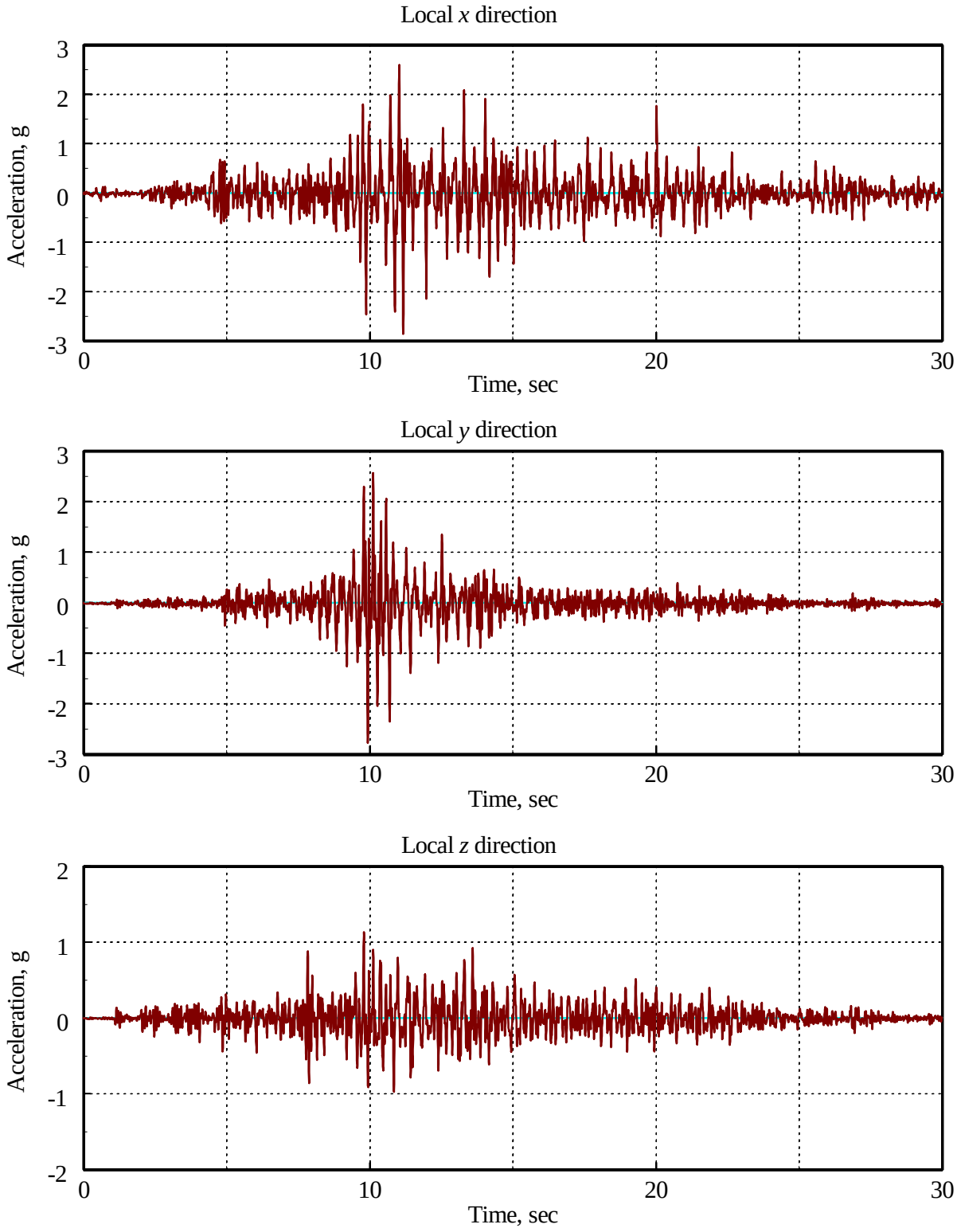

Figure 5-5 Input acceleration histories (Test Number 21: Tabas180) to the mathematical models

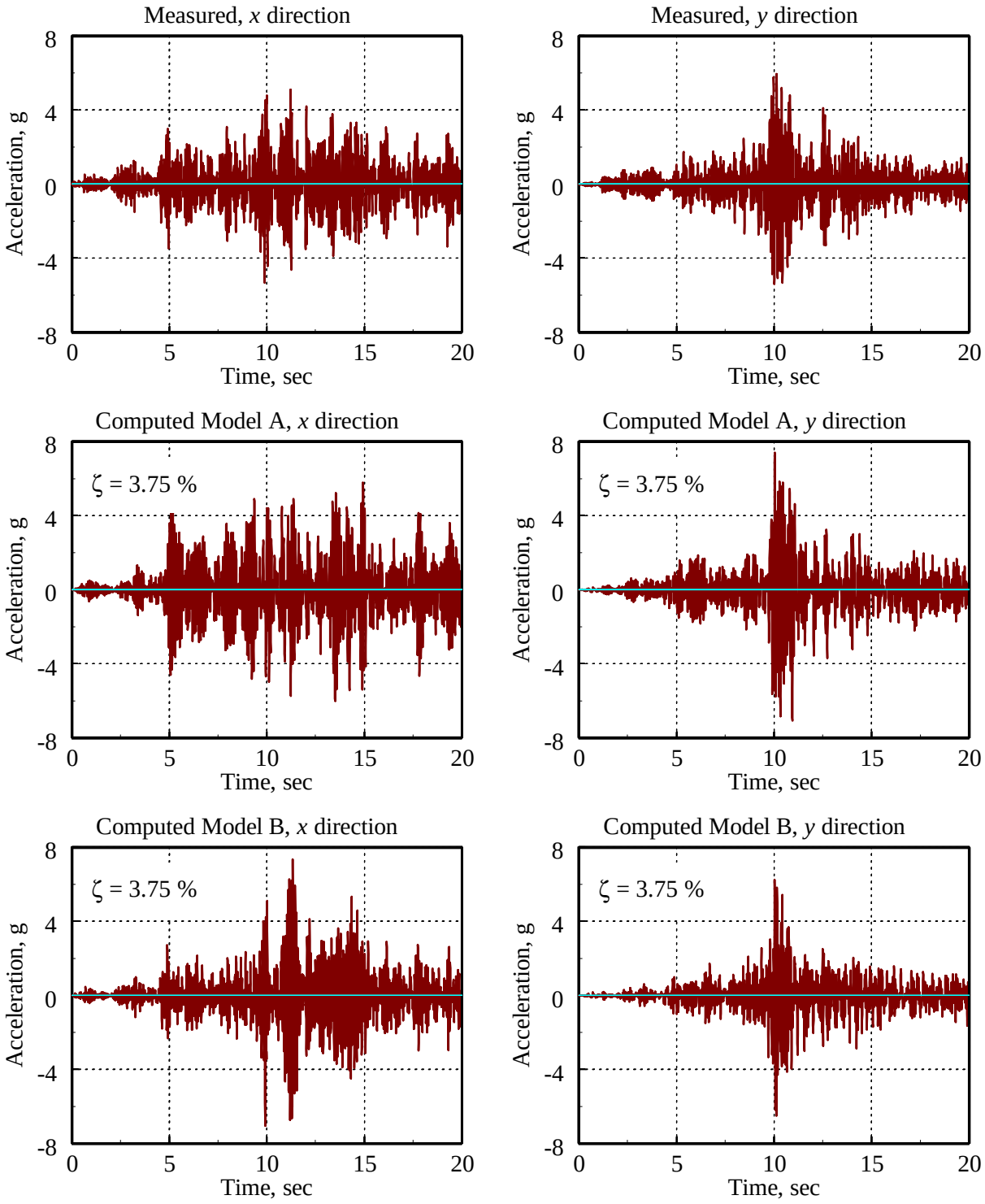

Figure 5-6 Comparison of measured and predicted acceleration histories at upper tip of bushing in the local coordinate system, Tabas180

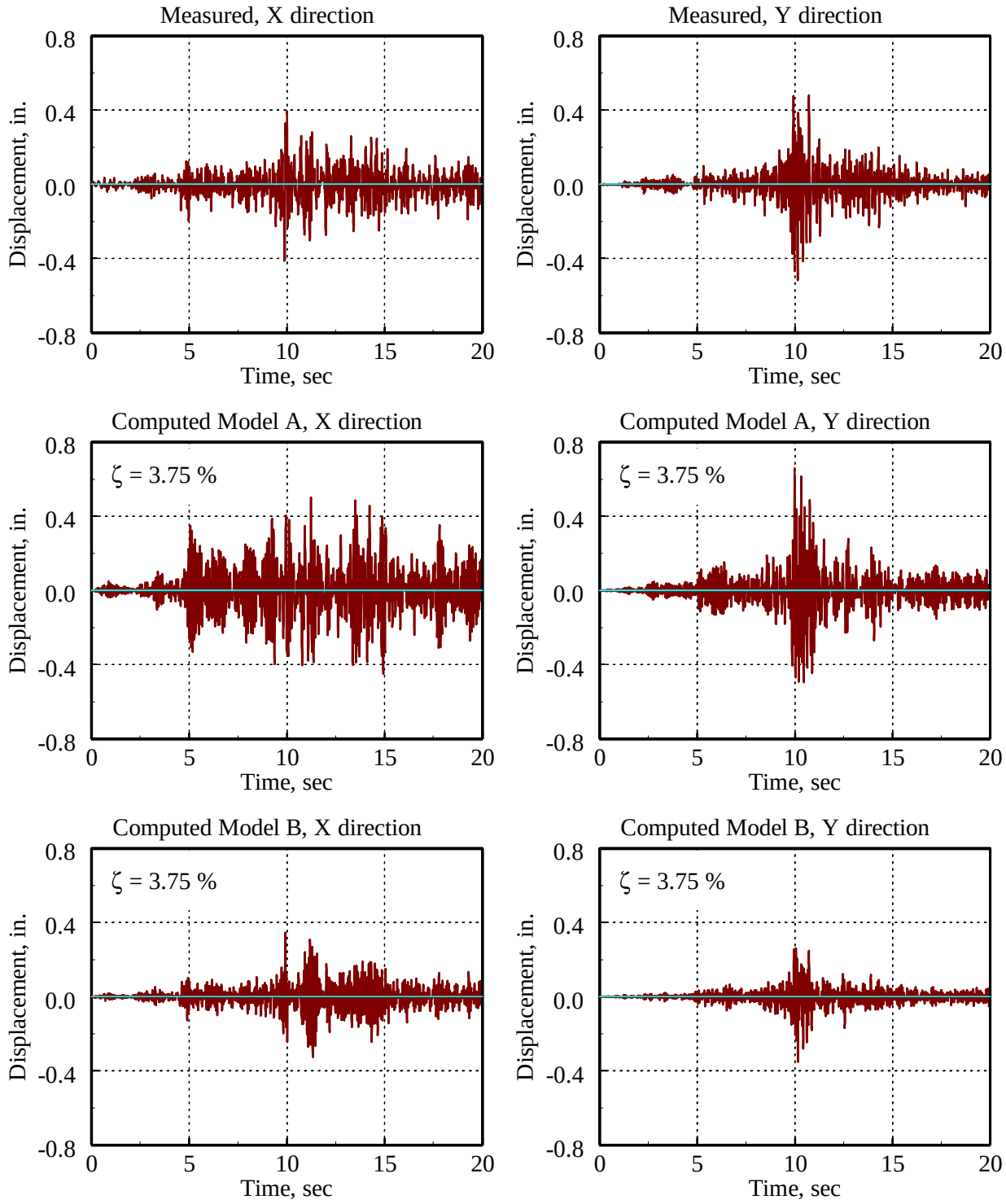

Figure 5-7 Comparison of measured and predicted displacement histories at upper tip of bushing in the global coordinate system, Tabas180

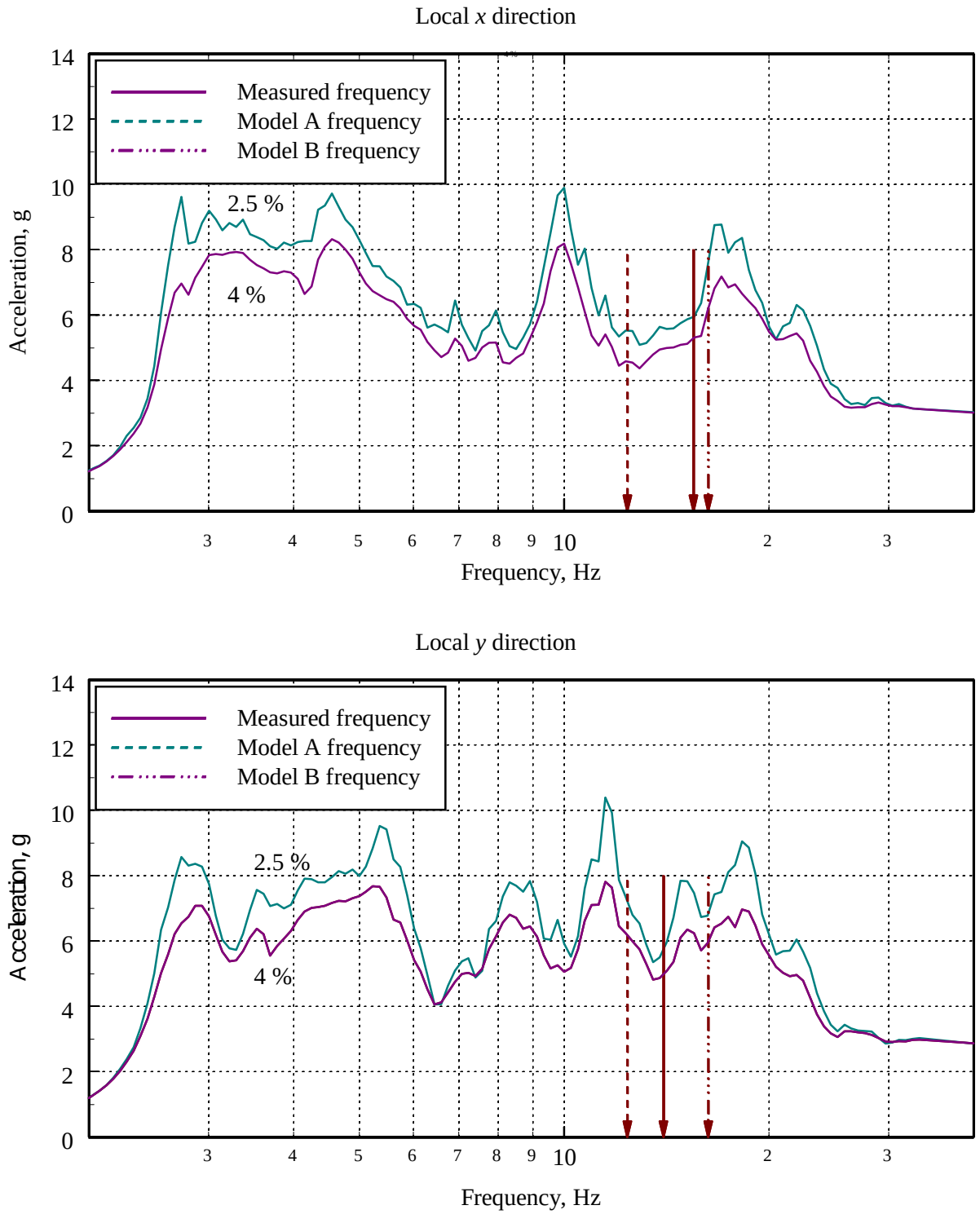

Figure 5-8 Tabas180 response spectra for horizontal earthquake shaking

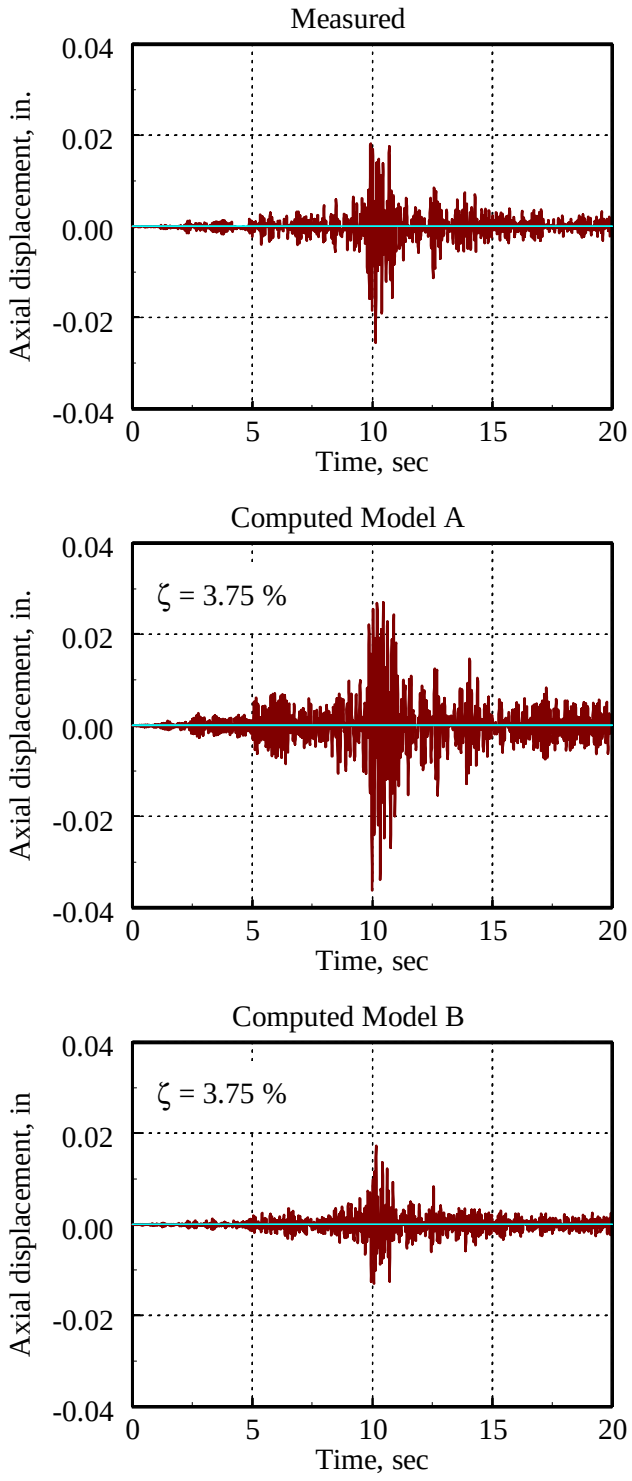

Figure 5-9 Comparison of measured and predicted gasket displacement histories, Tabas180

CHAPTER 6
SUMMARY AND CONCLUSIONS

6.1 Summary

6.1.1 Introduction

The reliability and safety of electrical transmission and distribution systems after an earthquake depend on the seismic response of individual substation components such as transformer bushings. Post-earthquake reconnaissance of electrical substations has identified porcelain transformer bushings as being particularly vulnerable to severe earthquake shaking.

Pacific Gas & Electric (PG&E) Company sponsored a research project to investigate the seismic response of new 196 kV transformer bushings manufactured by Asea Brown Boveri of Alamo, Tennessee. The six key objectives of the project were: 1) analyze, design, and build a mounting frame suitable for seismic testing of bushings ranging in size between 196 kV and 550 kV, 2) develop earthquake ground motion records suitable for the seismic evaluation, qualification, and fragility testing of 196 kV bushings, 3) test two 196 kV bushings on the earthquake simulator at the Pacific Earthquake Engineering Research (PEER) Center using levels of earthquake shaking consistent with those adopted for seismic qualification and fragility testing of electrical equipment, 4) reduce and analyze the data acquired from the earthquake simulator tests, 5) develop a three-dimensional mathematical model of a 196 kV porcelain bushing for parametric and future studies, and 6) draw conclusions about the seismic performance of porcelain transformer bushings, the likely failure modes of a bushing during severe earthquake shaking, and methods for modeling porcelain bushings.

6.1.2 Earthquake testing program

The earthquake testing was performed on the earthquake simulator at the Pacific Earthquake Engineering Research Center, which is headquartered at the University of California at Berkeley. The 20 ft by 20 ft (6.1 by 6.1 m) simulator can accommodate models up to 140 kips (623 kN) in weight and 40 ft (12.2 m) in height.

Two 196 kV bushings were supplied by Asea Brown Boveri for earthquake testing. Bushing-1 was designated for qualification testing and Bushing-2 for fragility testing.

For earthquake testing, the bushings were mounted on a support frame that was designed to accommodate larger (550 kV) bushings. The first three modal frequencies of the mounting frame alone were 72 Hz (global X direction), 78 Hz (global Y direction), and 113 Hz (θ_z). The mounting plate in the frame was sloped at 20 degrees measured to the vertical because a bushing qualified at this angle is deemed by IEEE 693 to be qualified for all angles between vertical and 20 degrees measured to the vertical.

Earthquake simulation testing of the bushings consisted of resonant search tests (sine-sweep and white-noise) and triaxial earthquake-history tests. The resonant search tests were undertaken to establish the dynamic characteristics of the bushings. The first modal frequency of the bushing was approximately 15 Hz; this frequency corresponded to motion in the local *x*-*y* plane. The first mode damping ratio for Bushing-1 prior to earthquake testing was approximately 2 percent of critical. No values of modal frequency and damping ratio for response along the local z-axis of the bushing could be evaluated using the resonant search tests.

The earthquake histories used for the triaxial shaking of the bushings were derived from sets of ground motion records recorded during the 1978 Tabas, Iran earthquake and the 1994 Northridge earthquake (Newhall station). Both sets of records were recorded in the near-field. The earthquake histories were initially matched to the IEEE spectrum. The Tabas station records were used for qualification testing, and both the Tabas and Newhall station records were used for fragility testing.

Bushings such as those tested as part of this research program are attached to the top of a transformer with torqued stainless steel bolts placed in over-sized, open-ended, slotted holes in the flange plate. During earthquake simulation, the bushing flange plate slipped with respect to the adaptor plate, and these bolts were checked and tightened as necessary after each test.

For Moderate Level qualification testing, the earthquake histories were matched to the 2- and 5-percent damped IEEE spectra with peak accelerations of 1.0g (horizontal shaking) and 0.8g (vertical shaking). The frequency content on the Tabas history was modified to suit the displacement and velocity limitations of the earthquake simulator. At this level of shaking, the porcelain stresses are required to be less than or equal to the ultimate value and show no evidence of oil leakage. Test Number 8 (Tabas100) was used for Moderate Level qualification of Bushing-1. The 2-percent damped spectral ordinates associated with the longitudinal (local *x* direction) and lateral (local *y* direction) response of the mounting frame exceeded those of the target spectrum in the frequency range of interest (10 to 20 Hz). The 2-percent damped spectral ordinates associated with the vertical (local *z* direction) response of the mounting frame equaled those of the target spectrum for frequencies between 10 and 20 Hz. The Tabas100 test produced no external damage in Bushing-1, the porcelain strains were less than 1 percent of the ultimate strain, and there was no evidence of oil leakage.

For High Level qualification, the ordinates of the target horizontal and vertical spectra are twice those of the spectra used for Moderate Level qualification. Although the objective of the research program was to only qualify Bushing-1 to the Moderate Level, the fragility testing sequence for Bushing-2 permitted the project team to investigate the response of this bushing to levels of earthquake shaking associated with High Level qualification. The 2-percent damped spectral ordinates associated with the longitudinal (local *x* direction) and lateral (local *y* direction) response of the mounting frame in Test Number 21 (Tabas180) exceeded those of the target High Level spectrum in the frequency range of interest (10 to 20 Hz). The 2-percent damped spectral ordinates associated with the vertical (local *z* direction) response of the mounting frame in Test Number 21 were slightly smaller than those of the target spectrum for frequencies between 10 and 20 Hz. The Tabas180 test produced no external damage in Bushing-2, the maximum porcelain strain was approximately 2 percent of the ultimate strain, and there was no evidence of oil leakage.

Test Number 22 (Tabas200) was the last test of Bushing-2. The peak acceleration response of the mounting frame in the local *x*-*y* plane was 2.7g. During this test, a minuscule amount of oil leaked from the gasket immediately above the flange plate. The peak accelerations at the upper tip of Bushing-2 during this test exceeded 6g. Displacement transducers installed around the perimeter of the bushing near the flange plate recorded relative displacements between the flange plate and the UPPER-1 porcelain unit (measuring gasket opening and closing) of more than 0.03 inch (0.8 mm)—the limiting value established by ABB for probable oil leakage.

Following earthquake testing, the bushings were returned to the ABB facility in Alamo, Tennessee, for tear down and electrical testing. Both bushings passed the requisite IEEE electrical tests, and there was no evidence of structural damage to the bushings.

6.1.3 Finite element analysis of a 196 kV transformer bushing

The earthquake-simulator testing program provided valuable information on the dynamic and earthquake-response characteristics of a 196 kV porcelain transformer bushing. The dynamic and earthquake response characteristics were further investigated by finite element analysis in order to a) ascertain whether porcelain bushings were readily amenable to such analysis, b) correlate the predicted and measured responses of a bushing to prescribed seismic input, and c) study the influence of gasket stiffness on the modal frequencies of a bushing.

Two linearly elastic mathematical models (Models A and B) of a 196 kV bushing were developed. Test and manufacturer data were used to calculate geometries and mechanical characteristics of the components of the bushing. Simple models of the nitrile rubber gaskets were implemented in the model. The lateral displacements of the aluminum core and the perimeter porcelain units were not constrained in Model A, but were constrained in Model B. The fundamental frequencies of Models A and B were 12.4 Hz and 16.3 Hz, respectively. These frequencies bracketed the measured fundamental frequencies of the bushing which ranged between 14.0 and 14.4 Hz in the local *x*-direction, and 15.4 and 15.8 Hz in the local *y*-direction.

The influence of gasket stiffness on the dynamic characteristics of a bushing was studied by varying the tangent compression modulus of the nitrile rubber over a range equal to one-half to twice the measured tangent modulus calculated at a contact pressure equal to 0.87 ksi (6 MPa). Only the properties of the gasket immediately above the flange-plate assembly were varied. A four-fold increase in tangent modulus produced a 60-percent change in the first mode frequency for Model A and a 40-percent change in the first mode frequency for Model B. A four-fold increase in tangent modulus did not proportionally reduce the contribution of gasket deformation to the first mode displacement of the upper tip of the bushing.

The earthquake analysis of the model used the local *x*-, *y*-, and *z*-acceleration histories of the mounting frame measured during Test Number 21: Tabas180. The peak accelerations of the three components were 2.86g, 2.77g, and 1.14g, in the local *x*-, *y*, and *z*-axes of the bushing, respectively. The modal damping ratio assumed for the analysis was 3.75 percent of critical. The computed peak accelerations exceeded the measured peak accelerations by up to 40 percent in the *x* direction and 25 percent in the *y* direction. The computed and measured relative displacements of the upper tip of the bushing with respect to the mounting frame were better correlated than the

absolute accelerations. Neither model reproduced well the shape of the measured response histories. The poor correlation between the measured and predicted responses can be attributed in part to the substantial differences in the acceleration response-spectrum ordinates at the measured frequencies of the bushing and at the fundamental frequencies of the two mathematical models.

6.2 Conclusions and Recommendations

6.2.1 Seismic response of 196 kV transformer bushings

Both 196 kV transformer bushings survived the effects of severe earthquake shaking. Bushing-1 passed the requirements for Moderate Level qualification, and Bushing-2 met the requirements for High Level qualification. Bushing-2 was subjected to seven earthquake simulations with input accelerations exceeding 1.0g and suffered no visible damage until after Test Number 22: a simulated earthquake which generated input accelerations of 2.7g (local *x*-direction), 2.9g (local *y* direction), and 1.2g (local *z* direction).

Based on the earthquake tests conducted as part of this research program, 196 kV ABB transformer bushings should be expected to perform well in extreme earthquake-loading environments. The bolted flange plate-to-transformer connection should be revised to prevent both slip and loss of bolt pre-tension during minor earthquake shaking. Any inspection of existing transformer bushings should include checking and re-tightening of these bolted connections. Loose flange-plate connections could lead to the premature failure of a transformer bushing.

6.2.2 Finite element analysis

The objectives of the finite element studies were to ascertain whether porcelain bushings were amenable to analysis using linearly elastic mathematical models, to correlate the predicted and measured responses of a bushing to prescribed seismic inputs, and to study the influence of gasket stiffness on the modal frequencies of a bushing.

Although the two SADSAP models of the 196 kV bushings captured the key dynamic properties of the 196 kV ABB bushing, reasonably well, neither model accurately reproduced its acceleration and displacement histories under earthquake simulation. Different assumptions regarding the relative lateral movement of the aluminum core and the perimeter porcelain units led to substantially different estimates of maximum acceleration and displacement response. The parametric studies on gasket stiffness clearly identified the need to model gaskets in a more rigorous manner than that used to date.

Better correlation between the computed and measured acceleration and displacement histories would be achieved if a) the modal frequencies of the models better matched the measured frequencies of the bushing, b) improved models of the nitrile rubber gaskets were implemented in the mathematical models, and c) the mathematical model was extended to include the mounting frame, the earthquake simulator platform, and the vertical servo-actuators beneath the platform.

6.2.3 Recommendations for future study

Procedures for seismic qualification

The 196 kV bushings were installed in a mounting frame without electrical connections for earthquake testing. For qualification of equipment attached to a foundation, IEEE 693 specifies a response spectrum for earthquake-simulator testing. The amplitude of the input motion for qualification of bushings is doubled to account for flexibility and ground-motion amplification in the transformer or support equipment. It is not known whether the IEEE 693 assumptions are reasonable, conservative, or non-conservative. Numerical (finite element) studies of transformer bushings and other turret structures should be undertaken to review the current specifications for equipment qualification. At a minimum, such studies should identify a) the stiffness characteristics of typical bushing support structures, b) the damping effects of the oil contained in the support structure, if any, c) the amplification of earthquake shaking effects, if any, through the support structure to the base of a bushing, and d) the importance of rotational input to a bushing resulting from flexibility in the upper plate of the transformer to which bushings are attached. Answers to these questions will provide valuable guidance to those tasked with revising the IEEE 693 *Recommended Practices for Seismic Design of Substations*.

Interconnected equipment

Although IEEE 693 acknowledges that physical (electrical) connections between substation equipment may detrimentally affect the seismic response of individual pieces of equipment, the testing procedures described in IEEE 693 may not adequately account for the effects of such connectivity. These physical connections can vary widely in flexibility and strength. There is substantial evidence from past earthquakes that such electrical connections may have precipitated bushing failures because of dynamic interaction between the interconnected equipment. Currently, analytical studies are under way to identify the important parameters affecting dynamic interaction between interconnected equipment. An experimental program should be pursued to investigate both the characteristics of standard interconnections and strategies to mitigate the effects of dynamic interaction.

Mathematical modeling of porcelain transformer bushings

Additional data on the mechanical characteristics of nitrile rubber gaskets is needed if improved mathematical models of bushings are to be developed. Nonlinear springs should be developed to model gaskets, and the constraint to relative lateral movement of the aluminum core and the perimeter porcelain units offered by the oil inside the bushing must be studied. Improved models of porcelain bushings that would be suitable for rigorous vulnerability studies could be developed with such information.

CHAPTER 7

REFERENCES

Abrahamson, N. 1996. "Nonstationary response-spectrum matching." Unpublished papers.

EERI. 1990. Loma Prieta Reconnaissance Report. *Earthquake Spectra,* Supplement to Volume 6, Oakland, Calif.: Earthquake Engineering Research Institute.

EERI. 1995. Northridge Reconnaissance Report. *Earthquake Spectra,* Supplement C to Volume 11, Oakland, Calif.: Earthquake Engineering Research Institute.

IEEE. 1997. *IEEE 693, Recommended Practices for Seismic Design of Substations.* Draft No. 6, Piscataway, N.J.: IEEE Standards Department.

Mathworks. 1997. *The Language of Technical Computing*. Natick, Mass.: The Mathworks, Inc.

Roberts, A.D. 1988. *Natural Rubber Science and Technology.* Oxford, U.K.: Oxford Science Publications.

Shinozuka, M., ed. 1995. *The Hanshin-Awaji Earthquake of January 17, 1995: Performance of Lifelines*. Technical Report NCEER-95-0015, Buffalo, N.Y.: National Center for Earthquake Engineering Research, State University of New York.

Wilson, E.L. 1992. *SADSAP, Static and Dynamic Structural Analysis Program,* Berkeley, Calif.: Structural Analysis Programs, Inc.

APPENDIX A

IEEE PRACTICE FOR EARTHQUAKE TESTING OF TRANSFORMER BUSHINGS

A.1 Introduction

The document IEEE 693 (IEEE 1997) entitled “Recommended Practices for Seismic Design of Substations” is used in the United States for the seismic qualification and fragility testing of electrical equipment such as transformer bushings. This recommended practice provides qualification requirements for substation equipment and supports manufactured from steel, aluminum, porcelain, and composites. Procedures for equipment qualification using analytical studies (static analysis, static coefficient analysis, and response-spectrum analysis) and experimental methods (response-history testing, sine-beat testing, and static pull testing) are described in the practice. The objective of the document is “... to secure equipment such that it performs acceptably under reasonably anticipated strong ground motion”.

IEEE 693 identifies eleven methods for experimental testing. The most rigorous method is earthquake-response analysis using earthquake ground motion records, the spectral ordinates of which equal or exceed those of a Required Response Spectrum (RRS). Categories of earthquake simulator testing include 1) single-axis, 2) biaxial (i.e., horizontal and vertical), 3) multiaxis, and 4) triaxial.

Section 9 of IEEE 693 describes seismic performance criteria for electrical substation equipment. Information on three seismic qualification levels (Low, Moderate, and High), Performance Levels, the Required Response Spectrum (RRS), the relation between PL and RRS, and acceptance criteria are provided.

The studies described in the body of this report employed triaxial earthquake simulator testing for the qualification and fragility testing of the 196 kV bushings. IEEE 693 writes text on six key topics related to the seismic qualification of transformer bushings:

- Performance level and performance factor
- Performance level qualification
- Support frame and mounting configuration
- Testing procedures
- Instrumentation
- Acceptance criteria

Each of these topics are elaborated upon in the following sections. For fragility testing, the amplitude of the seismic excitation is increased in small increments to determine the level of shaking that causes damage to the bushing, thereby establishing a point on a fragility curve.

A.2 Performance Level and Performance Factor

A Performance Level (PL) for substation equipment is represented in IEEE 693 by a response spectrum. The shape of this spectrum represents a broad-band response that envelopes earthquake effects in different areas considering site conditions that range from soft soil to rock. Three values of equivalent viscous damping are specified: 2 percent, 5 percent, and 10 percent. IEEE 693 states that very soft sites and hill sites might not be adequately covered by the PL shapes.

Three seismic performance levels are identified in IEEE 693: High, Moderate, and Low. In California, the relevant performance levels are High and Moderate. Equipment that is shown to perform acceptably in ground shaking consistent with the High Seismic Performance Level (see Figure A-1) is said to be seismically qualified to the High Level. Equipment that is shown to perform acceptably in ground shaking consistent with the Moderate Seismic Performance Level (see Figure A-2) is said to be seismically qualified to the Moderate Level.

IEEE 693 states that it is often impractical or not cost effective to test to the High or Moderate PL because a) laboratory testing equipment might be unable to attain the necessary high accelerations, and/or b) damage to ductile components at the PL, although acceptable in terms of component qualification, would result in the component being discarded following testing. For these reasons, equipment may be tested using accelerations that are one-half of the PL. The reduced level of shaking is called the Required Response Spectrum (RRS). The ratio of PL to RRS, termed the performance factor in IEEE 693, is equal to 2. The High and Moderate RRSs are shown in Figures A-3 and A-4, respectively. The shapes of the RRS and the PL are identical, but the ordinates of the RRS are one-half of the PL.

Equipment tested or analyzed using the RRS is expected to have acceptable performance at the PL. This assumption is checked by measuring the stresses obtained from testing at the RRS, and a) comparing the stresses to 50 percent (equal to the inverse of the performance factor) of the ultimate strength of the porcelain (assumed to be brittle) or cast aluminum components, and b) using a lower factor of safety against yield combined with an allowance for ductility of steel and other ductile materials.

A.3 Performance Level Qualification

Procedures for selecting the appropriate seismic qualification level for a site are presented in IEEE 693. Qualification levels are directly related to site-specific peak acceleration values calculated using a 2-percent probability of exceedance in 50 years. If the peak ground acceleration is less than 0.1g, the site is classified as Low. If the peak ground acceleration exceeds 0.5g, the site is classified as High. If the peak ground acceleration ranges in value between 0.1g and 0.5g, the site is classified as Moderate. Sites in California are classified as either Moderate or High.

A.4 Support Frame and Mounting Configuration

IEEE 693 writes that bushings 161 kV and larger must be qualified using earthquake-simulator testing. Recognizing that it is impractical to test bushings mounted on a transformer, IEEE requires bushings to be mounted on a rigid stand during testing. To account for the amplification of earthquake motion due to the influence of the transformer body and local flexibility of the

transformer near the bushing mount, the input motion as measured at the bushing flange shall match a spectrum with ordinates twice that of the Required Response Spectrum. The resulting spectra, termed the Test Response Spectra (TRS), for Moderate Level qualification are shown in Figure A-5.

A transformer bushing must be tested at no less than its in-service slope, which is defined as the slope angle measured from the vertical. IEEE 693 recommends that a bushing be tested at 20 degrees measured from the vertical. If so tested, a bushing is assumed to be qualified for use on all transformers with angles from vertical to 20 degrees. (A bushing installed at an angle greater than 20 degrees must be tested at its in-service angle.)

A.5 Testing Procedures for Transformer Bushings

Three types of earthquake-simulator testing are identified in IEEE 693 for the seismic qualification of transformer bushings: 1) earthquake ground motions, 2) resonant frequency search, and 3) sine-beat testing. Earthquake ground motion tests (termed *time-history shake table tests* in IEEE 693) and resonant frequency tests are mandatory; additional information on these two types of tests follow.

A.5.1 Resonant search tests

Sine-sweep or broad-band white noise tests are used to establish the dynamic characteristics (natural frequencies and damping ratios) of a bushing. These so-called *resonant search* tests are undertaken using uni-directional excitation along each principal axis of the earthquake simulator platform. If broadband white noise tests are performed, the amplitude of the white noise must not be less than 0.25g.

If sine-sweep tests are used, IEEE 693 specifies that the resonant search be conducted at a rate not exceeding one octave per minute in the range for which the equipment has resonant frequencies, but at least at 1 Hz; frequency searching above 33 Hz is not required. Modal damping is calculated using the half-power bandwidth method.

A.5.2 Earthquake ground motion tests

Triaxial earthquake simulator testing is mandated for the seismic qualification of 161 kV and above bushings. The Test Response Spectrum (TRS) for each horizontal earthquake motion must match or exceed the target spectrum. The TRS for the vertical earthquake motion shall be no less than 80 percent of target spectrum. Earthquake motions can be established using either synthetic or recorded histories. IEEE 693 recommends that 2-percent damping be used for spectral matching and requires at least 20 seconds of strong motion shaking be present in each earthquake record.

A.6 Instrumentation of Transformer Bushings

IEEE 693 states that porcelain bushings must be instrumented to record the following response quantities:

1. maximum vertical and horizontal accelerations at the top of the bushing, at the bushing flange, and at the top of the earthquake-simulator platform

2. maximum displacement of the top of the bushing relative to the flange

3. maximum porcelain stresses at the base of the bushing near the flange

A.7 Acceptance Criteria for Transformer Bushings

IEEE 693 writes that a bushing is considered to have passed the qualification tests if all the criteria tabulated below related to general performance, allowable stresses, and leakage are met. The data obtained from testing using ground motions compatible with the Test Response Spectrum (see Figure A-5) are used to assess general performance and allowable stresses. Oil leakage is checked for a higher level of earthquake shaking.

General Performance	No evidence of damage such as broken, shifted, or dislodged insulators. No visible leakage of oil or broken support flanges.
Allowable Stresses	The stresses in components are below the limiting values. (See Section A.2. For example, the stresses in the porcelain components associated with earthquake shaking characterized by the spectrum presented in Figure A-5 must be less than 50 percent of the ultimate value.)
Leakage	Bushings qualified by earthquake simulator testing shall have a minimum factor of safety of two against gasket leaks for loads imposed during application of the Test Response Spectrum. IEEE 693 states that an acceptable method to demonstrate this factor of safety is to have no leaks after shaking characterized by twice the Test Response Spectrum. (Such shaking corresponds to a Performance Factor equal to 1.0.)

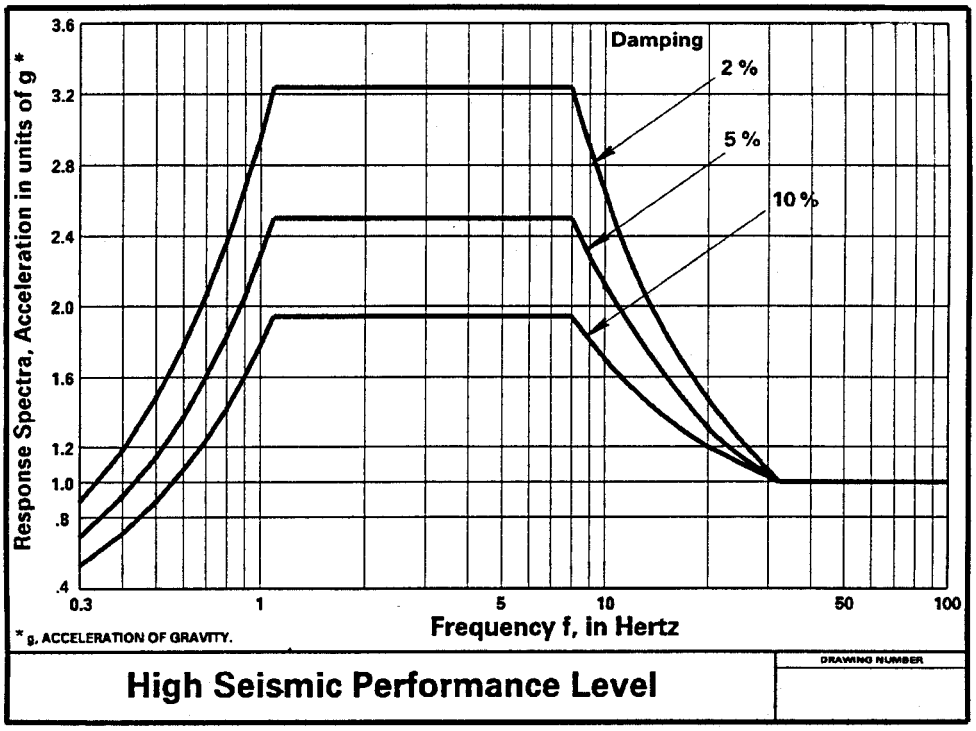

Figure A-1 Spectra for High Seismic Performance Level (IEEE, 1997)

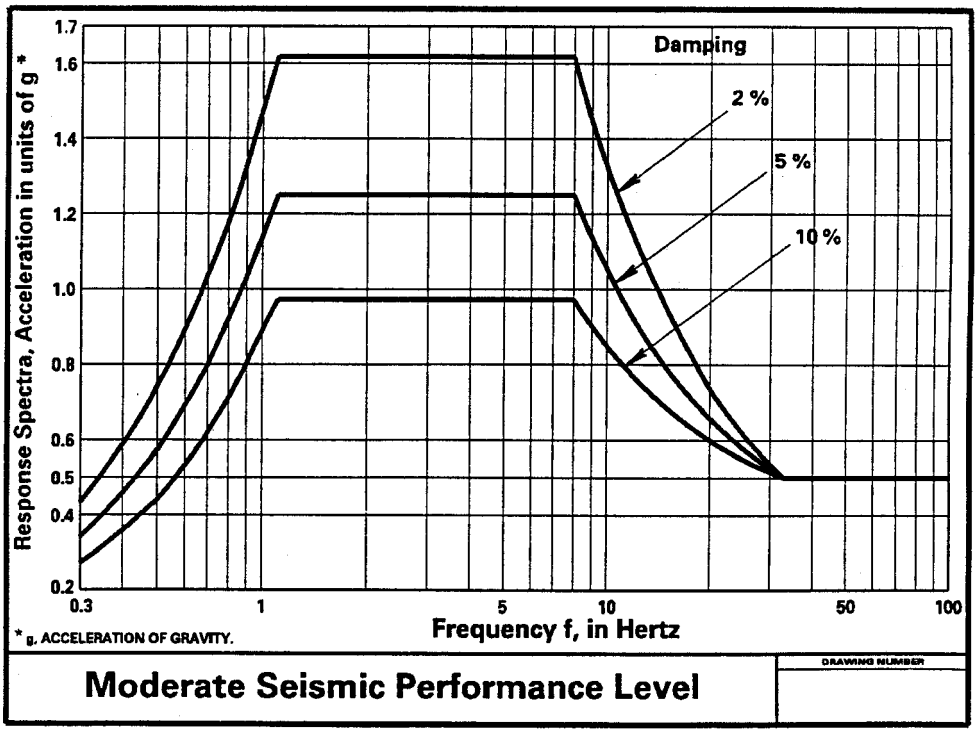

Figure A-2 Spectra for Moderate Seismic Performance Level (IEEE, 1997)

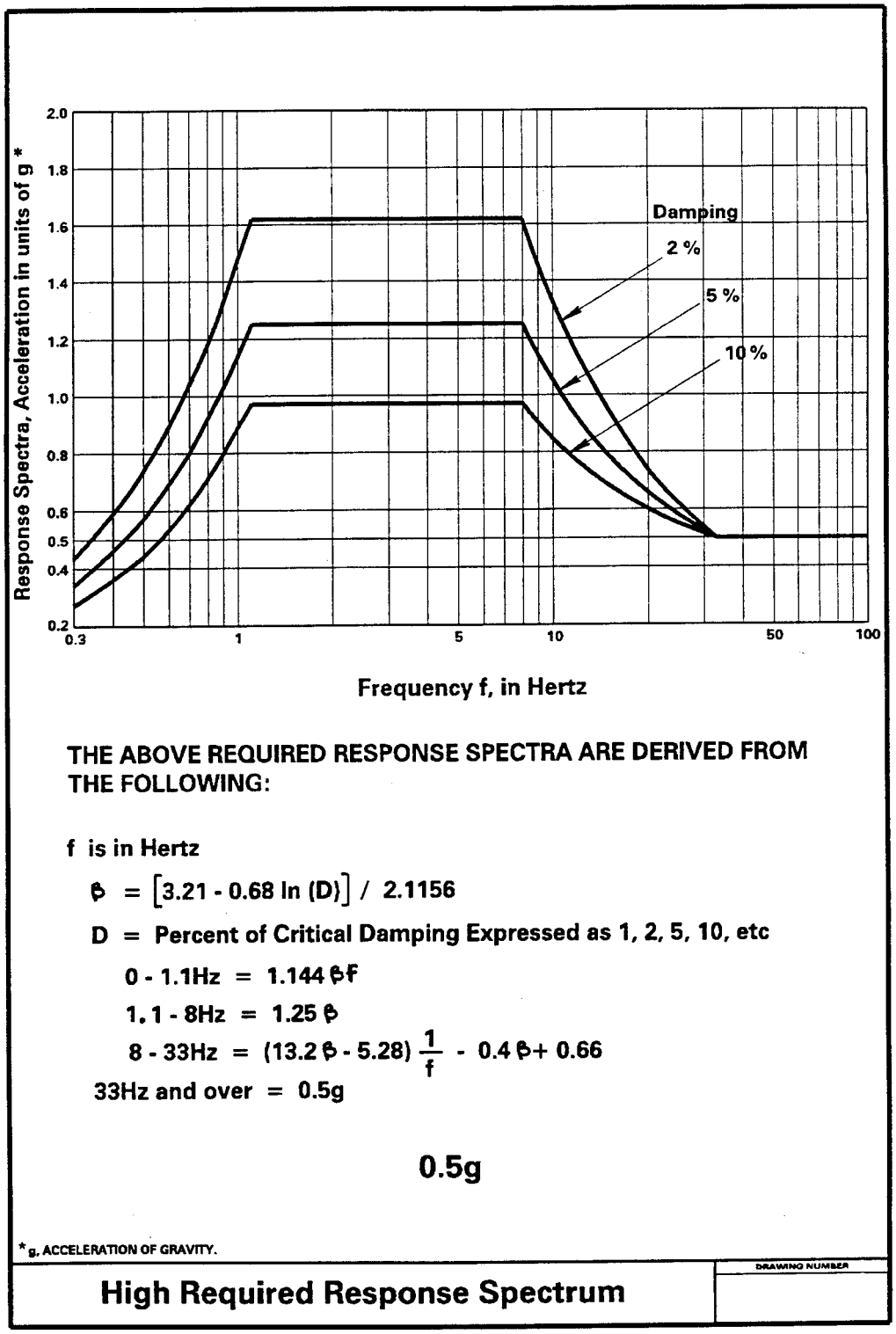

Figure A-3 Spectra for High Required Response Spectrum (IEEE, 1997)

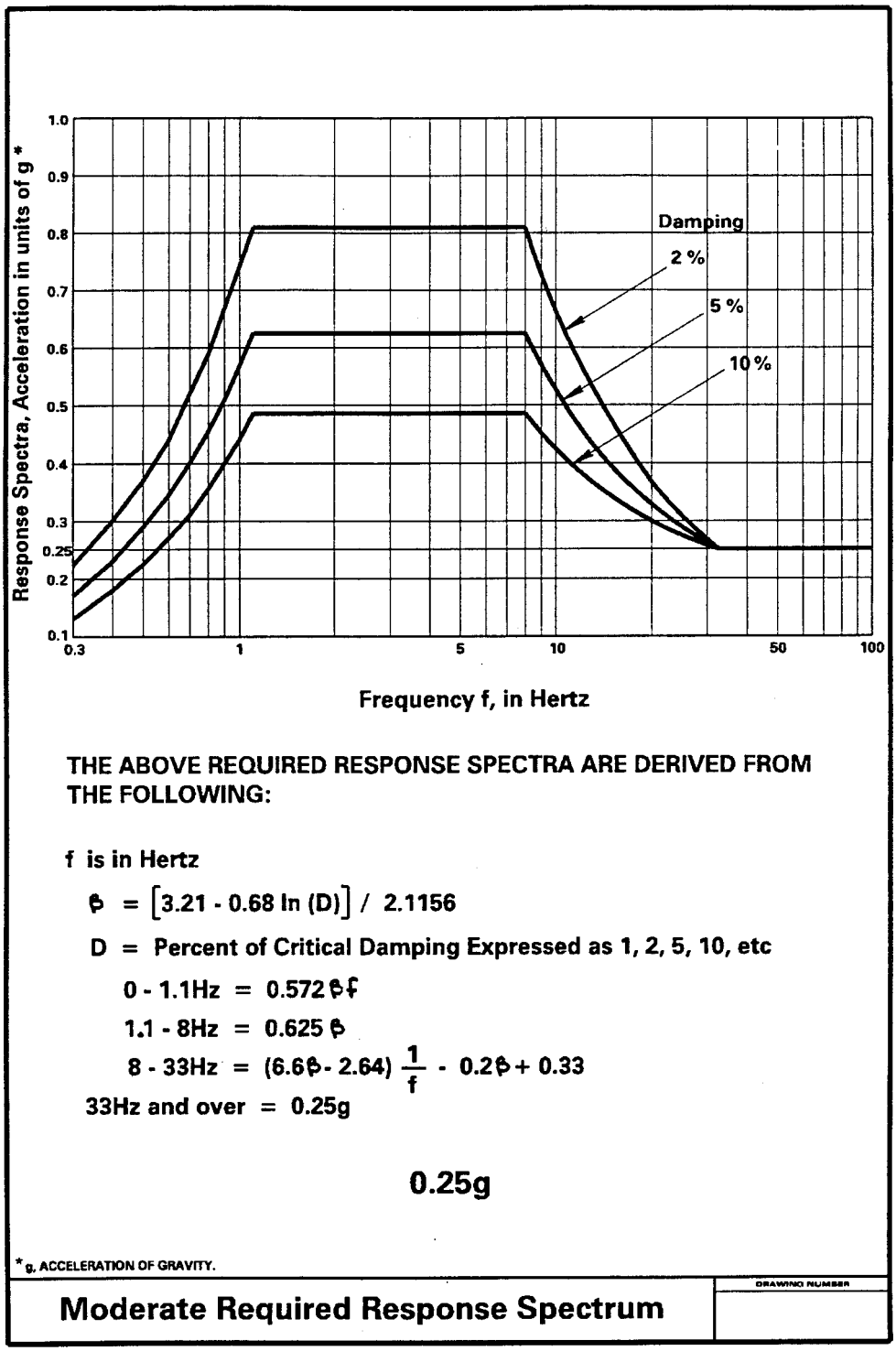

Figure A-4 Spectra for Moderate Required Response Spectrum (IEEE, 1997)

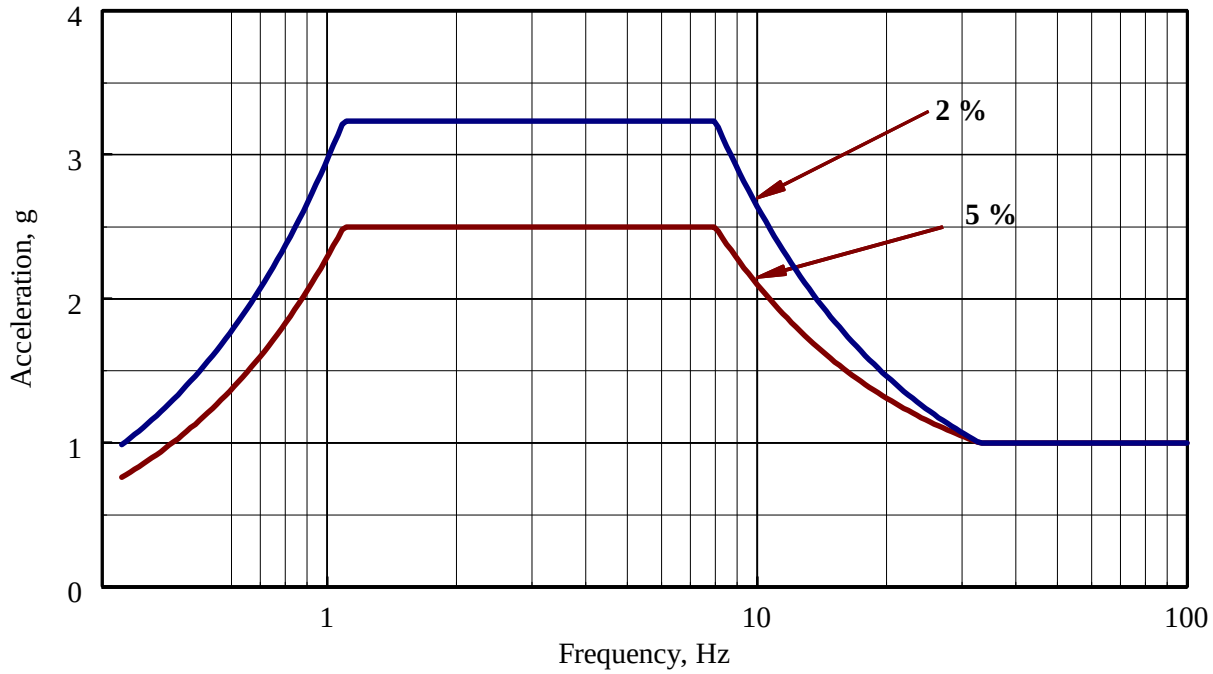

Figure A-5 Test Response Spectra for Moderate Level qualification of a transformer-mounted bushing

APPENDIX B

RESULTS OF ELECTRICAL TESTING

Electrical tests were conducted prior to and after the seismic tests to determine the functionality of the two 196 kV transformer bushings. The two key electrical response parameters are the capacitance measured between the top of bushing and the tap near the flange (designated as C_1) and between the tap and the grounded flange plate (designated as C_2). The capacitance is typically represented in terms of a power factor. A substantial increase in the power factors above the values measured during the fabrication and following earthquake simulation can represent failure of the bushing and could indicate internal structural damage in the bushing.

The two 196 kV bushings were tested at the ABB fabrication facility prior to shipment to California for testing. The power factor readings were recorded on the bushing identification plates.

The electrical test results conducted in the ABB facility indicated that there was no significant changes in the power factor readings in either bushing. The partial discharge value of 1.0 μV was less than the limiting value of 10 μV. Both bushings were pressure tested at 22 psi for 12 hours, and no leaks were observed. Both bushings were torn down; no evidence of internal damage was found in either bushing.

The following sheets present the results of the electrical tests as recorded by ABB technicians.

ABB
Alamo, Tennessee
CERTIFIED TEST REPORT

Apparatus: Condenser Bushing
Style: 196W0800AY
Rating: 196kV 800Amps
BIL: 900kV
Max L-G Voltage: 146kV
Serial: 7T00525802
Ambient Temperature: 22C

Customer: _____

Test Date: 04/03/97

1. Power Factor and Capacitance:
The power factor/capacitance test is conducted per IEEE Std. C57.19.00-1991 & Std. C57.19.01-1991. Test equipment includes a dissipation factor/capacitance bridge #062, and a dielectric test set for measurements above 10kV.
Before 60Hz Withstand

Measurement	Applied kV	Power Factor (%)	Capacitance (Pfd)
(C1) Stud to Tap	10	0.23	440
(C2) Tap to Flange	10	NA	3701
Stud to Flange	N/A	N/A	N/A

2.Tap Test:This bushing passed a 60Hz, one minute applied test: 20kV tap to flange.

3. Dry 60Hz Withstand and Partial Discharge:
The tests were conducted per IEEE Std. C57.19.00-1991, IEEE Std. C57.19.01-1991, specifications. The dielectric and partial discharge detection equipment is designed to meet or exceed IEEE 454-1973, C57.113-1988, and C63.2-1987 requirements which includes Hipotronics dividers, detectors, power sources to 1MV, and partial discharge detectors.

Test Voltage	Test Duration	Start	Finish
(kV)	(Min)	uV	uV
219	N/A	1	N/A
425	1	2	2
219	N/A	1	N/A

4. After 60Hz Withstand* *Nameplate information

Measurement	Applied kV	Power Factor (%)	Capacitance (Pfd)
(C1) Stud to Tap	10	0.25	441
(C2) Tap to Flange	10	N/A	3701
Stud to Flange	N/A	N/A	N/A

This bushing meets or exceeds all of the specified ANSI/IEEE test requirements. This includes an internal 22 psig oil pressure test for a minimum of one hour without resultant leakage. This unit was filled at the factory with PCB free (non-detectable) dielectric fluid in accordance with Federal poly chlorinate biphenyl (PCB) regulation 40 CFR 61, dated May 31, 1979. The analysis is verified per ASTM-D4059 using a H.P. model 5710 Gas Chromatograph with a minimum detection level of 0.8 ppm (accuracy +/(-) 5%). The contents of this report are a true and correct record of data obtained from tests performed at the ABB Power T&D Plant, Components Division; Alamo, TN.

5. Test Results: Passed

Test Specialist: Dennis Rogers Date: 04/03/97

Remarks: This Unit passed Cantilever at 600, 900, & 1000 lbs.
ETIPS 92-2314 7 ABB

ABB

Alamo, Tennessee

CERTIFIED TEST REPORT

Apparatus: Condenser Bushing Customer: _____

Style: 196W0800AY

Rating: 196kV 800Amps

BIL: 900kV

Max L-G Voltage: 146kV

Serial: 7T00525802

Ambient Temperature: 21C Test Date: 11/04/97

1. Power Factor and Capacitance:

The power factor/capacitance test is conducted per IEEE Std. C57.19.00-1991 & Std. C57.19.01-1991. Test equipment includes a dissipation factor/capacitance bridge #062, and a dielectric test set for measurements above 10kV.

Before 60Hz Withstand

Measurement	Applied kV	Power Factor (%)	Capacitance (Pfd)
(C1) Stud to Tap	10	.24	436
(C2) Tap to Flange	10	NA	3698
Stud to Flange	N/A	N/A	N/A

2.Tap Test:This bushing passed a 60Hz, one minute applied test: 20kV tap to flange.

3. Dry 60Hz Withstand and Partial Discharge:

The tests were conducted per IEEE Std. C57.19.00-1991, IEEE Std. C57.19.01-1991, specifications. The dielectric and partial discharge detection equipment is designed to meet or exceed IEEE 454-1973, C57.113-1988, and C63.2-1987 requirements which includes Hipotronics dividers, detectors, power sources to 1MV, and partial discharge detectors.

Test Voltage	Test Duration	Start	Finish
(kV)	(Min)	uV	uV
219	N/A	1	N/A
425	1	1	1
219	N/A	1	N/A

4. After 60Hz Withstand* *Nameplate information

Measurement	Applied kV	Power Factor (%)	Capacitance (Pfd)
(C1) Stud to Tap	10	.24	436
(C2) Tap to Flange	10	N/A	3699
Stud to Flange	N/A	N/A	N/A

This bushing meets or exceeds all of the specified ANSI/IEEE test requirements. This includes an internal 22 psig oil pressure test for a minimum of one hour without resultant leakage. This unit was filled at the factory with PCB free (non-detectable) dielectric fluid in accordance with Federal poly chlorinate biphenyl (PCB) regulation 40 CFR 61, dated May 31, 1979. The analysis is verified per ASTM-D4059 using a H.P. model 5710 Gas Chromatograph with a minimum detection level of 0.8 ppm (accuracy +/(-) 5%). The contents of this report are a true and correct record of data obtained from tests performed at the ABB Power T&D Plant, Components Division; Alamo, TN.

5. All Units rated 362kV & 1050kV BIL and above, received 5 full wave impulses, nominal 1.2 x 50 microseconds, prior to the 60 Hz withstand test.

6. Test Results: Passed

Test Specialist: Dennis Rogers Date: 11/04/97

Remarks: RMR5276. Unit had 18uV at 219 kV, Stopped tests. Removed Strain guage and cleaned. Reapplied voltage and unit operated at <1uV through withstand.

ETIPS 92-2314 7 ABB

ABB
Alamo, Tennessee
CERTIFIED TEST REPORT

Apparatus: Condenser Bushing
Style: 196W0800AY
Rating: 196kV 800Amps
BIL: 900kV
Max L-G Voltage: 146kV
Serial: 7T00525801
Ambient Temperature: 23C

Customer: _____

Test Date: 02/17/97

1. Power Factor and Capacitance:
The power factor/capacitance test is conducted per IEEE Std. C57.19.00-1991 & Std. C57.19.01-1991. Test equipment includes a dissipation factor/capacitance bridge #640, and a dielectric test set for measurements above 10kV.
Before 60Hz Withstand

Measurement	Applied kV	Power Factor (%)	Capacitance (Pfd)
(C1) Stud to Tap	10	.23	440
(C2) Tap to Flange	10	NA	3718
Stud to Flange	N/A	N/A	N/A

2.Tap Test:This bushing passed a 60Hz, one minute applied test: 20kV tap to flange.

3. Dry 60Hz Withstand and Partial Discharge:
The tests were conducted per IEEE Std. C57.19.00-1991, IEEE Std. C57.19.01-1991, specifications. The dielectric and partial discharge detection equipment is designed to meet or exceed IEEE 454-1973, C57.113-1988, and C63.2-1987 requirements which includes Hipotronics dividers, detectors, power sources to 1MV, and partial discharge detectors.

Test Voltage	Test Duration	Start	Finish
(kV)	(Min)	uV	uV
219	N/A	1	N/A
425	1	1	1
219	N/A	1	N/A

4. After 60Hz Withstand* *Nameplate information

Measurement	Applied kV	Power Factor (%)	Capacitance (Pfd)
(C1) Stud to Tap	10	.24	439
(C2) Tap to Flange	10	N/A	3718
Stud to Flange	N/A	N/A	N/A

This bushing meets or exceeds all of the specified ANSI/IEEE test requirements. This includes an internal 22 psig oil pressure test for a minimum of one hour without resultant leakage. This unit was filled at the factory with PCB free (non-detectable) dielectric fluid in accordance with Federal poly chlorinate biphenyl (PCB) regulation 40 CFR 61, dated May 31, 1979. The analysis is verified per ASTM-D4059 using a H.P. model 5710 Gas Chromatograph with a minimum detection level of 0.8 ppm (accuracy +/(-) 5%). The contents of this report are a true and correct record of data obtained from tests performed at the ABB Power T&D Plant, Components Division; Alamo, TN.

5. Test Results: Passed

Test Specialist: Dennis Rogers Date: 02/17/97

Remarks: This Unit passed Cantilever at 600, 900, & 1100 lbs.
ETiPS 92-2314 7 ABB

ABB

Alamo, Tennessee

CERTIFIED TEST REPORT

Apparatus: Condenser Bushing
Style: 196W0800AY
Rating: 196kV 800Amps
BIL: 900kV
Max L-G Voltage: 146kV
Serial: 7T00525801
Ambient Temperature: 21C

Customer: _____

Test Date: 11/04/97

1. Power Factor and Capacitance:

The power factor/capacitance test is conducted per IEEE Std. C57.19.00-1991 & Std. C57.19.01-1991. Test equipment includes a dissipation factor/capacitance bridge #062, and a dielectric test set for measurements above 10kV.

Before 60Hz Withstand

Measurement	Applied kV	Power Factor (%)	Capacitance (Pfd)
(C1) Stud to Tap	10	.24	436
(C2) Tap to Flange	10	NA	3714
Stud to Flange	N/A	N/A	N/A

2.Tap Test:This bushing passed a 60Hz, one minute applied test: 20kV tap to flange.

3. Dry 60Hz Withstand and Partial Discharge:

The tests were conducted per IEEE Std. C57.19.00-1991, IEEE Std. C57.19.01-1991, specifications. The dielectric and partial discharge detection equipment is designed to meet or exceed IEEE 454-1973, C57.113-1988, and C63.2-1987 requirements which includes Hipotronics dividers, detectors, power sources to 1MV, and partial discharge detectors.

Test Voltage	Test Duration	Start	Finish
(kV)	(Min)	uV	uV
219	N/A	1	N/A
425	1	1	1
219	N/A	1	N/A

4. After 60Hz Withstand* *Nameplate information

Measurement	Applied kV	Power Factor (%)	Capacitance (Pfd)
(C1) Stud to Tap	10	.24	436
(C2) Tap to Flange	10	N/A	3715
Stud to Flange	N/A	N/A	N/A

This bushing meets or exceeds all of the specified ANSI/IEEE test requirements. This includes an internal 22 psig oil pressure test for a minimum of one hour without resultant leakage. This unit was filled at the factory with PCB free (non-detectable) dielectric fluid in accordance with Federal poly chlorinate biphenyl (PCB) regulation 40 CFR 61, dated May 31, 1979. The analysis is verified per ASTM-D4059 using a H.P. model 5710 Gas Chromatograph with a minimum detection level of 0.8 ppm (accuracy +/(-) 5%). The contents of this report are a true and correct record of data obtained from tests performed at the ABB Power T&D Plant, Components Division; Alamo, TN.

5. All Units rated 362kV & 1050kV BIL and above, received 5 full wave impulses, nominal 1.2 x 50 microseconds, prior to the 60 Hz withstand test.

6. Test Results: Passed

Test Specialist: Dennis Rogers

Date: 11/04/97

Remarks: RMR5276

ETIPS 92-2314 7 ABB

APPENDIX C
SEISMIC TEST-QUALIFICATION REPORT

C.1 General

This appendix provides the information to support the seismic test-qualification report for which a template is provided in Appendix S of IEEE 693. Section C.2 reproduces page 149 of IEEE 693 for Bushing-1 and Bushing-2. Section C.3 presents information pertaining to the qualification data sheet.

The earthquake tests were witnessed by the authors of this report, representatives of Pacific Gas & Electric (Messrs. Ed Matsuda and Eric Fujisaki), and a representative of Asea Brown Boveri (Mr. Lonnie Elder).

C.2 Qualification Title Sheets

C.2.1 Bushing-1 (Serial No. 7T00525802)

Seismic Test-Qualification Report

Qualified to Moderate Level; 0.25g ZPA of the RRS

Equipment designation: 196W0800AY

Equipment rating: 196 kV

Equipment manufactured by: Asea Brown Boveri, Alamo, TN

Report prepared by: University of California, Berkeley

C.2.2 Bushing-2 (Serial No. 7T0052801)

Seismic Test-Qualification Report

Qualified to High Level; 0.5g ZPA of the RRS

Equipment designation: 196W0800AY

Equipment rating: 196 kV

Equipment manufactured by: Asea Brown Boveri, Alamo, TN

Report prepared by: University of California, Berkeley

C.3 Qualification Data Sheets

The table below cross-references the content listed on page 151 of IEEE 693 with the appropriate section(s) and table(s) contained in the body of the report.

Table C-1 Qualification Data Sheet

Data Sheet Content		
IEEE 693 Section No.	*Title*	*Comment or Section/Table No. in Report*
1.0	**General**	
a.	Supplemental work and options	Nil
b.	Equipment configuration	Sections 2.2 and 2.3
c.	Resonant frequency search data	Section 3.2
d.	Schedule of tests and witnesses	Section 4.4
e.	Test plan	Table 3-1
f.	Modifications, if any, to pass test	Nil
g.	Pretest calculations, if any	Nil
h.	Identification tags	Section 1.3
2.0	**Equipment Data**	-
a.	Resonant frequencies	Section 4.3
b.	Damping ratio	Section 4.3
c.	Displacements at tip of bushing	Section 4.4.6
d.	Equipment and structure reactions	NA
e.	Anchor details	NA
f.	Maximum input accelerations	Tables 3-2 and 4-3
g.	Table of measured accelerations	Table 4-4
h.	Table of measured porcelain strains	Table 4-5
i.	Materials types and strengths	Section 4-2
3.0	**Method of Testing**	-
a.	Testing cases	Chapter 3
b.	Location and date of test	Table 3-2
c.	Description of testing equipment	Section 2.2
d.	Serial numbers of equipment	Section 1.3
e.	Physical damage from testing	Nil
4.0	**Functional Testing**	Nil
5.0	**Video**	Delivered to PG&E

1. NA = Not Applicable

APPENDIX D
INSTRUMENT CALIBRATION

This appendix provides information on the manufacturer, model, range, and calibration factor for each transducer used for the earthquake-simulator testing. Channels 1 and 2 recorded the date and time, respectively.

Table D-1 Instrument calibration data

Channel Number	*Transducer*[1]	*Manufacturer*	*Model*	*Range*	*Calibration Factor*[2] *units/ bit span*
3	A	Setra Systems	141A	5 g	0.000305176
4	A		141A	5 g	0.000305176
5	A		141A	5 g	0.000305176
6	A		141A	5 g	0.000305176
7	A		141A	5 g	-0.000305176
8	A		141A	5 g	-0.000305176
9	A		141A	5 g	-0.000305176
10	A		141A	5 g	-0.000305176
11	LVDT	MTS	NA[3]	10 in.	-0.0006104
12	LVDT		NA	10 in.	-0.0006104
13	LVDT		NA	10 in.	0.0006104
14	LVDT		NA	10 in.	0.0006104
15	LVDT		NA	4 in.	0.0001526
16	LVDT		NA	4 in.	0.0001526
17	LVDT		NA	4 in.	0.0001526
18	LVDT		NA	4 in.	0.0001526
19	A	EG&G IC Sensors	ICS3022-005-P	10 g	-0.0006353
20	A		ICS3022-005-P	10 g	-0.0006086
21	A		ICS3022-005-P	10 g	-0.0006966
22	A		ICS3022-005-P	5 g	0.0002724
23	A		ICS3022-005-P	5 g	0.0002225
24	A		ICS3022-005-P	5 g	0.0002208
25	A		ICS3022-010-P	5 g	-0.0003319

Table D-1 Instrument calibration data

Channel Number	*Transducer*[1]	*Manufacturer*	*Model*	*Range*	*Calibration Factor*[2] *units/bit span*
26	A	EG&G IC Sensors	ICS3022-010-P	5 g	-0.0003284
27	A		ICS3022-010-P	5 g	-0.0003431
28	A		ICS3022-005-P	10 g	-0.0005951
29	A		ICS3022-005-P	10 g	-0.0006096
30	A		ICS3022-005-P	5 g	-0.0003363
31	LP	Celesco	PT-101-15A	15 in.	0.0006699
32	LP		PT-101-15A	15 in.	0.0006356
33	LP		PT-101-15A	15 in.	0.0006699
34	LP		PT-101-15A	15 in.	0.0006561
35	LP		PT-101-15A	15 in.	-0.0006419
36	LP		PT-101-15A	15 in.	0.0006383
37	LP		PT-101-15A	15 in.	0.0006585
38	LP		PT-101-15A	15 in.	0.0006597
39	SG	Measurements Group	EA-06-250A5-350/P	3 %	-0.390
40	SG		EA-06-250A5-350/P	3 %	-0.391
41	SG		EA-06-250A5-350/P	3 %	-0.399
42	SG		EA-06-250A5-350/P	3 %	-0.390
43	DCDT	Trans-Tek	243-0000	0.5 in.	0.0000430
44	DCDT		243-0000	0.5 in.	0.0000443
45	DCDT		243-0000	0.5 in.	0.0000444
46	DCDT		243-0000	0.5 in.	0.0000511
47	DCDT		243-0000	0.5 in.	0.0000439
48	DCDT		243-0000	0.5 in.	0.0000436
49	DCDT		243-0000	0.5 in.	0.0000452
50	DCDT		243-0000	0.5 in.	0.0000437

1. A = accelerometer; LVDT = displacement transducer; LP = linear potentiometer; SG = strain gage; DCDT = displacement transducer

2. 10 volts = 2^{14} bits

3. NA = Not available